ABSTRACT

REINERT, ALLISON MARIE. Granular Activated Carbon Adsorption of Micropollutants from Surface Water: Field-Scale Adsorber Performance and Scale-Up of Bench-Scale Data. (Under the direction of Detlef Knappe).

Micropollutants (MPs) are defined as compounds that occur in water at ng/L to μg/L concentrations. Many anthropogenic MPs, such as antibiotics, herbicides, insecticides, endocrine disrupting compounds, and personal care products, are ubiquitous in drinking water sources. As a result utilities are looking for economically feasible ways to remove these compounds during drinking water treatment. Granular activated carbon (GAC) adsorption is one effective treatment technology for controlling many MPs, but estimating GAC life and performance from pilot studies is expensive and time consuming. Bench-scale tests, such as the rapid small scale column test (RSSCT), have been developed as an economical and time saving alternative to pilot testing. However, approaches for predicting field-scale GAC adsorber performance from RSSCT data have remained elusive when MPs occur in the presence of natural organic matter (NOM).

The overall objectives of this research were to (1) determine the effectiveness of GAC for the removal of MPs that were added at ng/L concentrations to coagulated surface water and (2) develop a comprehensive scale-up approach for predicting field-scale MP removal from RSSCT data. Specifically, the effects of NOM on the scale-up of MP adsorption capacity and kinetics were assessed.

A pilot column was operated with bituminous coal-based GAC at an empty bed contact time (EBCT) of 7 minutes for 120,000 bed volumes (1.6 years). The GAC influent was spiked with 34 MPs (pesticides, endocrine disrupting chemicals,

pharmaceuticals, personal care products) at levels ranging from 10-500 ng/L. MP breakthrough curves were determined from paired influent and effluent samples. In the pilot column, dissolved organic carbon (DOC) breakthrough reached 50% after 13,000 bed volumes had been treated. At that point, none of the tested MPs reached measurable levels of breakthrough. These results suggest that GAC adsorption is an effective tool for the removal of MPs if GAC is primarily used for NOM control. At the completion of the pilot study, only 11 of the tested MPs exhibited breakthrough at levels greater than 10% of the influent concentration. Among the 34 MPs, the x-ray contrast agent iopromide was the least adsorbable followed by the flame retardant tributyl phosphate and the nicotine metabolite cotinine. Biodegradation of MPs likely contributed to the effectiveness of the pilot-scale GAC adsorber because, with the exception of caffeine, readily biodegradable MPs were not detected in the GAC effluent.

Two common RSSCT designs were evaluated for scale-up. One RSSCT was designed based on the proportional diffusivity (PD-RSSCT) approach, which assumes that MP diffusivity varies linearly with GAC particle size. The PD-RSSCT was operated for 350,000 bed volumes (8 months). A second RSSCT was designed based on the constant diffusivity (CD-RSSCT) approach, which assumes that MP diffusivity is independent of GAC particle size. The CD-RSSCT was operated for 250,000 bed volumes (2 months). As was the case for the pilot column, iopromide was the least adsorbable MP in both the PD- and the CD-RSSCT. During the PD-RSSCT, 26 MPs broke through to measurable levels, and31 broke through to measurable levels during the CD-RSSCT. Based on the CD-RSSCT results, the most adsorbable MPs were bisphenol A, ethinyl estradiol, triclosan, acetaminophen, carbaryl, chlorpyrifos, and diuron.

With the exception of iopromide in the CD-RSSCT, the RSSCTs overpredicted the MP adsorption capacity of the GAC. The difference in MP adsorption capacity was likely due to particle size-dependent GAC fouling that resulted from the adsorption of NOM. A fouling factor (Y), that addresses particle size-dependent GAC fouling, was calculated for each of the 11 MPs for which measureable breakthrough (10%) was reached in both the pilot study and the RSSCTs. The magnitude of Y was compound-specific. For the CD-RSSCT, a linear free energy relationship (LFER) was developed to relate Y to Abraham descriptors using principal component analysis (PCA). Abraham descriptors consist of excess molar refraction (E), dipolarity/polarizability (S), overall hydrogen bond acidity (A), overall hydrogen bond basicity (B), and the McGowan volume (V). For the CD-RSSCT, Y can be estimated from:

$$Y = (0.165 \pm 0.0406)(PC1) + (0.883 \pm 0.143)$$

n=11 r^2=0.90 adjusted r^2=0.89

where PC1 is the first principal component and is calculated from:

$$PC1 = -0.612S - 0.247A - 0.370B - 0.341V - 0.558E$$

For the PD-RSSCT, an LFER that effectively described the variability in Y could not be found. Instead, two distinct correlations between Y and the pH-dependent octanol water partition coefficient (log D) were found. However, no compound characteristic could be identified to place an MP on one or the other regression line.

While Y addresses differences in MP adsorption capacity between field-scale and RSSCT data, particle size-dependent differences in adsorption kinetics needed to be addressed as well. For both the CD- and the PD-RSSCT, results from the pore surface diffusion model (PSDM) suggested that the intraparticle diffusive flux of MPs varied

linearly with GAC particle size. While the PD-RSSCT design explicitly addresses the particle size-dependence of MP adsorption kinetics, the CD-RSSCT design does not. However, with the aid of the PSDM, CD-RSSCT data can be readily scaled by incorporating the linear dependence of the intraparticle diffusive flux on particle size.

For water treatment professionals looking to run RSSCTs in place of pilot tests to ascertain GAC service life for MP removal, the CD-RSSCT is the more convenient choice because the CD-RSSCT can to be completed in less time. Furthermore, Y, can be predicted with more confidence for the CD-RSSCT using the LFER developed in this research.

Granular Activated Carbon Adsorption of Micropollutants from Surface Water: Field-Scale Adsorber Performance and Scale-Up of Bench-Scale Data

by
Allison Marie Reinert

A thesis submitted to the Graduate Faculty of
North Carolina State University
in partial fulfillment of the
requirements for the degree of
Master of Science

Environmental Engineering

Raleigh, North Carolina

2013

APPROVED BY:

Detlef Knappe
Committee Chair

Joel Ducoste

Francis Lajara De Los Reyes

DEDICATION

This would not have been possible without the advice and encouraging words from my parents, Kevin and Kathleen, and my brother, Jared. Thank you for all your love and support in all of my endeavors.

BIOGRAPHY

Allison Marie Reinert was born in Pottstown, Pennsylvania on April 13, 1989 to Kevin and Kathleen Reinert. She grew up in Lansdale, Pennsylvania and later moved to Summerfield, North Carolina. Allison completed her Bachelor of Science in environmental engineering at Southern Methodist University in Dallas, Texas in 2011. After graduating from Southern Methodist University, she began her Master of Science degree in environmental engineering at North Carolina State University in Raleigh, North Carolina. Following completion of her graduate degree Allison will begin work as an Assistant Engineer at Hazen and Sawyer in Raleigh, NC.

ACKNOWLEDGMENTS

I would like to thank the following people and organizations for their participation and support of this project:

- Water Research Foundation for funding this project (4235)
- Hazen and Sawyer for their generous 2012 AWWA Scholarship
- Dr. Detlef Knappe for his constant guidance and knowledge for this project as well as the entirety of my graduate studies
- Anthony Kennedy, and Imma Ferrer and the entire Dr. Scott Summers research group for their analytical support, many conference calls, and technical advice throughout this research
- Dr. Joel Ducoste and Dr. Francis de los Reyes for serving on my committee and helping to shape me as a student and engineer throughout my time at NCSU
- David Black, Environmental Lab Manager, for always having an open door and a listening ear for our research and our lives
- James, Ken, Eric, and all of the other employees at the Orange Water and Sewer Authority (Carrboro, NC) for always giving me access to the basement, lending a helping hand, providing the water for this research, and checking in on my pilot column and me whenever I needed
- The Suffolk County Water Authority (Hauppauge, NY) employees, including Fil, Jeanne and Joe for their help, data analysis, and providing water for this research
- My family for their constant support and love

- My research group and friends including Meredith, Leigh-Ann, Dustin, Elisa, Viking, Amber, Rachel, and Bahareh, for their support and friendship
- Jason Patskoski for assisting in the statistical analysis and teaching me R-Project
- Everyone in the environmental lab and all those in office Mann 319-A for the food, conversation, fun, and support

TABLE OF CONTENTS

LIST OF TABLES

LIST OF FIGURES

ABBREVIATIONS

AdDesignS	Adsorption Design Software
ADI	Allowable Daily Intake
ANOVA	Analysis of Variance
C	Celsius
CCL3	Contaminant Candidate List 3
CD	Constant Diffusivity
CI	Chemical Ionization
CUR	Carbon Usage Rate
DI	Deionized Water
DOC	Dissolved Organic Carbon
DOM	Dissolved Organic Matter
DWEL	Drinking Water Equivalent Level
EPA	Environmental Protection Agency
GAC	Granular Activated Carbon
GC-MS/MS	Gas Chromatography Tandem Mass Spectrometry
GLM	Generalized Linear Model
HPLC	High Performance Liquid Chromatography
HPV	High Production Volume
IS	Internal Standard
L	Liter
LC-MS/MS	Liquid Chromatography Tandem Mass Spectrometry
LFER	Linear Free Energy Relationship
LOO	Leave One Out
MCL	Maximum Contaminant Level
MCLG	Maximum Contaminant Level Goal
mg	Milligram
mL	Milliliter
MLR	Multiple Linear Regression
MIB	Methylisoborneol
min	Minute
MP	Micropollutant
M	Molar (mole/Liter)

NCSU	North Carolina State University
ng	Nanogram
nm	Nanometer
NOM	Natural Organic Matter
OWASA	Orange Water and Sewer Authority
PC	Principal Component
PCA	Principal Component Analysis
PCP	Principal Care Product
PCR	Principal Component Regression
PD	Proportional Diffusivity
PRESS	Predicted Error Sum of Squares
PSDM	Pore Surface Diffusion Model
QSAR	Quantitative Structure-Activity Relationship
QSPR	Quantitative Structure-Property Relationship
RMSE	Root Mean Square Error
RSSCT	Rapid Small Scale Column Test
SCWA	Suffolk County Water Authority
SDWA	Safe Drinking Water Act
SPME	Solid Phase Microextraction
TOC	Total Organic Carbon
T	Tortuosity
UCMR3	Unregulated Contaminant Monitoring Rule 3
UV_{254}	Ultraviolet Absorbance at Wavelength of 254nm
VIF	Variation Inflation Factor
VOC	Volatile Organic Compound

CHAPTER 1: INTRODUCTION AND OBJECTIVES

MOTIVATION

The removal of trace levels of organic contaminants from drinking water supplies has received increased public attention. Personal care products (PCPs), pharmaceuticals, pesticides, and endocrine disrupting compounds are some contaminant groups of concern that are present in drinking water supplies throughout the United States. Typically compounds in these contaminant groups occur at ng/L to µg/L levels (Boyd et al., 2003). Due to the minute levels of contamination, these organic pollutants have garnered the name micropollutants (MPs). Collectively, these compounds are important for human health because many MPs are toxic. Possible kidney, liver, cardiovascular, and reproductive problems can occur in humans when prolonged consumption of regulated MPs above the maximum contaminant level (MCL) occurs (EPA NPDWR 2012). Many MPs are not regulated by the United States Environmental Protection Agency (EPA), but possible additional and stricter regulations could be forthcoming.

Typically, micropollutants are not well removed by conventional drinking water treatment processes, such as coagulation, flocculation and sedimentation, and as a result additional treatment options must be explored (Corwin et al., 2012). One treatment option for the removal of MPs is granular activated carbon (GAC) adsorption. GAC has most commonly been used for the control of taste and odor compounds and more recently for the removal of natural organic matter (NOM)/disinfection byproduct (DBP) precursors

(Summers et al., 2011). GAC adsorber performance for MP removal depends on the chemical characteristics of the GAC surface, GAC pore size distribution and surface area, background water matrix, contaminant properties, and non-steady state mass transfer processes (Patni et al., 2008). Typically, design parameters for full-scale GAC adsorbers are derived from time consuming and expensive pilot tests. Results from pilot tests are also used to select GAC type (Crittenden et al., 1986). By maintaining the same GAC particle size, bed depth, and hydraulic loading rate, pilot testing effectively simulates full-scale GAC adsorber performance. Since particle size and hydraulic loading rate, and therefore empty bed contact time (EBCT) are kept constant between pilot and full scale adsorbers, contaminant breakthrough in the pilot occurs on the same time scale as at the full scale. As a result, pilot testing requires a large volume of water and is time consuming and expensive.

Studies have been conducted to find alternative ways to assess GAC adsorber performance in a more timely and cost effective manner. In response to this need, rapid small-scale column tests (RSSCTs) were developed by Crittenden et al (1986, 1987). By using principles of similitude, dimensionless parameters, are kept constant in field- and bench-scale adsorbers. By reducing GAC particle size at the bench-scale, adsorber performance evaluations can be conducted over a compressed time scale. Two common rapid small scale column test (RSSCT) design approaches that can be used to asses GAC service life and MP removal performance are the proportional diffusivity design (PD or PD-RSSCT) and the constant diffusivity (CD or CD-RSSCT) design. When NOM is present at concentrations that are substantially higher than those of the MPs, it has been suggested that the PD-RSSCT is more suitable to simulate MP removal (Corwin and Summers, 2009). The

CD-RSSCT, on the other hand, effectively simulates the removal of pollutants at higher concentrations from waters with low NOM concentrations (Crittenden et al., 1991; Summers et al., 1995). However, a scale-up approach for predicting MP removal from surface water has not been developed, to date.

RESEARCH OBJECTIVES

The main objectives of this research were to (1) conduct a pilot test to evaluate the effectiveness of GAC adsorption for the removal of MPs from coagulated surface water, (2) evaluate the two common RSSCT designs, the CD-RSSCT and the PD-RSSCT, for the predicting field-scale MP removal and, (3) develop a comprehensive scale up procedure that will ultimately save utilities time and money when determining GAC adsorber life and performance.

APPROACH

To meet the research objectives, the following tasks were completed:

1. Designed, built, and operated GAC pilot column at the Orange Water and Sewer Authority (OWASA) to evaluate the removal of 34 MPs.
2. Designed, built, and operated a PD-RSSCT to evaluate the removal of 34 MPs.
3. Designed, built, and operated a CD-RSSCT to evaluate the removal of 34 MPs.

4. Analyze pilot and RSSCT data set to develop a scale-up approach that permits the prediction of field-scale GAC performance from RSSCT data

The pilot test for the evaluation of the removal of 34 MPs was performed at the drinking water treatment plant of the Orange Water and Sewer Authority (OWASA) in Carrboro, North Carolina. Corresponding RSSCTs were conducted at North Carolina State University. MPs were spiked into coagulated and settled surface water, and targeted influent MP concentrations ranged from 10 to 500 ng/L in all tests. The same bituminous coal based GAC was used for the pilot test and the RSSCTs. The pilot column was operated at an EBCT of 7 minutes for 120,000 bed volumes (1.6 years). The corresponding PD-RSSCT was operated for 350,000 bed volumes (8 months), and the CD-RSSCT was operated for 250,000 bed volumes (2 months). Pilot and RSSCT data were described with the pore surface diffusion model (PSDM) to determining GAC service life and to calculate parameters of GAC scale-up.

CHAPTER 2: BACKGROUND

MICROPOLLUTANTS (MPs)

Over 84,000 chemicals are currently in the commercial market place and approximately 700 new chemicals are introduced into the market annually (EPA, 2010). The database CAS REGISTRY, which has been produced by the Chemical Abstracts Service since 1907, currently contains more than 33 million organic and inorganic substances (Binetti et al., 2008). An exponential increase in the number of new chemicals synthesized and added to the database has been occurring over the last several years (Binetti et al., 2008). As such, the occurrence of micropollutants being released into the environment has also increased. Sources of MPs in surface waters include run-off from agricultural lands, sewer leaks, and wastewater discharges. Water contaminated with micropollutants can threaten human and aquatic life. For example, feminization of fish from increased levels of hormone and endocrine disrupting compounds in surface waters is one well documented example of a harmful impact MPs can have on the environment (Baynes et al., 2012).

Table 2.1: Study Micropollutants

Pharmaceutical	**Antibiotic, Antimicrobial**	**Hormone, Endocrine Disrupting Chemical**	**Herbicide**	**Insecticide**
Acetaminophen	Erythromycin	Bisphenol A	2,4-D	Aldicarb
Carbamazepine	Sulfamethoxazole	Ethinyl estradiol (EE2)	Acetochlor	Carbaryl
Diclofenac	Triclosan		Atrazine	Chlorpyrifos
Gemfibrozil	Trimethoprim		Clofibric acid	Diazinon
Ibuprofen			Diuron	Dimethoate
Naproxen			Metolachlor	Malaoxon
Warfarin			Molinate	Methomyl
			Prometon	
			Simazine	
Nicotine Metabolite	**Stimulant**	**X-Ray Contrast Agent**	**Taste and Odor**	**Flame Retardant**
Cotinine	Caffeine	Iopromide	Methylisoborneol	Tributyl Phosphate

Regulations

Information regarding the potential hazards is relatively unknown for many MPs. “Minimal toxicity data” are available for about a quarter of the US High Production Volume (HPV) chemicals. Acute and chronic toxicity, developmental and reproductive toxicity, mutagenicity, ecotoxicity, and environmental fate are some of the categories included in the “minimal toxicity data” set. The remaining 75% of the chemicals have even less data and information available.

In this research 34 MPs were studied (Table 2.1).

Based on current research and toxicity reports, the U.S. EPA has established Maximum Contaminant Levels (MCLs) for four of the MPs evaluated in this research (Table 2.2). MCLs are established under the Safe Drinking Water Act (SDWA) and indicate the maximum allowable level for a compound in drinking water and are enforceable by law. The MCLs aim to meet the Maximum Contaminant Level Goal (MCLG), which is defined as the level of contamination which has no known or anticipated human health effects. Apart from MCLs, Table 2.2 summarizes the potential health effects for the four regulated MPs.

Table 2.2: Regulated MPs

Compound	**MCL (mg/L)**	**Potential Health Effects from Long-Term exposure above the MCL**
2,4-D	0.07	Kidney, Liver and Adrenal Gland Problems
Aldicarb	0.003	Neurological Problems
Atrazine	0.003	Cardiovascular and Reproductive System Problems
Simazine	0.004	Blood problems

Source: National Primary Drinking Water Regulations: List of DW Contaminants and MCLs (EPA 2012)

Even though many of the MPs in this study are not currently regulated by federal standards, future EPA regulations on emerging trace organic contaminants are expected. Six of the MPs studied in this research have been placed on the third Contaminant Candidate List (CCL3) as shown in Table 2.3, and thus are being considered for future regulation (EPA 2012, a). Additionally, the Unregulated Contaminant Monitoring Rule 3 (UCMR3) includes EE2 from the list of MPs studied in this research. The UCMR3 requires potable water systems to

monitor contaminants placed on the list from January 2012 through December 2015 to ascertain if future regulations will be necessary (EPA 2012, b).

Table 2.3: CCL3 Compounds

Compound	**Potential Health Effects**
Acetochlor	Probable human carcinogen, thyroid disrupter
Diuron	Liver problems, cell necrosis
Erythromycin	Gastrointestinal and cardiovascular problems
Ethinyl estradiol	Endocrine system problems
Metolachlor	Kidney and liver problems, cardiovascular and nervous systems problems
Molinate	Reproductive system problems

Additionally initiatives to determine safe levels of MPs have been conducted to ascertain allowable daily intakes (ADIs) and drinking water equivalent levels (DWELs). ADIs are the amounts of a specific substance that be ingested on a daily basis over a lifetime without an appreciable health risk. DWELs are the lifetime health advisory that is obtained from the contaminants reference dose and incorporates a drinking water relative source contribution that accounts for the total exposure from all possible sources (EPA 2012, c). ADIs and DWELs for some of the MPs in this research are shown in Table 2.4.

Table 2.4: MP Allowable Daily Intakes and Drinking Water Equivalent Levels

Compound	ADI (µg/kg-day)	DWEL (µg/L)
Acetaminophen	340	12,000
BPA	50	1,800
Caffeine	2,500	87,500
Carbamazepine	0.34	12
Diclofenac	67	2,300
Diuron	2	70
Gemfibrozil	1.3	46
Ibuprofen	0.97	34
Simazine	--	4
Sulfamethoxazole	510	18,000
Triclosan	75	26,000

MP Removal by Activated Carbon Adsorption

Granular activated carbon adsorption has been proven as an effective treatment option for the removal of trace organic contaminants from drinking water sources. Within adsorption processes, the carbon is referred to as the adsorbent and the contaminant is referred to as the adsorbate. Carbon is an effective adsorbent because it is a highly porous material with a large internal surface area. Carbon is a heterogeneous adsorbent that contains a range of pore sizes. Micropores are less than 20 Å (2 nm) in width and are the principal location for MP adsorption. Mesopores are between 20 Å (2 nm) and 500 Å (50 nm) in width and facilitate adsorbate diffusion to the adsorption sites. When contaminants move through a GAC bed, they diffuse into the carbon pores and adsorb to the internal structure of the carbon (Crittenden et al., 2005). GAC adsorption occurs in four key steps (Figure 2.1 through Figure 2.4). In the first step the adsorbate, diffuses through the bulk liquid to the film surrounding the GAC grain. Second, film mass transfer occurs when the adsorbate passes through the

liquid film surrounding the GAC particle to the carbon surface. Next, intraparticle diffusion occurs. Intraparticle diffusion can consist of both pore diffusion and surface diffusion. These two diffusion processes dictate the rate at which the MP travels to the adsorption site within the carbon pore. With pore diffusion, the MP travels directly through the pore water to the adsorption site. With surface diffusion, the MP travels along the surface of the pore until it reaches the final adsorption site (Knappe, 1996).

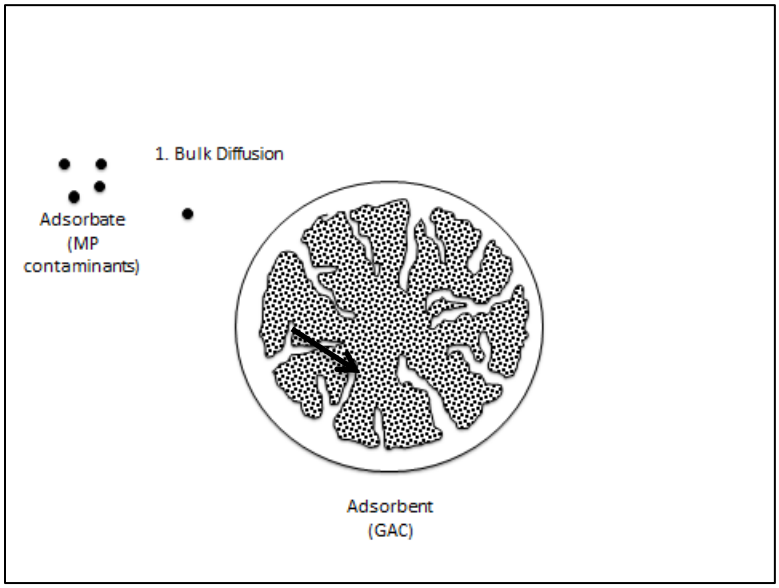

Figure 2.1: Bulk Diffusion

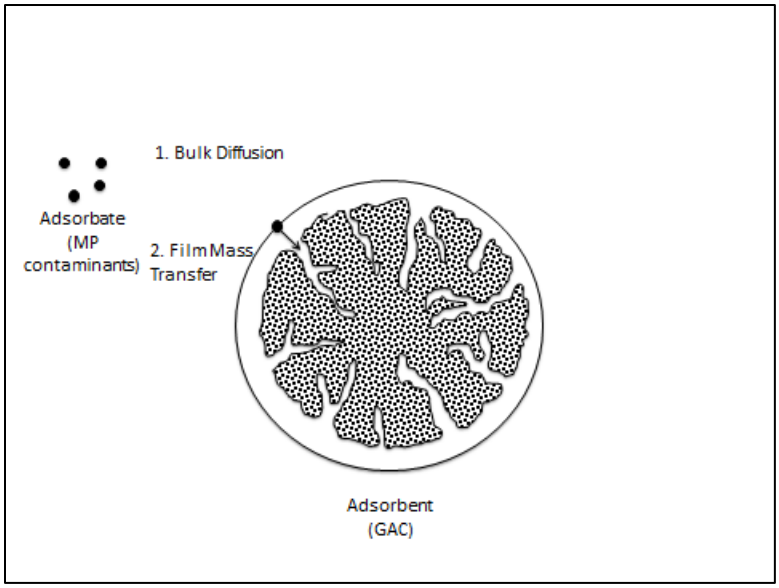

Figure 2.2: Film Mass Transfer

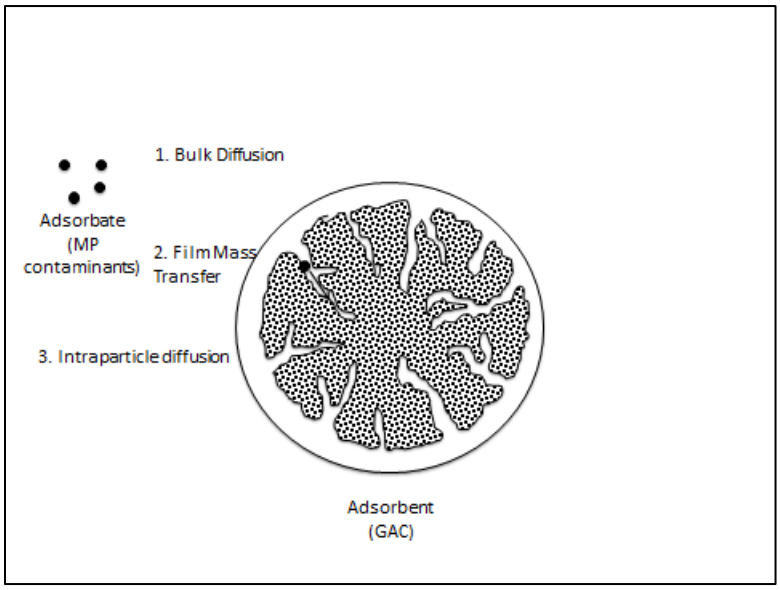

Figure 2.3: Intraparticle Diffusion

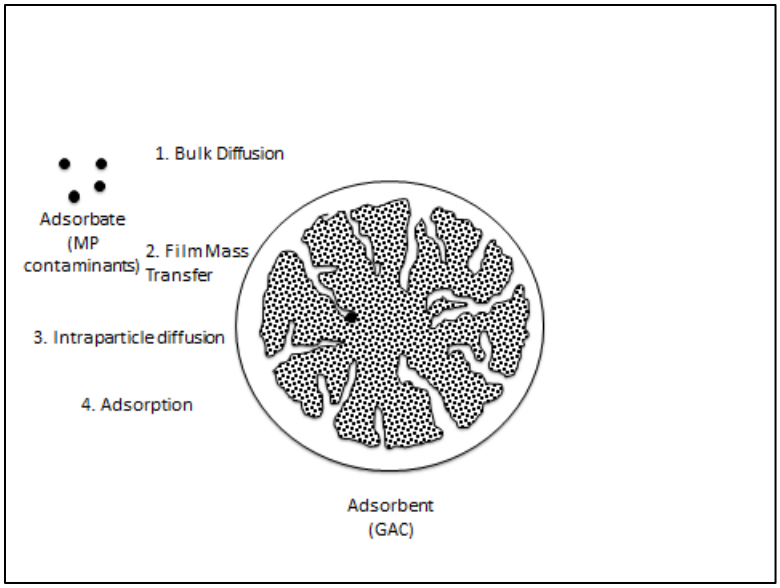

Figure 2.4: Adsorption

In single adsorbers or adsorbers in series the mass transfer zone (MTZ) of the adsorbate moves through the GAC bed as the influent end of the adsorber becomes saturated with adsorbate. Eventually, the MTZ of the adsorbate moves far enough to the bottom reaches of the filter such that measurable concentrations of adsorbate are observed in the effluent and breakthrough occurs. As the MTZ leaves the GAC adsorber, MP concentrations in the GAC adsorber effluent increases. Once the breakthrough concentration of a MP reaches a predetermined level, the GAC in the adsorber must be replaced (Dyksen et al., 1995). A typical breakthrough curve for a MP leaving a GAC column is shown in Figure 2.5.

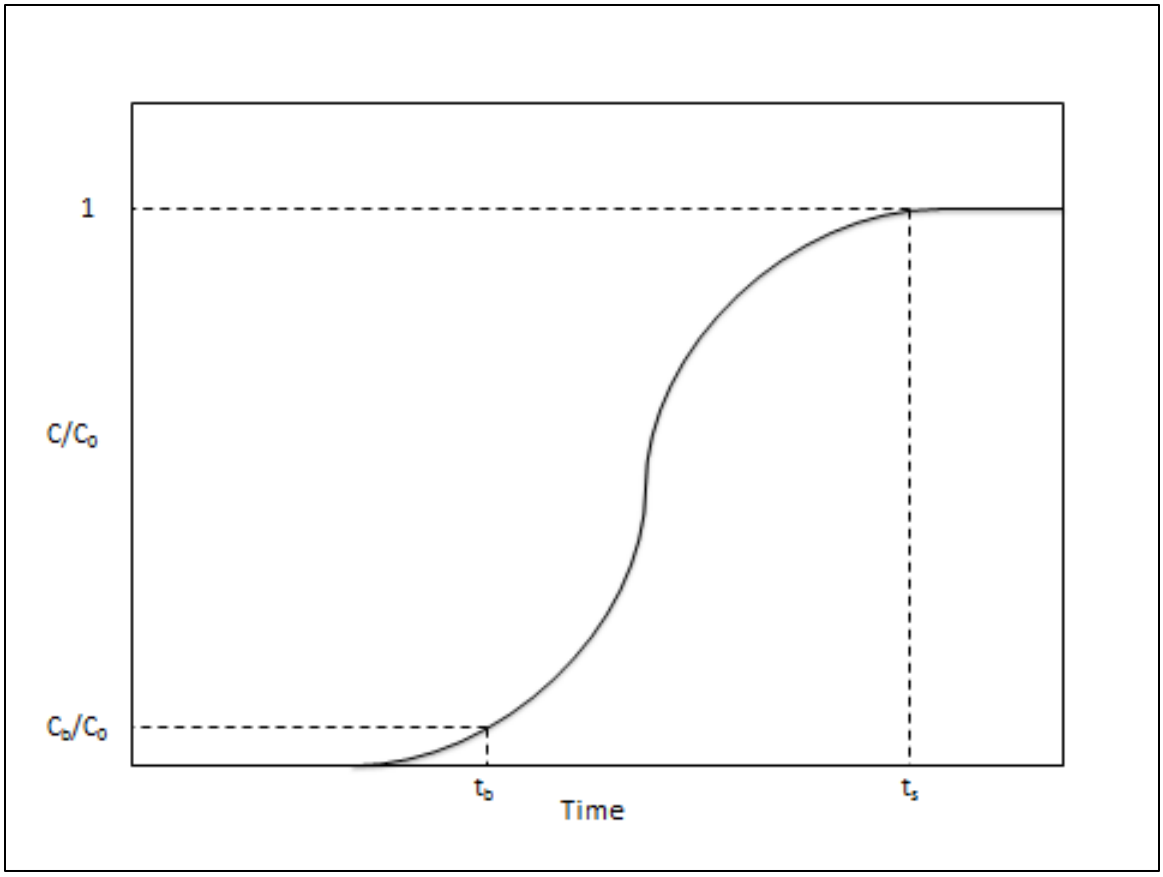

Figure 2.5: Micropollutant Breakthrough Curve

In Figure 2.5, C is the effluent concentration, C_0 is the initial influent concentration, and C_b is the breakthrough concentration at which the GAC needs to be replaced, t_b is the time to a target level of MP breakthrough (i.e. a certain percentage of the influent concentration, the MCL of a regulated MP, or the reporting limit of an analytical method), and t_s is the time to saturation.

GAC adsorber performance for MP removal from surface waters is strongly impacted by natural organic matter (NOM) adsorption. NOM preloading occurs when the mass transfer zone of NOM moves through the fixed bed at a faster rate than the target compound(s) and

loads the carbon ahead of the MTZ of the target compound, as shown in Figure 2.6 (Kilduff et al., 2002). NOM preloading has two effects: (1) direct competition for adsorption sites, which decreases the adsorption capacity for MPs and (2) pore blockage and restriction, which decreases the rate of MP adsorption. MP breakthrough will occur with or without NOM, but in the presence of NOM, MP breakthrough occurs faster because of the two NOM preloading effects. A small, strongly adsorbing fraction of NOM directly competes for MP adsorption sites (Summers, Knappe, and Snoeyink, 2010). Therefore, a larger, weakly adsorbing fraction of NOM blocks pores and slows MP adsorption kinetics (Summers, Knappe, and Snoeyink, 2010). Adsorption of NOM continually decreases the GAC adsorption capacity for MPs. The NOM concentration in a GAC adsorber is typically highest near the influent end of the filter adsorber and then gets progressively lower towards the effluent side of the filter. Therefore, the effluent end of the adsorber initially has larger remaining capacity to adsorb MPs. Over time, as the filter run continues, the NOM concentration becomes uniform throughout the GAC filter and therefore reduces MP adsorption capacity throughout the entire bed (Summers, Knappe, and Snoeyink, 2010). Additionally, the presence of NOM has been shown to nearly eliminate the surface diffusion aspect of adsorption and increase the length of the path each adsorbate takes to reach an adsorption site (Dyksen et al., 1995). NOM effect on carbon pores and therefore GAC effectiveness and life is shown in Figure 2.6.

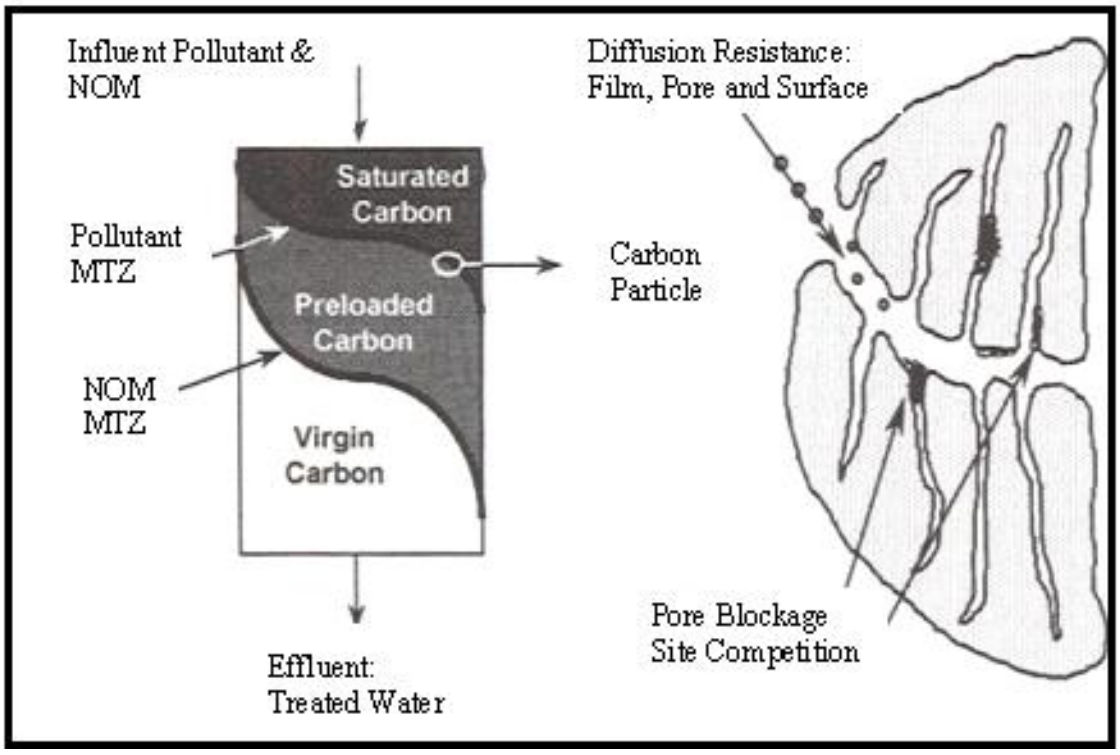

Source: Kilduff et al., 2002
Figure 2.6: NOM Preloading

Because of the shape of the MTZ, not all of the GAC will be saturated at the targeted breakthrough concentration (C_b). This inefficiency can be minimized by operation GAC adsorbers in series or in parallel. Furthermore, if only a single GAC filter is available, shutdown of the treatment system is required until new or regenerated carbon can be replaced into the adsorber (Creek and Davidson, 2000).

Biodegradation of Micropollutants

Previous research has indicated that some micropollutants are susceptible to biodegradation within biologically active filters (Zearley et al., 2012). Biodegradation of MPs occurs either through catabolism or cometabolism. With catabolism, the MPs are the primary substrate used by the microorganisms in the filter to obtain energy. With cometabolism, the biodegradable fraction of dissolved organic matter (DOM) is the primary substrate for the microorganisms, and the MPs are secondary substrates that are only broken down if DOM is present. Four trends of biodegradation have been identified for micropollutants: (1) steady state removal throughout the filter, (2) increasing removal to steady state (acclimation) throughout the filter, (3) decreasing removal throughout the filter over time, and (4) no removal within the filter (Zearley et al., 2012). Additionally, removal rates have been categorized into four types: (1) recalcitrant which indicates less than 15% removal, (2) slow biodegradation which indicates 15-50% removal, (3) fast biodegradation which indicates 50-85% removal, and (4) very fast biodegradation which indicates greater than 85% removal (Zearley et al., 2012). The biodegradation classification of the MPs selected in this research is shown in Table 2.5.

Table 2.5: Biodegradation Classification of MPs

Contaminant	Biodegradation Classification*
2,4-D	Fast
Acetaminophen	Fast
Acetochlor	Recalcitrant
Aldicarb	Slow
Atrazine	Recalcitrant
Bisphenol A (BPA)	Very Fast
Caffeine	Fast
Carbamazepine	Recalcitrant
Carbaryl	Recalcitrant
Chlorpyrifos	Fast
Clofibric Acid	Slow
Cotinine	Slow
Diazinon	Recalcitrant
Diclofenac	Slow
Dimethoate	Fast
Diuron	Recalcitrant
Erythromycin	N/A
Ethinyl Estradiol (EE2)	Recalcitrant
Gemfibrozil	Fast
Ibuprofen	Very Fast
Iopromide	Recalcitrant
Malaoxon	Slow
Methomyl	Recalcitrant
Metolachlor	Recalcitrant
Methylisoborneol (MIB)	Very Fast
Molinate	Very Fast
Naproxen	Fast
Prometon	Recalcitrant
Simazine	Recalcitrant
Sulfamethoxazole	Recalcitrant
Tributyl Phosphate	Slow
Triclosan	Very Fast
Trimethoprim	Very Fast
Warfarin	Slow

*Classifications from Zearley et al. (2012)

MIB and endocrine disrupting compounds have been shown to degrade in biologically active filters (Elhadi et al., 2006, McDowell et al., 2007, Westerhoff et al., 2005), and Zearley et al. (2012) confirmed that these compounds are rapidly biodegraded. Based on the findings of Zearley et al. (2012), 18% of the MPs studied exhibited very fast biodegradation, 21% fast biodegradation, and 21% slow biodegradation. Furthermore, 38% were recalcitrant. In order to achieve steady-state levels of MP degradation in a biologically active filter, an acclimation period is necessary. The acclimation period is particularly important when MPs are degraded by cometabolism because the secondary substrate utilization requires the growth of microorganisms not initially present in the biofilter. Research is still ongoing to understand all aspects of the biodegradation of micropollutants.

PLACEMENT OF GAC ADSORBERS IN SURFACE WATER TREATMENT PLANTS

Both upflow and downflow GAC contactors are common in water treatment. Upflow contactors are more prevalent in wastewater treatment and downflow contactors are common to drinking water treatment. Downflow adsorbers can be further split into two designs: gravity-driven GAC adsorbers and pressure-driven GAC adsorbers. The choice between implementing a gravity system or a pressure system is largely driven by cost. Gravity-driven systems are often used for large surface water treatment plants in order to reduce the construction cost and footprint. Pressure driven system are typically used for smaller treatment plants and wellhead treatment in groundwater systems. Additionally, GAC filters

can be operated as filter adsorbers or post-filter adsorbers. Figure 2.7 illustrates the treatment train placement options for filter adsorbers and post-filter adsorbers.

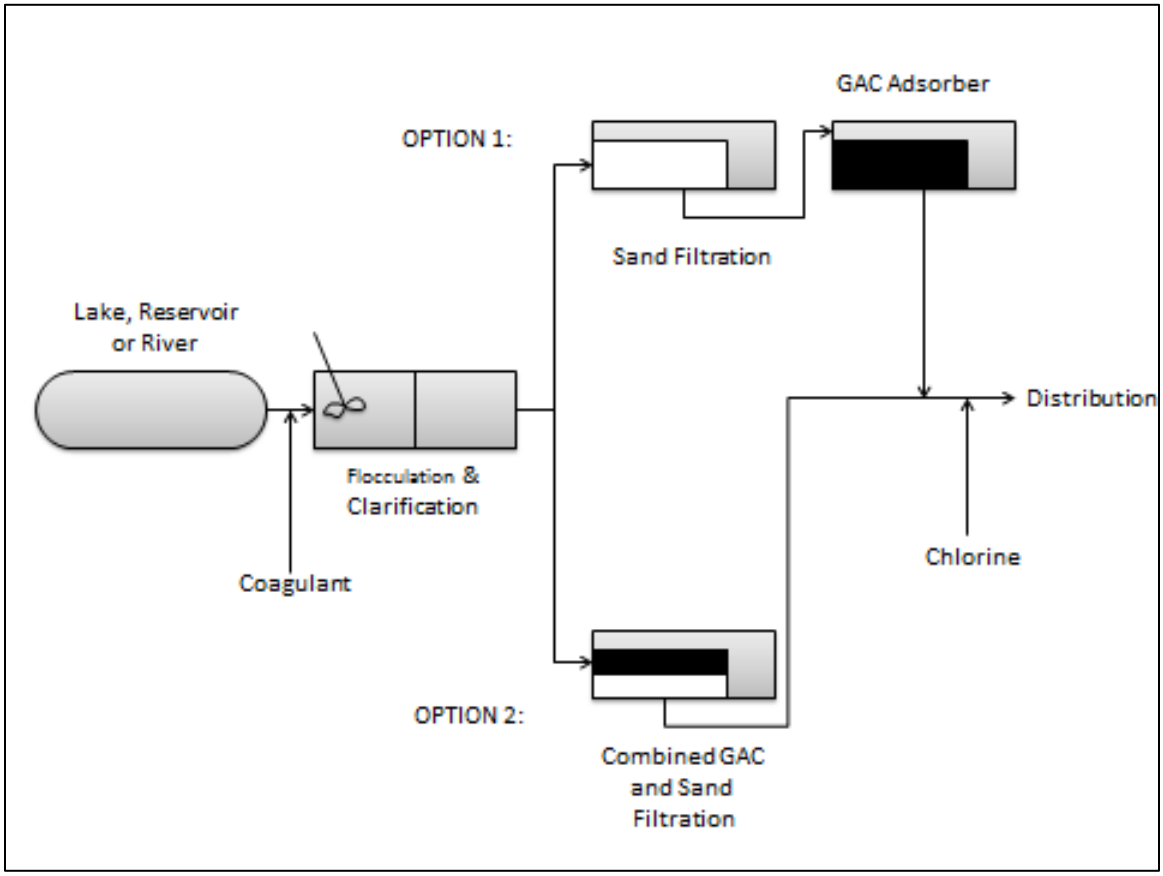

Figure 2.7: GAC Contactor Placement Options in Treatment Train

Option 1 in Figure 2.7 is the post-filter adsorber and option 2 is the filter adsorber. Filter-adsorbers function to remove both turbidity and dissolved organic chemicals, including micropollutants. Filter adsorbers have a typical EBCT of 5-10 minutes require frequent backwashing. Post-filter adsorbers are designed and operated to primarily remove organic

chemicals and have an EBCT of 10-20 minutes (Owen 1998). Only light and infrequent backwashing is required for post-filter adsorbers.

DESIGN OF ACTIVATED CARBON ADSORBERS

When designing GAC adsorbers several important factors must be taken into consideration. GAC base material, GAC size, EBCT, and backwashing all impact the performance of the GAC contactor. GAC prepared from base materials such as lignite, bituminous coal, wood and coconut can be utilized. Bituminous coal-based GAC has been used for NOM and micropollutant control in surface waters. Coconut shell-based GAC can be effective for removing contaminants with low molecular weights (i.e. VOCs) from groundwater and lignite-based GAC is often used for taste and odor control. Lastly, wood-based GAC is often used for biologically active carbon filters that need to support biological growth (Summers et al., 2011, Fotta, 2012). Particle size of the GAC also plays an important role in adsorption efficiency (Summers, Knappe, and Snoeyink, 2010). U.S. Standard Mesh sizes of 12x40 and 8x30 are common in in full-scale GAC adsorbers. A mesh size of 12x40 equates to GAC particle sizes between 0.425 and 1.70 mm, and 8x30 equates to carbon particles sizes between 0.60 and 2.36 mm. The smaller the particle size, the faster the rate of adsorption kinetics and the later the onset of contaminant breakthrough. But a smaller particle size also increases head loss within the filter, which may require more frequent backwashing and therefore reduce net water production. The available head as well as required net water production may dictate which particle size is used (Summers et al., 2011).

The EBCT is also important to GAC adsorber design. The EBCT typically ranges from 5 to 30 minutes when designing GAC adsorbers for the control of synthetic organic compounds (Crittenden et al., 2005). Short EBCTs lead to high carbon usage rates and increasing the EBCT lowers carbon usage rates in a nonlinear manner. Higher carbon usage rates mean that more frequent GAC regeneration or replacement is needed (i.e. operation and maintenance costs increase). For MP removal, very long EBCTs can lead to increased NOM fouling and higher carbon usage rates. Therefore, the carbon adsorber should be designed and operated at an optimal EBCT established from pilot studies (Roberts and Summers, 1982).

Backwash frequencies should also be considered for the design and operation of carbon adsorbers (Summers et al., 2011). Utilities backwash filters to remove trapped particles and reduce headloss that builds up during a filter run. Backwashing expands and mixes the bed. Mixing the bed can cause contaminants to desorb from GAC particles that were initially within or above the mass transfer zone of the contaminant but migrated below the mass transfer zone after backwashing (Summers et al, 2011). In that case, there is a higher MP concentration on the carbon surface than what would be expected based on the MP concentration in the water, thus potentially creating a concentration gradient that favors desorption (Corwin and Summers, 2011). Desorption, however, does not always occur. Corwin and Summers (2010) showed that backwashing RSSCTs did not result in MP desorption. If displacement does occur for certain compounds it can lead to higher than anticipated effluent concentrations, but appropriately timed backwashing and carbon replacement or reactivation can alleviate this problem. Furthermore, for carbon adsorber design, levels of removal efficiency must also be balanced with cost.

RAPID SMALL SCALE COLUMN TESTS (RSSCTS)

RSSCT Design

The RSSCT was first developed by Crittenden et al. (1986, 1987) to rapidly evaluate GAC life and effectiveness at the bench-scale. There are three primary advantages for using RSSCTs as opposed to pilot testing. First, RSSCTs can be completed in a fraction of the time, secondly, these tests do not require extensive isotherm or kinetic studies to obtain a full-scale performance prediction, and finally RSSCTs utilize a much smaller volume of water (Sontheimer et al., 1988). One disadvantage of RSSCTs is that they do not reflect (1) long-term capacity reductions due to background organic matter fouling, (2) biological removal of NOM or MPs, or (3) seasonal trends due to the shorter run time. RSSCTs conducted over several different seasons can be used to approximate seasonal trends that affect GAC performance (Sontheimer et al., 1988). Mass transfer models serve as the basis for scaling down full-scale GAC adsorbers to the bench-scale. In order to maintain perfect similarity between the full-scale and small-scale columns, Crittenden et al. (1986) stipulated that the dimensionless pore solute distribution parameter (D_g), pore diffusion modulus (Ed), surface diffusion modulus (Ed_S), Peclet number (Pe), and the Stanton number (St) have to be kept constant (Table 2.6).

Table 2.6: Dimensionless Parameters for RSSCT Design

Parameter	Equation	Equation Number
Pore solute distribution parameter	$D_g = \frac{\varepsilon_p(1-\varepsilon)}{\varepsilon}$	(2.1)
Pore diffusion modulus	$Ed = \frac{4D_p \times D_g \times t}{d_p^2}$	(2.2)
Surface diffusion modulus	$Ed_s = \frac{4D_s \times C_F \times t}{d_p^2}$	(2.3)
Peclet number	$Pe = \frac{L \times v}{D_x}$	(2.4)
Stanton number	$St = \frac{2k_f \times (1-\varepsilon) \times t}{d_p \times \varepsilon}$	(2.5)

The necessary parameters to calculate the dimensionless groups in Table 2.6 are the intraparticle porosity (ε_p), bed porosity (ε), pore diffusion coefficient (D_p), fluid residence time in packed bed (t), particle diameter (d_p), surface diffusivity (D_s), capacity factor (C_F), bed length (L), fluid velocity (v), dispersion coefficient (D_x), and film mass transfer coefficient (k_f). The capacity factor (C_F) is determined from the following equation:

$$C_F = \frac{q_0 \times \rho_b}{C_0 \times \varepsilon} \tag{2.6}$$

Where q_0 is the solid phase concentration in equilibrium with the influent aqueous phase concentration C_0, and ρ_b is the apparent bed density.

The Biot number is also an important parameter that ideally is kept constant between the large and small column. The Biot number (Bi) is used to determine the relative importance of the internal or external mass transfer resistance:

$$Bi = \frac{k_f \times d_p \times \tau}{2D_L \times \varepsilon_p} \tag{2.7}$$

Where τ is tortuosity and D_L is the diffusivity of the target compound in water (Sontheimer et al., 1988). Biot numbers are calculated for both surface diffusion (Bi_S) and pore diffusion (Bi_P) and then compared to one another to determine which type of adsorption controls the overall adsorption rate. For internal diffusion to control the adsorption rate, Bi must have a value greater than 100 (Sontheimer et al., 1988).

Since RSSCTs are conducted with crushed and sieved GAC and pilot tests with the as-received carbon, several equations were developed to relate the design of the large column to that of the small column. The essential RSSCT design equations are shown in Table 2.7.

Table 2.7: Essential RSSCT Design Equations

Parameter	Equation	Relationship
Scaling Factor (SF)	$SF = \left[\frac{d_{p,LC}}{d_{p,SC}}\right]$	Provides initial basis for bench scale design dependence on GAC particle diameters
Diffusion Coefficients (D)	$D_{SC} = \left[\frac{d_{p,SC}}{d_{p,LC}}\right]^{X} D_{LC} = [SF]^{-X} D_{LC}$	Dependence of intraparticle diffusivity on particle size
Empty Bed Contact Time (EBCT)	$\frac{EBCT_{SC}}{EBCT_{LC}} = \left[\frac{d_{p,sc}}{d_{p,LC}}\right]^{2} \times \left[\frac{D_{LC}}{D_{SC}}\right]$	Empty bed contact time is related to the size of GAC in each adsorber and the dependence of intraparticle diffusivity on particle size
Design Factor (DF)	$\frac{EBCT_{SC}}{EBCT_{LC}} = \left[\frac{d_{p,sc}}{d_{p,LC}}\right]^{2-X} = \left[\frac{t_{SC}}{t_{LC}}\right] = [SF]^{X-2} = DF$	Provides relationship between scaling factor, empty bed contact time, intraparticle diffusivity, and times to run the large column and small column

The parameters required in the RSSCT design equations (Table 2.7) include the GAC particle diameter (d_p) for the large column (subscript LC) and the small column (subscript SC), intraparticle diffusivity (D), diffusivity factor (X), and empty bed contact time (EBCT).

There are two common RSSCT design approaches, the constant diffusivity (CD) approach and the proportional diffusivity (PD) approach. In the CD-RSSCT design, the diffusivity factor, X, is equal to zero; i.e., intraparticle diffusivity does not depend on GAC particle diameter. Therefore the design factor for the CD-RSSCT becomes:

(2.8)

$$DF = SF^{-2}$$

The CD-RSSCT is used when target compounds are present at higher concentration and when little background natural organic matter is present (e.g. low TOC groundwater).

On the other hand, intraparticle diffusivity is assumed to be directly proportional to GAC particle size for the PD-RSSCT design approach. As a result, the diffusivity factor, X, is equal to 1, and the design factor becomes:

(2.9)

$$DF = SF^{-1}$$

The PD-RSSCT design is used to simulate NOM adsorption and may also offer advantages for simulating MP removal in the presence of NOM (Corwin and Summers, 2009). The PD-RSSCT design equations result in long columns and thus large head loss and large water requirement (Crittenden et al., 1987). Therefore the following additional equation, which introduces the minimum Reynolds number (Re_{min}), is typically used to reduce the column length and hydraulic loading rate.

(2.10)

$$\frac{v_{SC}}{v_{LC}} = \left[\frac{d_{p,LC}}{d_{p,SC}}\right] \times \left[\frac{Re_{Sc,min}}{Re_{LC}}\right]$$

Recommended minimum Reynolds numbers range from 0.023 to 0.13 for organic chemicals and NOM and are dependent on the molecular weight of the target compounds (Crittenden et al., 1987). The equations used to calculate $Re_{sc,min}$ are as follows:

(2.11)

$$Re_{SC,min} = \frac{500}{S_c}$$

Where S_C is the Schmidt number

(2.12)

$$S_c = \frac{v}{D_L}$$

In Equation 2.12, *v* is the kinematic viscosity and D_L is the diffusivity of the smallest target compound in water. D_L (cm^2/s) is calculated using the following equation (Crittenden et al., 1989):

(2.13)

$$D_L = \frac{1.326 \times 10^{-3}}{u^{1.14} \times V_b^{0.589}}$$

where u is the dynamic viscosity (centipoise) and V_b is the molal volume at the normal boiling point (cm^3/gram-mole). V_b can be estimated from the McGowan Method, ChemSketch, or the Joback Group Contribution Method. The Joback Group Contribution Method was used for this research.

Fouling, based on the presence of NOM, is also an important factor to consider when scaling up RSSCT data. Fouling occurs when NOM reduces the adsorption capability of the GAC particles. It has been hypothesized that pore blockage as well as competition for adsorption sites by the NOM are the main mechanisms for decreased GAC effectiveness (Corwin and Summers 2010). As GAC pore size increases NOM fouling increases due to the increased percentage of total surface area behind blocked pores. In order to account for the

fouling from NOM in the PD-RSSCT, Corwin and Summers (2010) introduced a fouling index. The fouling index is used to scale the bed volumes from the RSSCT to those expected at the field-scale. The fouling index can be calculated by the following equation:

$$Fouling\ Index = SF^{Y} = \left[\frac{d_{p,LC}}{d_{p,SC}}\right]^{Y} \tag{2.14}$$

The bed volumes for the field scale adsorber can be scaled by using the fouling index:

$$\#BVs_{pilot\ scale\ predicted} = \frac{\#BVs_{RSSCT}}{Fouling\ Index} = \frac{\#BVs_{RSSCT}}{SF^{Y}} \tag{2.15}$$

Where Y is the fouling factor in Equation 2.14 and Equation 2.15.

To date, two hypotheses have been developed regarding factors that control the magnitude of Y. Corwin (2010) proposed that the magnitude of Y increases as the ratio of the influent MP concentration to influent DOC concentration decreases. Fotta (2012), on the other hand, suggested that Y increases as the octanol-water partition coefficient (Log K_{OW}) of the target compound increases.

PORE SURFACE DIFFUSION MODEL (PSDM)

Both pore diffusion and surface diffusion can occur in parallel within GAC particles. Therefore, a combination of pore and surface diffusion is used to describe breakthrough curves obtained from field-scale adsorbers and RSSCTs. The PSDM in AdDesignS is a finite

element model that is commonly used to describe contaminant breakthrough curves. Required input parameters include adsorbate properties, adsorbent properties, kinetic parameters, and equilibrium parameters. Adsorbate properties can be entered manually, or, for certain adsorbates, the properties can be imported from the Software to Estimate Physical Properties (StePP) database. The entire set of inputs for the PSDM model is shown in Table 2.8.

Table 2.8: PSDM Inputs

Type	Parameter	Notes
Water Properties	Pressure	Entered manually or keep default values
	Temperature	
Adsorbate Properties	Name	Entered manually or imported through StEPP Export File.
	Molecular Weight	
	Molar Volume at Normal Boiling Point	
	Boiling Point	
	Initial Concentration	
	Liquid Density	
	Solubility	
	Vapor Pressure	
	Refractive Index	
	CAS Number	
Equilibrium Parameters	Freundlich K	Entered manually or estimated within AdDesignS
	Freundlich 1/n	
Kinetic Parameters	Tortuosity (τ)	Entered manually or estimated within AdDesignS
	Surface-to-Pore-Diffusion Flux Ratio (SPDFR)	
	Film Mass Transfer Coefficient	
Fixed Bed Properties	Bed Length	Entered manually or chosen from an adsorber database
	Bed Diameter	
	Bed Mass	
	Flow Rate	
	EBCT	
	Apparent Bed Density	
	Bed Porosity	
	Superficial Velocity	
	Intersitial Velocity	
Adsorbent Properties	Name	Entered manually or chosen from an adsorbent database
	Apparent Particle Density	
	Particle Radius	
	Particle Porosity	
	Particle Shape Factor	
Simulation Parameters	Total Run Time	Entered manually or keep default values
	First Point Displayed	
	Time Step	
	Number of Axial Elements	
Number of Collocation Points	Axial Direction	Entered manually or keep default values
	Radial Direction	

The output from PSDM describes the normalized effluent concentration (C/C_0) of the target compound(s) as a function of GAC service time, bed volumes treated, and specific throughput.

LINEAR FREE ENERGY RELATIONSHIPS (LFERS) AND ABRAHAM DESCRIPTORS

Intermolecular interactions play an important role in GAC adsorption. In GAC adsorber systems, adsorptive exchange of an MP from the aqueous phase to a condensed phase (micropore filling) as well as to an adsorbed phase (surface adsorption) is possible. The reverse of the two scenarios, i.e. desorption, is also possible. In order to understand the possible molecular interactions between the organic MP and the carbon surface, a thorough understanding of the strength and type of bonds formed and broken is necessary. One parameter used to understand intermolecular interactions is the partitioning coefficient in two-phase systems, K_{12}, where subscript 1 indicates the first phase and subscript 2 indicates the second phase. The magnitude of K_{12} relative to a reference compound is indicative of which types of intermolecular interactions are important.

One approach to predict the behavior of MPs is the development of quantitative structure-property relationships (QSPRs). A QSPR is a mathematical relationship between the structure of a compound, as expressed by compound-specific descriptors, and the property being determined (e.g., partitioning coefficient). Linear free energy relationships (LFERs) are one example of QSPRs. This empirical approach is used to predict and evaluate

partition coefficients of organic compounds in different two-phase systems. The most common approach used for LFERs is to express the unknown free energy transfer of a given compound in the two-phase system of interest by one or several other known free energy terms. LFERs can be single-parameter or multi-parameter relationships that take into consideration the types of molecular interactions and the factors that determine the free energy cost of sorption site formation. The Abraham descriptors or organic compounds are commonly used to predict partition coefficients. The five Abraham descriptors, from which LFERs are developed, are shown in Table 2.9.

Table 2.9: Abraham Descriptors and Definitions

Descriptor Definition	Dipolarity/ Polarizability	Hydrogen Bonding Acidity	Hydrogen Bonding Basicity	McGowan Molecular Volume	Gas-Hexadane Partition Coefficient	Excess Molar Fraction
Old Symbol	π^*	α	β	V_w	--	--
New Symbol	S	A	B	V	L	E

Polarizability, S, is the measure of the change in a molecule's electron distribution in response to an applied electric field, which can also be induced by electric interactions with solvents or ionic reagents. S is used to provide insight into a molecule's internal structure. The hydrogen bond acidity and basicity gives information about the compound’s solubility and permeability. Additionally, the A and B descriptors help to explain electron donor/acceptor and H bond donor/acceptor interactions. The molecular volume of a compound directly relates to its transport characteristics. The McGowan method is a

fragment contribution method that calculates the molecular volume (McGowan, 2010). The gas-hexadane partitioning coefficient indicates the affinity of a compound for the gas phase. Lastly, the excess molar fraction is the difference between the partial molar property of a component in a mixture and that of the pure component. The excess molar fraction gives information about how the compound will react in mixtures.

If a partitioning process deals with a transfer from the gas phase to a condensed phase the descriptor L is used in conjunction with descriptors S, A, B, and E in the following equation (Clark et al., 2009):

$$SP = c + eE + sS + aA + bB + lL \tag{2.16}$$

where SP is the equilibrium constant for a given partitioning process, c is the intercept, and e, s, a, b, and l are coefficients found by multiple linear regression. In partitioning processes concerning the transfer from one condensed phase to another, the descriptor V is used in conjunction with descriptors S, A, B, and E in the following equation (Clark et al., 2009):

$$SP = c + eE + sS + aA + bB + vV \tag{2.17}$$

where v is the coefficient for the McGowan molecular volume. Again, coefficients e, s, a, b, and v are determined by multiple linear regression. Equation 2.17 has typically been used to describe sorption processes (Sprunger et al., 2007, Eriksson et al., 2003, Walker et al., 2003, and Clark et al., 2009).

CHAPTER 3: MATERIALS AND METHODS

MATERIALS

Water

Coagulated, settled water from the Jones Ferry Water Treatment Plant (Carrboro, NC) was used in this study. This water is derived from the Orange Water and Sewer Authority (OWASA) Cane Creek Reservoir or University Lake. Typical raw water characteristics are shown in Table 3.1.

Table 3.1: Typical Raw Water Characteristics

Parameter	**Value**
pH	7.3
DOC	4.9 mg/L
UV_{254}	0.14 cm^{-1}
Alkalinity	37.0 mg/L as $CaCO_3$
Hardness	40.6 mg/L as $CaCO_3$
Bromide	15.9 µg/L

Source: Dunn, 2011

After coagulation, sedimentation, and cartridge filtration, the TOC concentration was 2 mg/L (range: 1.40 - 2.82 mg/L) and the pH was 6. The pilot influent water was pulled directly from the settling basin at OWASA and filtered through a 5-µm filter cartridge into two 100-gallon polyethylene barrels.

The coagulated and settled feed water for the RSSCTs was periodically collected from the settling basin at OWASA and filtered through a 5-µm filter cartridge on-site into polypropylene carboys. At the North Carolina State University Environmental Lab, the water was transferred into a 55-gallon stainless steel drum and stored at 4°C. The night before use, the RSSCT influent was pulled out of the 55-gallon stainless steel drum with a stainless steel hand pump and transferred to a glass carboy. The glass carboy was allowed to equilibrate to the laboratory temperature of 25ºC over night.

Adsorbates

In this study, 34 MPs were selected to evaluate GAC performance. MPs included pharmaceuticals, herbicides, endocrine disrupting compounds, insecticides, and a taste and odor compound. All 34 micropollutants and representative characteristics are summarized in Table 3.2.

Table 3.2: Micropollutants and Their Characteristics

Micropollutant	**Uses**	**Log K_{OW}****	**Log D (at pH 6 and 25°C)***	**pKa *****	**C_S* (g/L)**	**C_S^{pH6} * (g/L)**
2,4-D	Herbicide	2.94	-0.52	2.73	0.42	999
Acetaminophen	Antibiotic	0.0926	0.48	9.4	15	15
Acetochlor	Herbicide	3.15	3.05	-	0.70	0.70
Alidcarb	Insecticide	1.71	0.92	-	4.0	4.0
Atrazine	Herbicide	2.94	2.64	1.7	0.069	0.069
Bisphenol A	Hormone, Endocrine Disrupting Chemical	4.48	3.64	-	0.071	0.071
Caffeine	Stimulant	0.95	-0.63	<0	58	58
Carbamazepine	Pharm-aceutical	3.64	1.89	-	0.22	0.22
Carbaryl	Insecticide	2.94	2.34	-	0.11	0.11
Chlorpyrifos	Insecticide	6.34	5.00	-	1.63E-3	1.63E-3
Clofibric Acid	Herbicide	3.59	-0.34	-	0.56	1000
Cotinine	Nicotine Metabolite	1.02	0.05	-	23	23
Diazinon	Insecticide	4.74	3.77	-	0.022	0.022
Diclofenac	Pharm-aceutical	4.13	2.72	4.2	3.8E-3	2.30
Dimethoate	Insecticide	1.2	1.37	-	3.90	3.90
Diuron	Herbicide	2.72	2.68	-	0.56	0.56
Erythromycin	Antibiotic, Anti-microbial	-0.89	-0.12	8.88	37	420
Ethinyl Estradiol	Hormone, Endocrine Disrupting Compound	4.29	4.11	10.5	3.9E-3	3.9E-3
Gemfibrozil	Pharm-aceutical	4.45	3.03	4.5	0.063	11
Ibuprofen	Pharm-aceutical	3.56	1.91	4.9	0.19	68
Iopromide	X-Ray Contrast Agent	-1.17	-2.66	6.5	160	160

Table 3.2 Continued

Malaoxon	Insecticide	3.65	0.79	-	38	38
Methomyl	Insecticide	0.65	0.60	-	11	11
Metolachlor	Herbicide	3.17	3.03	-	0.51	0.51
Methylisoborneol	Taste and Odor Compound	3.00	-	-	2.2	2.2
Molinate	Herbicide	2.59	3.19	-	0.64	0.64
Naproxen	Herbicide	2.88	1.69	4.2	0.11	15
Prometon	Herbicide	2.92	2.86	4.30	0.59	0.59
Simazine	Herbicide	2.58	2.28	1.62	0.14	0.14
Sulfamethoxazole	Antibiotic, Antimicrobial	-0.0551	0.43	1.7	3.94	3.42
Tributyl Phosphate	Flame Retardant	6.55	3.83	-	0.64	0.64
Triclosan	Antibiotic, Anti-microbial	5.42	5.34	8.0	1.2E-3	1.3E-3
Trimethoprim	Antibiotic, Anti-microbial	0.70	-0.48	7.1	0.49	1.0
Warfarin	Pharma-ceutical	2.33	2.33	-	0.019	5.5

* From SciFinder
** From SPARC
*** From Rossner et al. (2009)

The CAS number, purity used, stock concentration, and target influent spiking concentrations of the 34 MPs are shown in Table 3.3.

Table 3.3: Adsorbate Characteristics and Spiking Amounts

Compound Name	CAS Registry Numbers	Purity	Stock Concentration (mg/L)	Influent Target Concentration (ng/L)
2,4-D	94-75-7	99.0%	1	100
Acetaminophen	103-90-2	99.0%	2	200
Acetochlor	34256-82-1	97.3%	2	200
Aldicarb	116-06-3	99.9%	2	200
Atrazine	1912-24-9	97.2%	0.1	10
Bisphenol A	80-05-7	99.0%	8000	500
Caffeine	50-08-2	100%	1	100
Carbamazepine	298-46-4	100%	1	100
Chlorpyrifos	2921-88-2	99.9%	1	500
Clofibric Acid	882-09-7	97.0%	2	200
Cotinine	486-56-6	98.0%	1	100
Diazinon	333-41-5	98.3%	1.5	10
Diclofenac	15307-86-5	99.0%	2	200
Dimethoate	60-51-5	99.4%	1	100
Diuron	330-54-1	99.5%	1	100
Ethinyl Estradiol	57-63-6	98.0%	8000	500
Erythromycin	114-07-8	100%	1	100
Gemfibrozil	25812-30-0	100%	2	100
Ibuprofen	158687-27-1	98.0%	5	200
Iopromide	73334-07-3	97.9%	5	500
Malaoxon	1634-78-2	93.0%	2	500
Methomyl	16752-77-5	99.9%	2	200
Metolachlor	51218-45-2	98.0%	2	200
MIB	2371-42-8	100%	1	200
Molinate	2212-67-1	98.6%	2	120
Naproxen	22204-53-1	99.9%	2	200
Prometon	1610-18-0	99.6%	1	100
Simazine	122-34-9	96.0%	0.5	50
Sulfamethoxazole	723-46-6	100%	2	200
Tributyl Phosphate	126-73-8	99.0%	1	100
Triclosan	3380-34-5	97.0%	8000	500
Trimethoprim	738-70-5	99.0%	1	100
Warfarin	81-81-2	99.0%	1	100

Granular Activated Carbon

Norit GAC1240 (bituminous coal-based, Norit Americas) was evaluated in this research. GAC properties are shown in Table 3.4. GAC was used in the as-received form (12x40 US Standard Mesh, d_p=0.92 mm) for the pilot test and was crushed and sieved for both the CD- and PD-RSSCTs. The 100 x 200 (d_p = 0.11 mm) and 60 x 80 (d_p = 0.21 mm) US Standard Mesh fractions were collected and used for the PD-RSSCT and CD-RSSCT experiments, respectively.

Table 3.4: GAC Characteristics

Carbon Characteristic	Value
Apparent Bed Density (g/mL)	0.45
Iodine Number (mg/g)	1079
Molasses Number	250
% Moisture (as packaged)	2
Abrasion Number (Ro-Tap)	77
% +12 Mesh	0.4
% - 40 Mesh	0.3

Pilot Test

The pilot test was designed and initiated by Mastropole (2011). The pilot column was operated from March 2011 through October 2012. During the pilot test, a total of 120,000 bed volumes were treated. A schematic of the pilot test is shown in Figure 3.1 The numbered components in Figure 3.1 are as follows (Mastropole, 2011):

1. 1 gallon glass volatilization trap (half full; spike to ~2*C_0)
2. 100 gallon polypropylene feed barrel (US Plastics 5319)

3. Valve (Swagelok SS-4P4T)
4. Teflon tubing with ¼” Swagelok stainless steel fittings
5. Pump (Cole Parmer 7523-70 drive and 7090-62 PTFE diaphragm pump head)
6. Pressure relief valve (Swagelok SS-RL3S4-MO)
7. 25 mm x 1200 mm glass chromatography column with epoxy coating (Ace Glass 5820-40)
8. 2” ID acrylic tubing (McMaster-Carr 8486K348) to protect glass column
9. Pressure gauge (Wika, 100 psi)
10. GAC filter to treat pilot column effluent (EBCT = 60 minutes, 4” ID acrylic pipe, McMaster-Carr 8486K578)
11. Plywood backboard
12. Norit GAC 1240 (bituminous coal-based, as-received grain size)
13. ~ 8 cm of 2 mm glass beads
14. Needle Valve (Swagelok (SS-1RS4)
15. PTFE Column adapter for each end of column (Ace glass 5838-78)

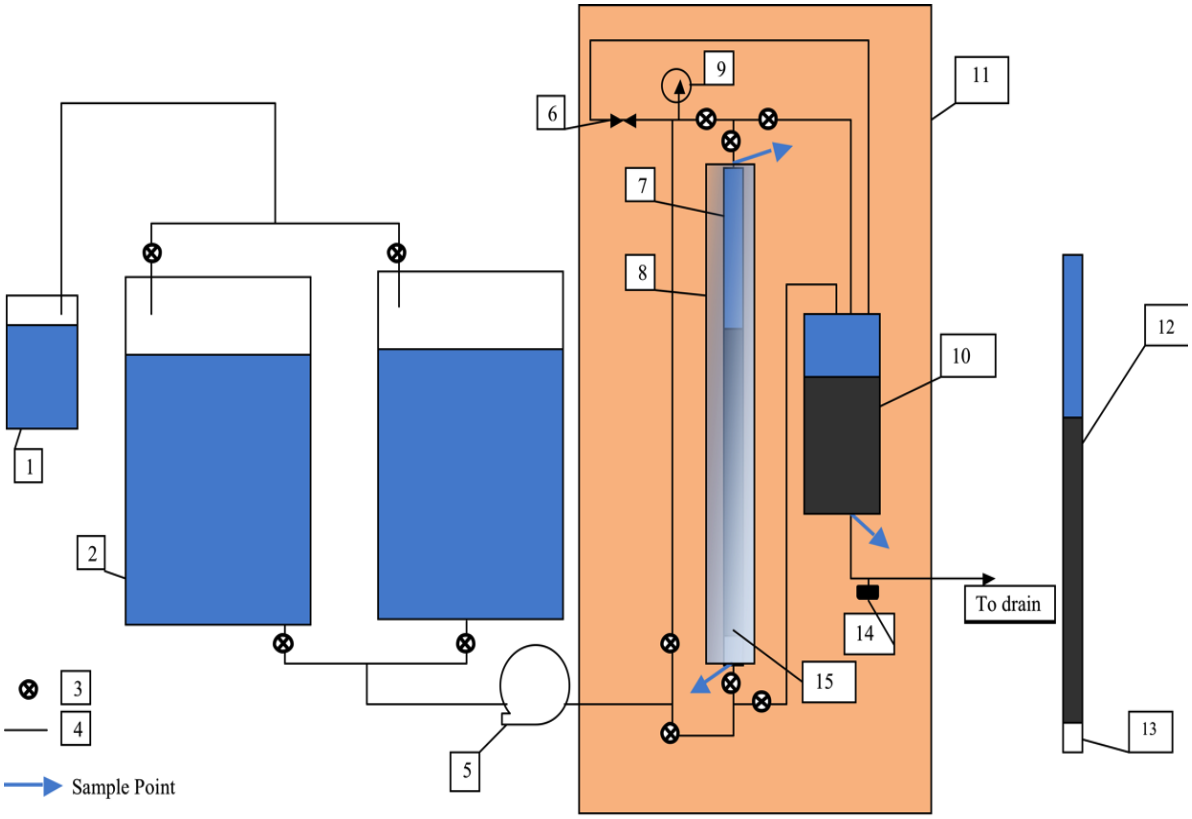

Figure 3.1: Schematic of OWASA Pilot

Rapid Small Scale Column Tests (RSSCTs)

A CD-RSSCT and a PD-RSSCT were completed in this research. Both RSSCTs were designed and initiated by Mastropole (2011). The CD-RSSCT was operated from June 2011 to August 2011 and the PD-RSSCT was operated from March 2011 through November 2011. In the CD-RSSCT, 250,000 bed volumes of water were treated and 350,000 bed volumes were treated in the PD-RSSCT. The RSSCT setup that was used is illustrated in Figure 3.2. The numbered components for Figure 3.2 are as follows (Mastropole 2011):

1. 26-L glass carboy influent tank (American Brewmaster)
2. Pump (PD-RSSCT: Alltech HPLC pump Model 301, CD-RSSCT: Cole Parmer modular gear pump 75211-22, 73003-14)
3. 1 gallon glass volatilization trap (3.5 L spiked to ~2*C_0)
4. Air release port
5. Glass wool pre-filter
6. Pressure gage (Ashcroft 436-06, 0-100psi)
7. Valve (Swagelok SS-4P4T)
8. 3/16” PTFE tubing w/ ¼” stainless steel fittings
9. Column (PD-RSSCT: 3/16” PTFE tubing, CD-RSSCT: 19/64” PTFE tubing)
10. Crushed GAC media (PD-RSSCT: 100 x 200 mesh, CD-RSSCT: 60 x 80 mesh)
11. Glass wool packing platform
12. 26-L Glass carboy effluent tank
13. Influent sample port
14. Sample port

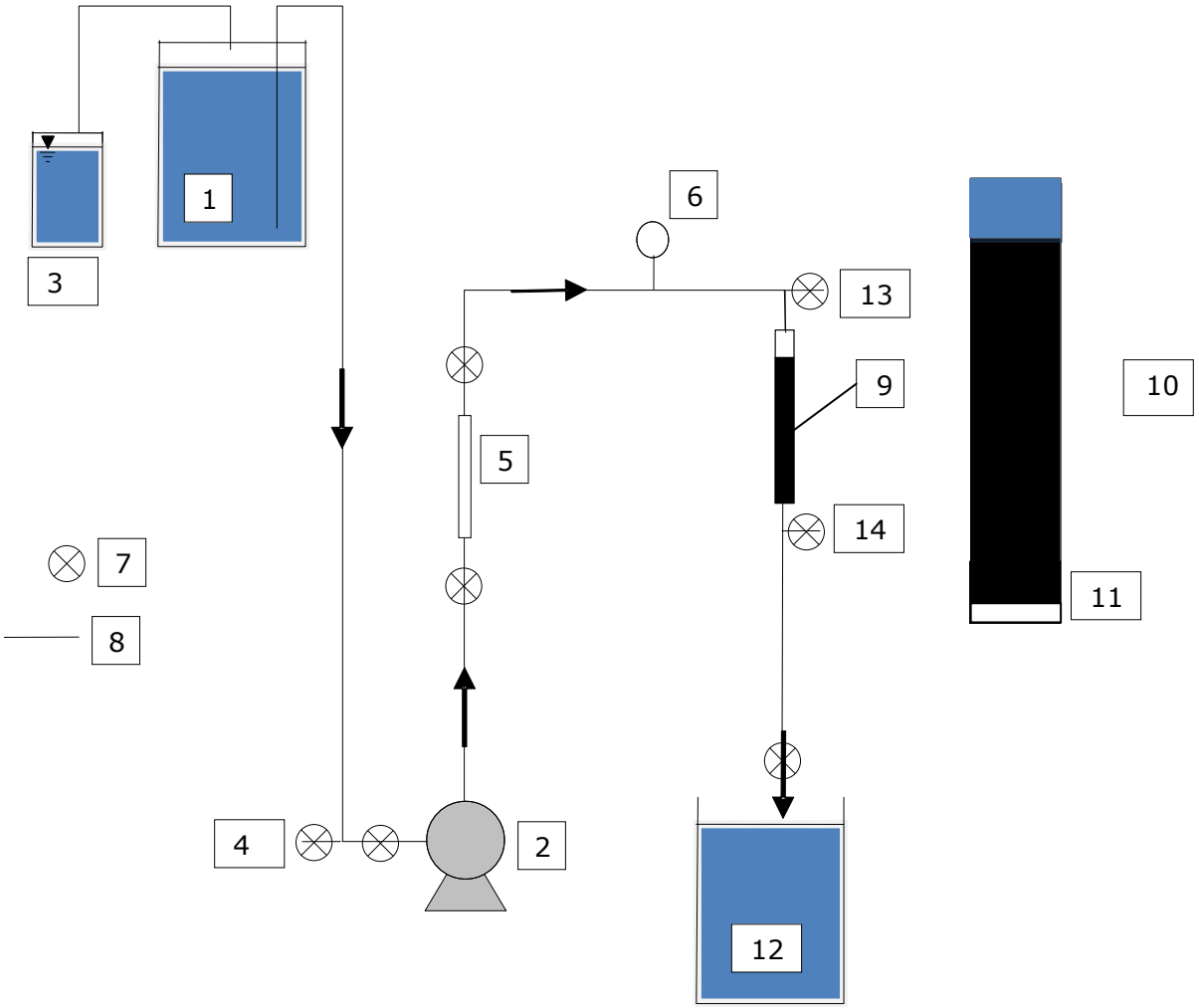

Figure 3.2: PD-RSSCT and CD-RSSCT Schematic

METHODS

GAC Preparation

The pilot column at OWASA used the as-received carbon. GAC for the RSSCTs was crushed with a mortar and pestle and then sieved to separate and collect the targeted particle size. The targeted particle size for the PD-RSSCT was the 100 x 200 U.S. Standard Mesh fraction and the targeted particle size for the CD-RSSCT was the 60 x 80 U.S. Standard Mesh fraction. Three- inch diameter brass sieves were used (McMaster-Carr, Cleveland, OH) and an electrical sieve shaker was used to assist in sieving (Humboldt Manufacturing Company, Raleigh, NC). The following protocol was used when preparing the carbon:

- A small volume of carbon was crushed using a ceramic mortar and pestle.
- Periodically, the carbon was transferred to the top-most sieve (100 U.S. Standard Mesh for the PD-RSSCT and the 60 U.S. Standard Mesh for the CD-RSSCT) until the surface of the sieve was covered by carbon. Then the sieve cover was installed.
- The sieves were stacked in the following order for the PD-RSSCT (top to bottom): sieve cover, 100 U.S. Standard Mesh sieve, 200 U.S. Standard Mesh sieve, and the catch pan. For the CD-RSSCT, the sieves were stacked in the following order: sieve cover, 60 U.S. Standard Mesh sieve, 80 U.S. Standard Mesh sieve, and the catch pan.
- The sieves were secured by screws on the sieve shaker table and allowed to shake for 7 minutes with the hammer operating.

- The sieve shaker was turned off and the bottom catch pan was emptied into a waste container to remove the carbon fines (<200 U.S. Standard Mesh sieve for the PD-RSSCT and <80 U.S. Standard Mesh sieve for the CD-RSSCT) and the catch pan was wiped clean with a Kimwipe.
- The catch pan was returned to the bottom of the sieves and shaken by hand for 2 minutes.
- Steps 5 and 6 were repeated until no carbon was visible in the bottom catch pan
- GAC that did not pass through the top sieve was returned to the mortar for more crushing and the process was repeated. GAC retained by the middle sieves was collected and stored for experimental use.
- Once the correct amount of GAC for the RSSCT was sieved and placed in a beaker, the carbon was rinsed with deionized water until the water above the carbon appeared clear (approximately 10 to 15 rinses).
- The beaker of crushed and rinsed carbon was covered with aluminum foil and placed in a 105°C oven to dry for 24 hours.
- The beaker of GAC was removed from the oven and placed in a desiccator for storage.
- The proper amount of GAC necessary for the particular RSSCT was weighed out and placed in a separate beaker
- The weighed GAC was placed in DI water and degassed under vacuum overnight (at least 6 hours) to remove any trapped air bubbles.

The RSSCT column was made out of Teflon tubing and was packed with glass wool. To load the carbon, the bottom of the column was covered with parafilm and then filled with DI water. The degassed and wetted carbon was loaded into the column with a glass eye dropper. Once the column was filled, the parafilm was removed and the carbon column was connected to the RSSCT setup (Figure 3.2). For the pilot column, the glass column contained 8 cm of glass beads with a wire mesh underneath for support at the effluent end. The degassed and wetted carbon was then loaded into the glass column and attached to the rest of the pilot setup (Figure 3.1). After adding all of the GAC into the pilot column, the column was backwashed with DI water to 20% bed expansion for 10 minutes. At the end of the backwash cycle, the pump flowrate was slowly decreased to maintain stratification of the bed.

Preparation of Stock Solutions for RSSCT Influent Tank and Pilot Influent Tank

The detailed procedure for preparing MP stocks used to spike the influent tanks of the RSSCTs and the pilot is described by Mastropole (2011).

Column Operation

Operating conditions for the pilot, the PD-RSSCT, and the CD-RSSCT are shown in Table 3.5.

Table 3.5: Comparison of Operating Conditions for the Pilot Test, PD-RSSCT, and CD-RSSCT

Experiment	Pilot	PD-RSSCT	CD-RSSCT
EBCT (min)	7.0	0.82	0.38
Column Diameter (cm)	2.54	0.476	0.754
Mean GAC Particle Diameter (mm)	0.92	0.11	0.21
Bed Depth (cm)	58.3	9.26	13.5
GAC mass (g)	136	0.76	1.41
Flow Rate (mL/min)	42.2	2.0	16.1
Hydraulic Loading Rate (m/hr)	5.0	6.7	21.6
Experiment Duration (days)	602	207	79
Volume of Water Required (gal)	9670	158	484

Pilot Operation

The OWASA pilot was operated at an EBCT of 7 minutes with a hydraulic loading rate of 5 m/h which translated into a flow rate of 42.2 mL/min (Table 3.5).

The pilot setup consisted of two 100 gallon drums that held influent water for the pilot column. Both tanks were filled but only one tank was spiked and put online at a time. When one of the tanks was empty, the other tank was spiked and put online. The empty drum was then washed with non-spiked influent water and Star San-Acid Sanitizer (5-Star Chemical Company and Supply Inc, Commerce City, Colorado) and refilled and allowed to equilibrate with the ambient temperature. The following procedure by Mastropole (2011) was followed when preparing and spiking pilot column feed tanks:

1. 100-gallon food-grade polypropylene drum was filled to the 100 gallon line with OWASA water pulled from the treatment process train after conventional settling and prior to chlorination and pre-filtered with a 5 µm cartridge filter (Whirlpool). The drum was allowed to sit open to the atmosphere for at least 3 days (6 days was typical) to equilibrate the water to room temperature.

2. A length of PTFE tubing was lowered into the opening of the drum so that the bottom end is submerged at least halfway down from the water line and secured to the side of the drum opening with waterproof tape.

3. An auto-pipette fitted with polypropylene tips was used to spike the correct amount of stock from each prepared stock bottle. Table 3.2 lists the micropollutants and their target influent concentrations for the pilot study.

4. A 60-mL polypropylene syringe (Becton-Dickinson) was used to rinse the tubing with deionized water. The tubing was rinsed with at least 120 mL of deionized water after spiking.

5. The tubing was then removed from the side of the drum and used to stir the water for at least a minute.

6. The drum lid was closed and tightened and the feed tank sat for at least 30 minutes prior to being put online.

RSSCT Operation

To conduct the RSSCTs, the following procedure as prepared by Mastropole (2011) was followed when preparing and spiking the RSSCT influent carboys:

1. 26 L glass carboy was filled to the 24 L line with OWASA water pumped with a stainless steel hand pump out of a 55-gallon stainless steel drum. The glass carboy was allowed to sit on the bench surface over night to equilibrate the water to room temperature.
2. The next day, a length of PTFE tubing was lowered into carboy so that the bottom end was submerged at least halfway down from the water line and secured to the side of the glass carboy with waterproof tape.
3. An auto-pipette fitted with a polypropylene tip was used to spike the desired amount of stock from each prepared stock bottle. Table 3.2 lists the micropollutants and their corresponding target concentrations for the RSSCT studies.
4. A 20-mL polypropylene syringe (Becton-Dickinson) was used to rinse the tubing with deionized water. The tubing was rinsed with at least 60 mL of deionized water after spiking.
5. The tubing was then removed from the side of the carboy and used to stir the water for at least a minute.
6. The glass carboy was then put connected to the HPLC pump.

Pilot and RSSCT Sampling

Effluent samples were taken prior to influent samples. For each influent and effluent sample, two 250-mL bottles were filled headspace free. One 250-mL bottle was sent to the University of Colorado for MP analysis by LC-MS/MS and the remaining bottle was analyzed at North Carolina State University for BPA, triclosan, and EE2. In addition, two 40-mL samples were taken at each sampling point and at each sampling time. One 40-mL vial was taken for UV_{254} and DOC analysis and the remaining 40-mL vial was taken headspace-free for MIB analysis.

The 40-mL samples for UV_{254} and DOC analysis were filtered on-site using a 0.45 µm PVDF syringe filter. Upon return to the NCSU lab, the 250-mL samples were filtered through a 0.45-µm glass fiber filter with a vacuum filter apparatus. UV_{254} absorbance was analyzed on the sampling day. Two drops of 2 M HCl were added for sample preservation and the vial stored at $4^{o}C$ until DOC analysis could be conducted. Samples for BPA, triclosan, and EE2 were collected and analyzed for a large portion of the study but were later stopped because the CD-RSSCT showed no breakthrough. All samples were stored headspace-free in a refrigerator at $4^{o}C$ until analysis.

Instrumental Analysis

Analysis of 2-Methylisoborneol with GC-MS/MS

The procedure for the analysis of MIB in the aqueous-phase was developed by Yuncu (2010). Aqueous-phase concentrations of MIB were analyzed with a gas chromatograph (GC) (Varian 3800, Palo Alto, CA) equipped with a split/splitless injector, a 30-m column (Factor Four VF-5ms low bleed, I.D. 0.25 mm, film thickness 0.25 µm, Palo Alto, CA), and a mass spectrometer (MS) (Varian Saturn 2200, Palo Alto, CA) that was used in the chemical ionization (CI) tandem mass spectrometry (MS/MS) mode. The GC oven temperature was maintained at 50ºC for 1 minute, increased to 200ºC at 10ºC/min and held at 200ºC for 2 minutes, and finally increased to 240ºC at 10ºC/min and finally held at 240ºC for 5 minutes. Upon sample collection, 10-mL aliquots were transferred to 20-mL autosampler vials (Varian, Palo Alto, CA) that contained 2.5 g of NaCl. Isoborneol was used as the internal standard and was spiked at a concentration of 20 ng/L. Prior to analysis, analytes in samples were concentrated using headspace solid-phase microextraction (SPME) using a 1-cm 50/30 52 µm DVB/Carboxen/PDMS fiber (Supelco, St. Louis, MO). The SPME fiber was exposed to the headspace of the sample vial at a temperature of 65ºC for 30 minutes. The SPME fiber was then inserted into the injector of the GC oven (T= 250ºC, time = 4 minutes). The method quantification limit for MIB was 1 ng/L. The GC-CI/MS/MS method used for analysis of MIB was adapted from the standard operating procedure developed by the Metropolitan Water District of Southern California (MWDSC).

Analysis of Micropollutants with LC-MS/MS

The procedure for the analysis of all micropollutants, except MIB, BPA, and Triclosan was developed by Imma Ferrer at the University of Colorado-Boulder. The extraction experiments were performed using an automated sample preparation with extraction columns system (GX-271 ASPEC, Gilson, Middleton, WI, USA) fitted with a 25-mL syringe pump for dispensing the water samples through the sample extraction cartridges. Water samples were extracted with Oasis HLB cartridges (200 mg, 6mL) obtained from Waters (Milford, MA, USA). The cartridges were conditioned with 4 ml of methanol followed by 6 ml of HPLC-grade water at a flow rate of 1 ml/min. The water samples (100mL) were then loaded at a flow rate of 10 mL/min. Elution of the analytes from the cartridge were carried out with 6 mL of methanol. The solvent was then evaporated to 0.5-mL with a stream of nitrogen at a temperature of 45ºC in a water bath using a Turbovap concentration workstation (Caliper Life Sciences, Mountain View, CA, USA). The samples were then be transferred to vials and analyzed by LC/MS-MS. The mass spectrometry analyses (LC/MS-MS) allowed for the separation of the water extracts through use of an HPLC system (consisting of vacuum degasser, autosampler and a binary pump) (Agilent Series 1290, Agilent Technologies, Santa Clara, CA, USA) equipped with a reversed phase C_{18} analytical column of 50 mm x 2.1 mm and 1.8 μm particle size (Zorbax Eclipse Plus). Column temperature was maintained at 25ºC. The injected sample volume was held constant at 15 μL. The optimized chromatographic method held the initial mobile phase composition constant for 1.7 min, followed by a linear gradient after 10 min. The flow-rate used was 0.4

mL/min. A 4-min post-run time was necessary after each run. The HPLC system connects to a triple quadruple mass spectrometer Model 6460 Agilent (Agilent Technologies, Santa Clara, CA, USA) that is equipped with electrospray Jet Stream technology which can operate in positive and negative ion mode.

Analysis of BPA, Triclosan, and EE2

The procedure for the analysis of BPA, triclosan and EE2 in the aqueous-phase was developed by Mastropole (2011). Aqueous-phase concentrations of BPA, triclosan and EE2 were analyzed with a gas chromatograph (GC) (Varian 3800, Palo Alto, CA) equipped with a split/splitless injector, a 30-m column (Factor Four VF-5ms low bleed, I.D. 0.25 mm, film thickness 0.25 μm, Palo Alto, CA), and a mass spectrometer (MS) (Varian Saturn 2200, Palo Alto, CA) that was used in the chemical ionization (CI) tandem mass spectrometry (MS/MS) mode. The GC oven temperature was maintained at 50ºC for 1 minute, increased to 190ºC at 25ºC/min and held at 190ºC for 1 minute, and finally increased to 290ºC at 10ºC/min and finally held at 290ºC for 3 minutes and 24 seconds. The optimal method run time to ensure analyst separation was determined to be 20 minutes by the Varian Software. Upon sample collection, 18-mL aliquots were transferred to 20-mL autosampler vials (Varian, Palo Alto, CA) that contained 1.5 g of NaCl. 17α-ethinyl estradiol-2,4,16,16-d4 was used as the internal standard and was spiked at a concentration of 200 ng/L. Prior to analysis, analytes in samples were concentrated using solid-phase microextraction (SPME) using a 1-cm 85 μm polyacrylate SMPE fiber (Supelco, St. Louis, MO). The sample vial was first incubated at

60ºC for 30 seconds followed by 2 minutes of rest. The SPME fiber was exposed to the sample at a penetration depth of 16 mm (measured from the bottom of the vial) for 60 minutes The SPME fiber was then inserted into the injector of the GC oven (T= 280ºC, time = 8 minutes, depth = 54 mm).

Analysis of Total Organic Carbon/Dissolved Organic Carbon

Dissolved organic carbon (DOC) was measured with TOC analyzer (Model TOC-VCSN, Shimadzu Scientific, Columbia, MD) in accordance with Standard Method 5310C (APHA, 2005).

Analysis of UV_{254}

Ultraviolet absorbance (UV_{254}) was analyzed at a wavelength of 254 nm using a HACH spectrophotometer (DR5000, Hach Company, Loveland, CO, USA) in accordance with Standard Method 5910 (APHA, 2005).

Description of Breakthrough Data with Pore Surface Diffusion Model

MP breakthrough curves were described with a pore surface diffusion model (PSDM). The adjustable parameters were the Freundlich K value and the intraparticle diffusive flux. The Freundlich K value is specified by the user, and an initial value was

estimated by calculating the apparent Freundlich capacity parameter K* as follows (Corwin 2010):

$$K^* = \left[\frac{BV_{50}}{\rho_{bed}}\right] \tag{3.1}$$

where BV_{50} is the bed volumes required for the compound of interest to reach 50% breakthrough in the effluent and ρ_{bed} is the apparent density of the GAC bed.

The software used for this research was the Adsorption Design Software (AdDesignS). The RSSCT was modeled by fitting the modeled output for a particular contaminant to the corresponding experimental breakthrough data. The Freundlich 1/n value was set equal to 1 (Corwin, 2010), and the surface to pore diffusion flux ratio (SPDFR) was initially assumed to be negligible (1E-30). Next, the tortuosity (τ) value or SPDFR value was adjusted to match the slope of the breakthrough curve established by the data. Tortuosity can take a value of 1 or greater. Larger tortuosity values decrease the slope of the breakthrough curve. If the modeled output was still too flat to match the experimental data at $\tau = 1$, surface diffusion was invoked in addition to pore diffusion by increasing the SPDFR value. Once the best fit was achieved, the results from the RSSCT were used to model the pilot. Using the τ and SPDFR values for the RSSCT, the total normalized RSSCT flux was calculated as:

(3.2)

$$RSSCT\ Flux = \frac{1}{\tau}$$

If SPDFR = 1E-30, or (3.3)

$$RSSCT\ Flux = SPDFR + 1$$

If SPDFR was > 1E-30

The total normalized pilot flux was then calculated by multiplying the total normalized RSSCT flux by the scaling factor (SF) as follows:

(3.4)

$$Pilot\ Flux = SF \times RSSCT\ Flux$$

The value of the pilot flux determines the SPDFR and τ values for the pilot. The three possible scenarios are listed in Table 3.6.

Table 3.6: PSDM SPDFR Values

Option 1	Option 2	Option 3
Pilot Flux >1	Pilot Flux =1	Pilot Flux<1
SPDFR= Pilot Flux-1 τ = 1	SPDFR= negligible (1E-30) τ = 1	SPDFR= negligible (1E-30) τ = 1/Pilot Flux

The pilot breakthrough curve for a particular contaminant was modeled using the applicable option from Table 3.6. The K value for the plot was estimated from K*, or if 50% breakthrough was not reached, by trial and error until a good fit was obtained.

Film mass transfer also played an important role in the PSDM. Film mass transfer is the rate at which an adsorbate travels through the aqueous film that surrounds the GAC

particles in the column. AdDesignS estimates the film mass transfer coefficient with the Gnielinksi relationship.

After describing the pilot and RSSCT data with the PSDM, Equation 3.5 was used to compare the pilot and RSSCT model parameters to find the fouling factor (Y). The fouling factor accounts for the delayed onset of breakthrough for the RSSCT as compared to the pilot.

$$SF^{Y} = \left[\frac{K_{RSSCT}}{K_{Pilot}}\right] \tag{3.5}$$

Where Y is solved for by using:

$$Y \quad = \left[\frac{Log(K_{RSSCT}/K_{Pilot})}{Log(SF)}\right] \tag{3.6}$$

Obtaining Abraham Descriptors

The Abraham descriptors were obtained from ACD Laboratories for the 21 compounds that were used to develop and apply LFERS. The Abraham descriptors for the 21 compounds are shown in Table 3.7.

Table 3.7: Abraham Descriptors

Compound	S	A	B	V	E
MP Training Set					
Acetochlor	1.63	0	0.94	2.14	1.11
Atrazine	1.17	0.32	0.96	1.6196	1.51
Caffeine	1.72	0.05	1.28	1.3632	1.5
Carbamazepine	2.06	0.39	0.92	1.81	2.12
Cotinine	1.54	0	1.14	1.3867	1.24
Iopromide	4.87	1.65	3.36	3.82	4.33
Methomyl	0.91	0.21	0.85	1.21	0.77
Metolachlor	1.62	0	0.98	2.28	1.12
Prometon	1.26	0.26	1.19	1.8377	1.2
Simazine	1.2	0.33	0.95	1.4787	1.55
Tributyl Phosphate	0.72	0	1.25	2.24	0.25
VOCs (Fotta, 2012)					
1,1-Dichloroethane	0.37	0.09	0.02	0.6352	0.22
1,2-Dichloroethane	0.48	0	0.1	0.6352	0.30
1,1,2-Trichloro-Trifluoroethane	0.31	0	0.04	0.8104	0.2
1,1,1-Trichloroethane	0.44	0	0.01	0.7576	0.31
1,2-Dichloroethene	0.56	0	0.09	0.5922	0.4
1,1-Dichloroethene	0.46	0	0.1	0.5922	0.35
MPs used to apply LFER in predictive mode					
Diclofenac	1.95	0.7	0.67	2.025	1.81
Diuron	1.66	0.44	0.77	1.5992	1.27
Naproxen	1.49	0.57	0.75	1.7851	1.54

The box and whisker plots in Figures 3.3 to 3.7 illustrate the value ranges for each Abraham descriptor.

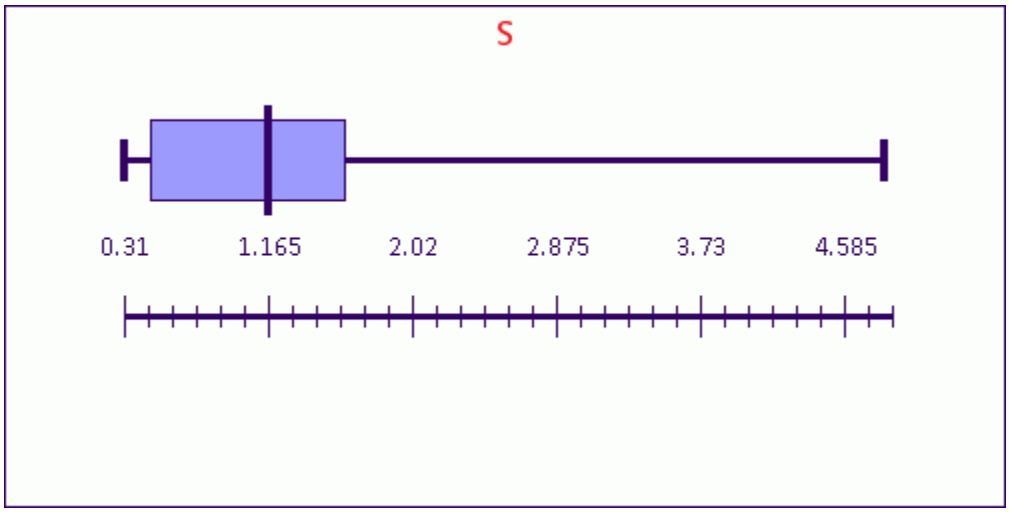

Figure 3.3: S-Dipolarizability/Polarizability Values for 11 MPs and 6 VOCs

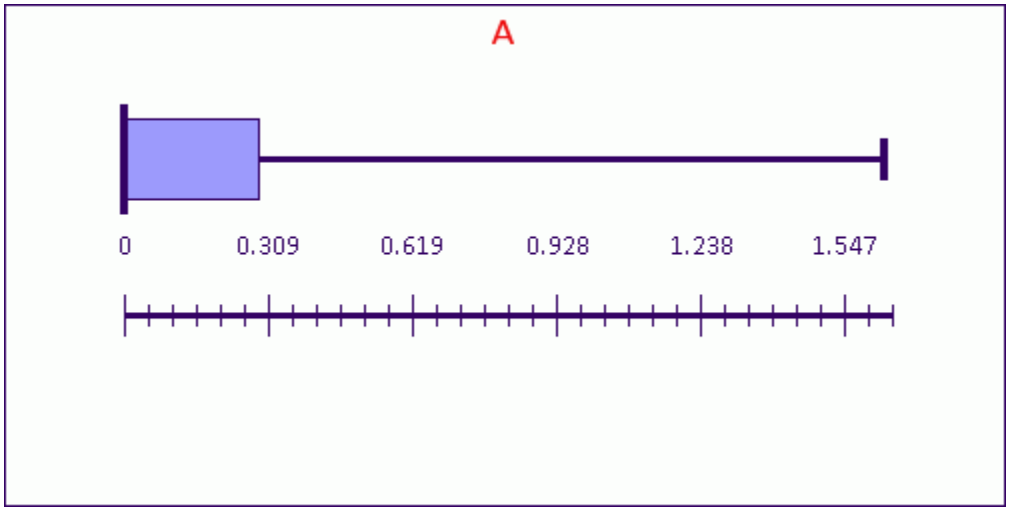

Figure 3.4: A-Hydrogen Bond Acidity Values for 11 MPs and 6 VOCs

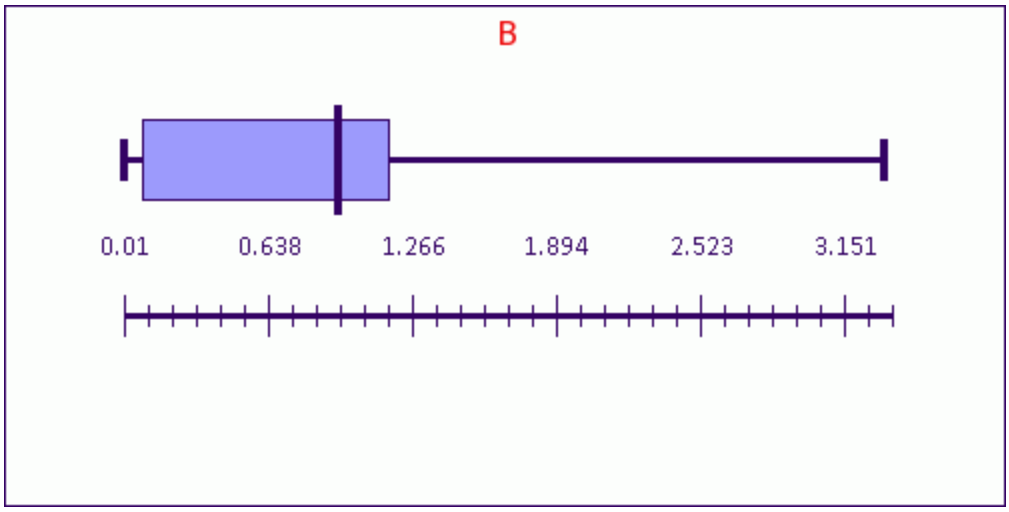

Figure 3.5: B-Hydrogen Bond Basicity Values for 11 MPs and 6 VOCs

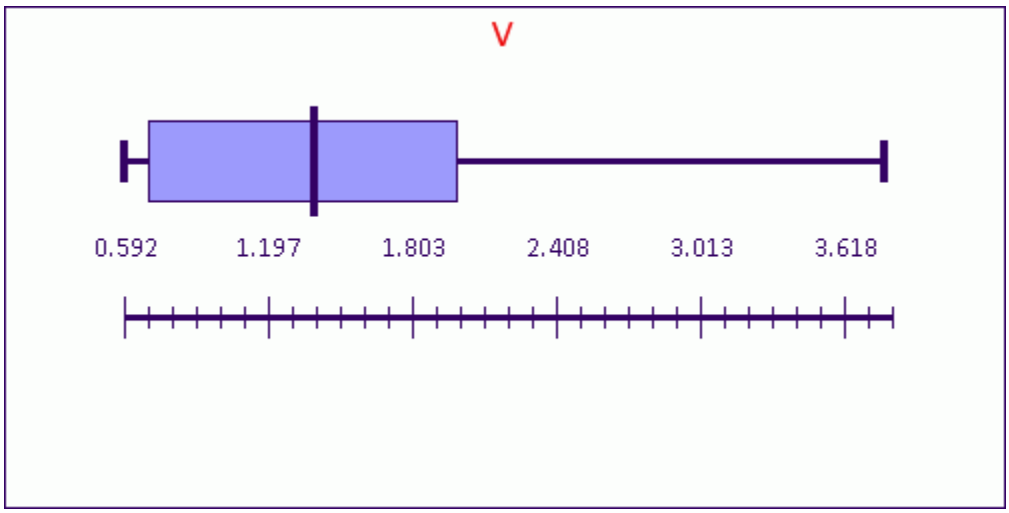

Figure 3.6: V-McGowan Molar Volume Values for 11 MPs and 6 VOCs

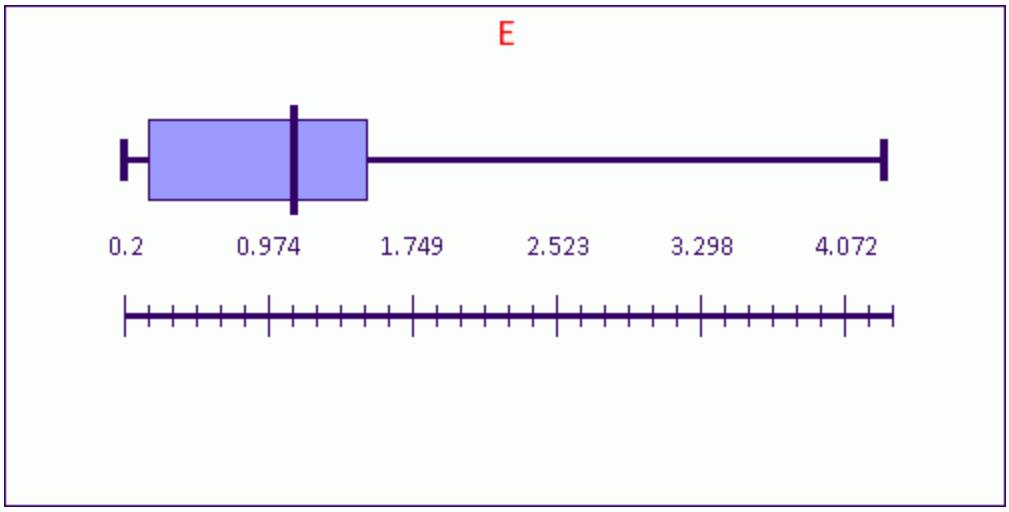

Figure 3.7: E-Excess Molar Fraction Values for 11 MPs and 6 VOCs

Principal component analysis (PCA) was conducted to relate Y-values obtained from either the CD-RSSCT or the PD-RSSCT to Abraham solubility parameters. The training set consisted of the Y-values that were determined for the 11 MPs for which comparisons between the pilot data and the RSSCT data could be made. The training set for the PD-RSSCT also included Y-values for 7 VOCs that were determined by Fotta (2012).

Multicolinearity was identified among the five Abraham descriptors using the variation inflation factor (VIF) through the use of R-project (University of Auckland). VIF values larger than 10 indicated that the independent variables were correlated and the results for the VIF analysis are shown in Table 3.8.

Table 3.8: VIF Values for CD-RSSCT and PD-RSSCT

Test	Abraham Descriptor	VIF Value
CD-RSSCT	S	50.97
	A	21.14
	B	13.77
	V	6.06
	E	52.29
PD-RSSCT	S	29.15
	A	5.76
	B	13.48
	V	8.29
	E	24.43

For the CD-RSSCT, only V, the McGowan molecular volume was not correlated with the other Abraham descriptors. For the PD-RSSCT, A, the hydrogen bond acidity, and V, were not correlated with the other Abraham descriptors.

PCA transforms correlated variables into uncorrelated principal components (PCs) within a regression equation. The first PC in the equation accounts for as much of the variability in the data set as possible and if enough variability is not explained by the first PC then another PC is created. Essentially, the PCs define a new coordinate system for the data. For this research, PCA regression models were obtained using R-Project and verified using Microsoft Excel. The generalized linear model (GLM) procedure of R-Project was applied for parameter identification. GLM supplied an r^2 and an adjusted r^2 for each regression model created. The r^2, or the coefficient of determination, indicates how much variation can be explained by the model. The adjusted r^2 explains how much variation is being explained by the model but it takes into account the number of variables being used. The Microsoft Excel

Solver generalized linear regression model was used to verify that the parameters for the LFER found in R-project were in agreement.

The significance of individual variables was quantified by p-values. Individual p-values were calculated to ascertain whether at the 95% confidence level the coefficient was statistically different from zero ($p<0.05$).

The leave one out (LOO) method was used to ascertain the predictive ability of the LFER developed with the five Abraham descriptors through R-project and Microsoft Excel. The LOO method was evaluated with the predicted error sum of squares (PRESS) when used with R-project. A small PRESS value indicated stronger predictive abilities of the LFER. Within Microsoft Excel, the LOO method was completed manually by leaving out one MP in the training set at a time, solving for a new regression equation, and then comparing how the predicted Y-value compared to the experimentally determined Y-value. LOO analysis ensures that the original regression was not influenced by one single data point more than others.

CHAPTER 4: RESULTS AND DISCUSSION

In this chapter, results from the pilot study and the RSSCTs are presented and discussed. The data were collected to assess the effectiveness of GAC for MP removal from surface water. In addition, the RSSCT data were used in conjunction with the pilot data to develop a scale up procedure. A linear free energy relationship (LFER) was developed to predict fouling factors from Abraham descriptors for MPs. Using the LFER in conjunction with the PSDM, a comprehensive scale-up procedure for predicting full-scale GAC adsorber performance from bench scale RSSCTs is presented.

PILOT STUDY

Pilot column operation started on March 3, 2011, and the pilot was operated for a period of 1.6 years. The pilot column had an EBCT of 7 minutes and 120,000 bed volumes were treated. A total of 12 sampling campaigns were conducted throughout the pilot test. GAC characteristics and operating conditions for the pilot study are listed in Tables 3.3 and 3.4, respectively.

The objectives for the pilot study were to:

1. Determine the effectiveness of GAC for the removal of micropollutants from coagulated surface water
2. Use MP breakthrough data to support the development of a scale-up procedure

At the completion of the pilot study, a total of 11 MPs were detected in the GAC effluent at levels that exceeded 10% of the influent concentration, and their breakthrough curves are shown in Figure 4.1. In addition, the DOC and UV_{254} breakthrough curves are shown for reference.

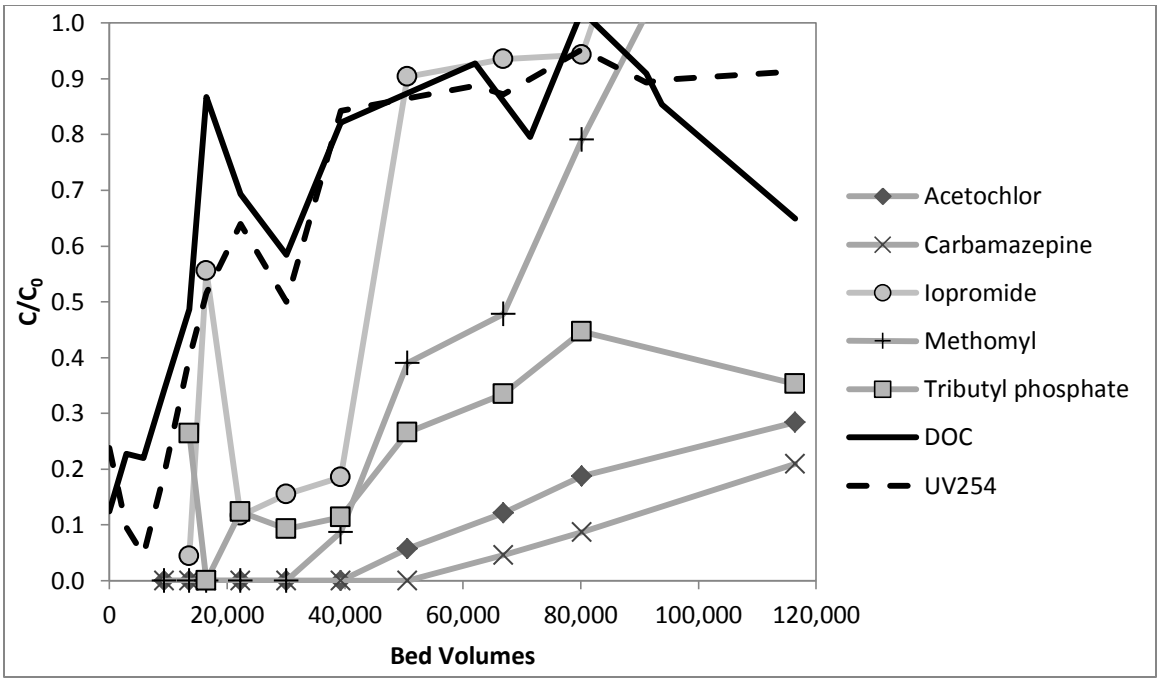

(a)

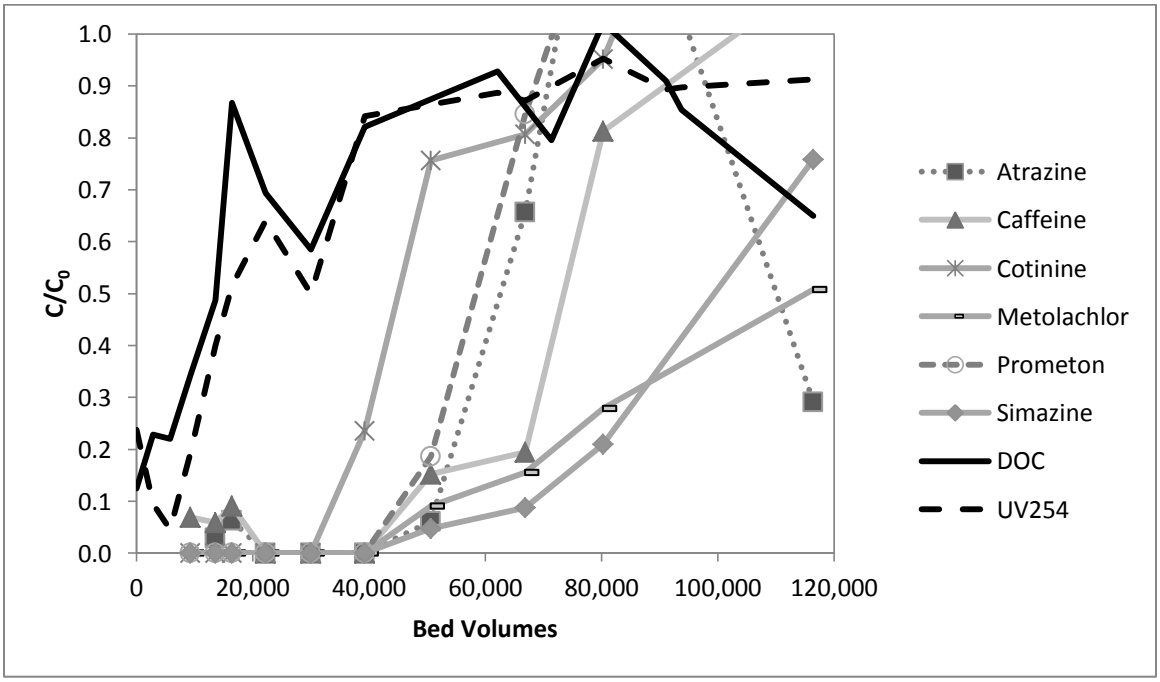

(b)

Figure 4.1: MP Breakthrough Curves for Pilot-Scale Adsorber (separated into two panels for visual clarity)

The question of the effectiveness of GAC for adsorbate removal was answered by comparing the bed volumes of water that could be processed until 10% contaminant breakthrough was reached. Based on the analytical methods used, the reporting limit was about 10% for most MPs. As shown in Figures 4.1 and 4.2, DOC breakthrough occurred prior to the breakthrough of all 34 MPs. DOC breakthrough reached 50% at about 13,000 bed volumes which would be a typical stopping point for the operation of a GAC adsorber if the main treatment objective was TOC or DBP precursor removal. For an EBCT of 7 min, 13,000 bed volumes would equate to about 2 months of operation and to a CUR of 0.29 lb/1000 gallons (34.7 mg/L).

The bed volumes that could be processed to 10% and 20% breakthrough, GAC life, and carbon usage rates (CURs) for the 11 MPs, which measureable breakthrough was obtained, are compared in Table 4.1. The most weakly adsorbed MP, iopromide, did not begin to break through until about 20,000 bed volumes as shown in Figure 4.1 (panel A). Breakthrough at 20,000 bed volumes would be approximately equal to 3 months of continuous filter operation. The CURs for the 11 MPs at 10% breakthrough ranged from 0.042 lb/1000 gal for carbamzepine to 0.183 lb/1000 gal for iopromide (Table 4.1). No measureable breakthrough was observed for the remaining 23 MPs evaluated in this study.

Table 4.1: GAC Life and Bed Volumes to 10% and 20% Breakthrough of MPs Detected in Pilot Column Effluent. (Results to 50% DOC breakthrough are shown for reference)

Compound	Breakthrough (%)	Bed Volumes to Indicated % Breakthrough*	Bed Life (Days)	CUR (mg/L)	CUR (lb/1000 gal)
DOC	50	13,000	63	34.7	0.289
Acetochlor	10	68,900	334	6.6	0.055
	20	82,300	400	5.5	0.046
Atrazine	10	84,300	410	5.5	0.046
	20	101,800	450	4.4	0.037
Caffeine	10	43,200	210	10.4	0.087
	20	51,400	250	8.7	0.073
Carbamazepine	10	88,500	430	5.0	0.042
	20	110,000	530	4.0	0.034
Cotinine	10	28,800	140	15.6	0.130
	20	36,000	175	12.5	0.104
Iopromide	10	20,600	100	21.9	0.183
	20	26,700	130	16.8	0.140
Methomyl	10	40,100	200	11.3	0.094
	20	47,300	230	9.5	0.079
Metolachlor	10	54,500	265	8.3	0.069
	20	71,000	345	6.4	0.053
Prometon	10	40,100	195	11.3	0.094
	20	51,400	250	8.7	0.073
Simazine	10	63,800	310	7.1	0.059
	20	76,100	370	5.9	0.049
Tributyl Phosphate	10	36,000	175	12.5	0.104
	20	49,400	240	9.1	0.076

* Bed volumes to 10% and 20% MP breakthrough are based on PSDM fits

The relative adsorbability of the MPs in the pilot was determined from the time to 10% breakthrough. Weakly adsorbing compounds such as iopromide, cotinine, and tributyl phosphate reached 10% breakthrough before 40,000 bed volumes had been treated. The remainder of the compounds that broke through to 10% were considered moderately adsorbable and reached 10% breakthrough before 85,000 bed volumes had been processed.

The remaining 23 micropollutants that did not reach measurable detection during pilot operation were considered strongly adsorbable.

One reason why MP breakthrough was not observed for such a large number of MPs may be attributable to biological removal. MPs identified as having very fast biodegradation consisted of BPA, ibuprofen, MIB, molinate, triclosan, and trimethoprim (Table 2.5, Zearley et al., 2012). Furthermore, compounds identified as having fast biodegradation consisted of 2,4-D, acetaminophen, caffeine, chlorpyrifos, dimethoate, gemfibrozil, and naproxen (Table 2.5, Zearley et al., 2012). None of the compounds that were classified as being biodegradable at a very fast or fast rate were detected in the pilot effluent, with caffeine being the exception. While 12 of the 23 MPs that did not break through were readily biodegradable (fast or very fast), all 11 MPs that had broken through at the completion of the pilot study were classified as slowly biodegradable or recalcitrant, with the exception of caffeine (Table 2.5). It is likely that biodegradation and therefore enhanced removal of MPs was more effectively simulated at the pilot-scale than at the bench-scale. The longer run time of the pilot column allows the microorganisms to grow and attach to the GAC surface and acclimate to the MP influent concentrations.

CD-RSSCT STUDY

The RSSCT based on the constant diffusivity design was operated for 2 months (250,000 bed volumes). The objectives for the CD-RSSCT study were to:

1. Determine the effectiveness of GAC for the removal of micropollutants

2. Determine the suitability of the CD-RSSCT design for scale-up

Breakthrough was obtained for all MPs but chlorpyrifos, BPA, triclosan, and ethinyl estradiol (EE2) through a total of 8 sampling events. Thus, a very complete data set was obtained in a relatively short amount of time.

The 29 MPs that were detected at measureable levels in the CD-RSSCT are shown in Figures 4.2 to 4.6. For clarity, compounds were grouped by the following compound classifications: antibiotics/antimicrobials, herbicides, insecticides, pharmaceuticals, and other.

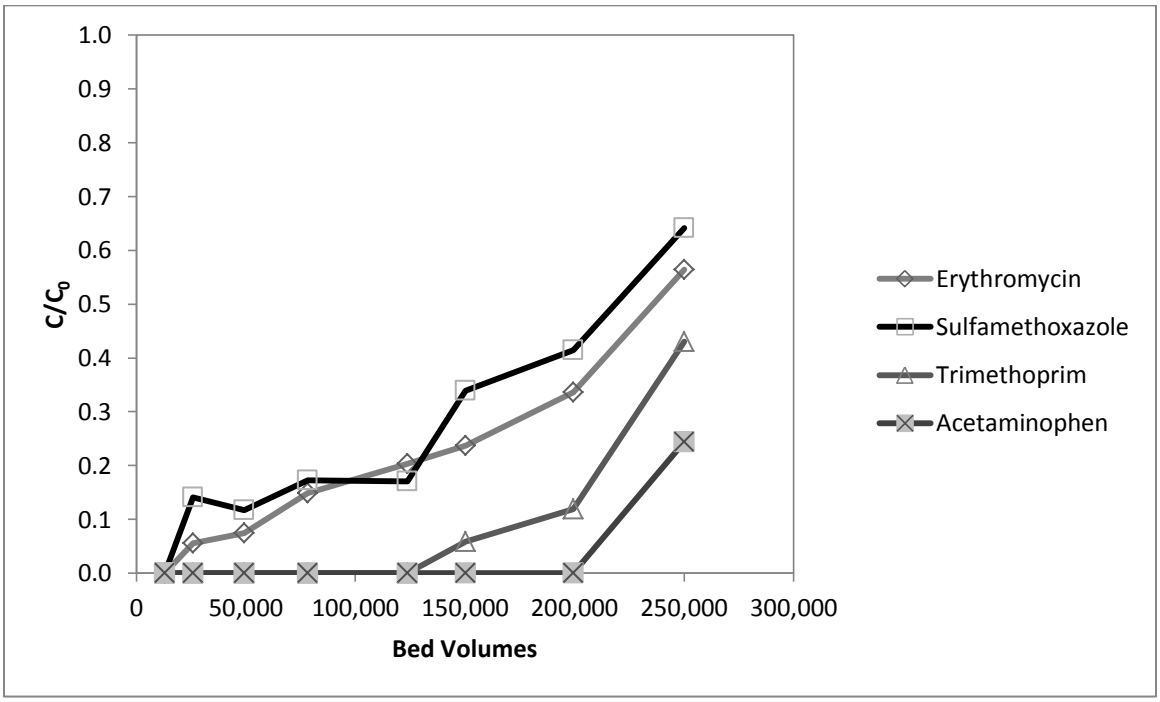

Figure 4.2: Breakthrough Curves for Antibiotic/Antimicrobial Compounds from CD-RSSCT

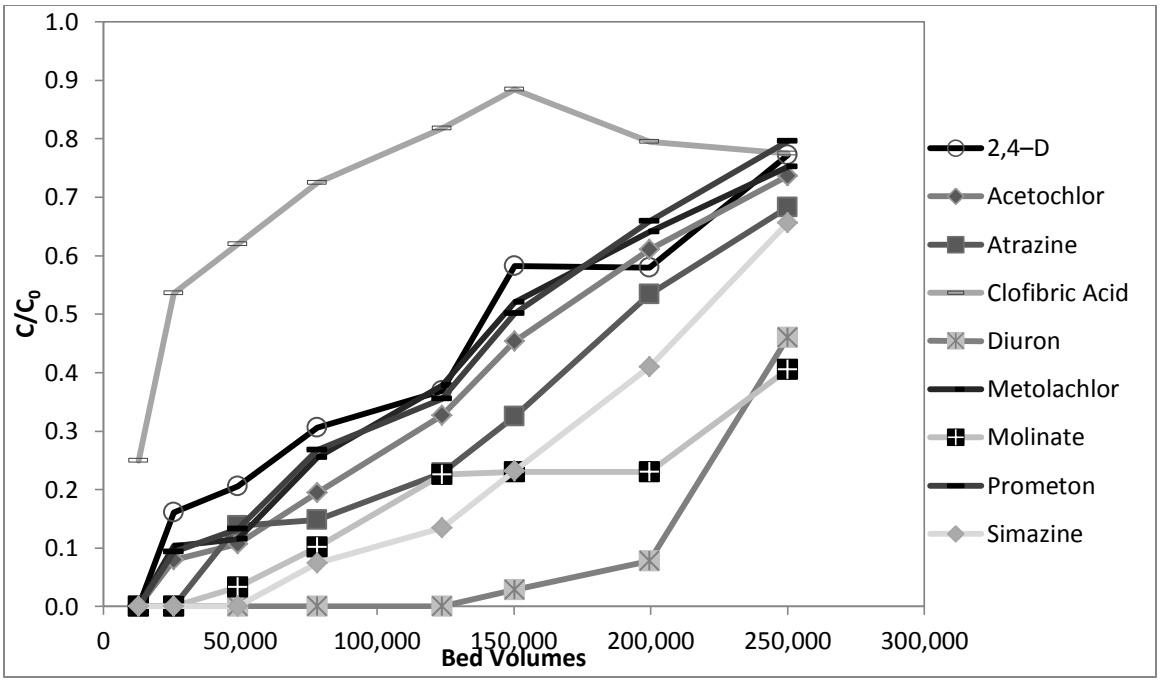

Figure 4.3: Breakthrough Curves for Herbicide Compounds from CD-RSSCT

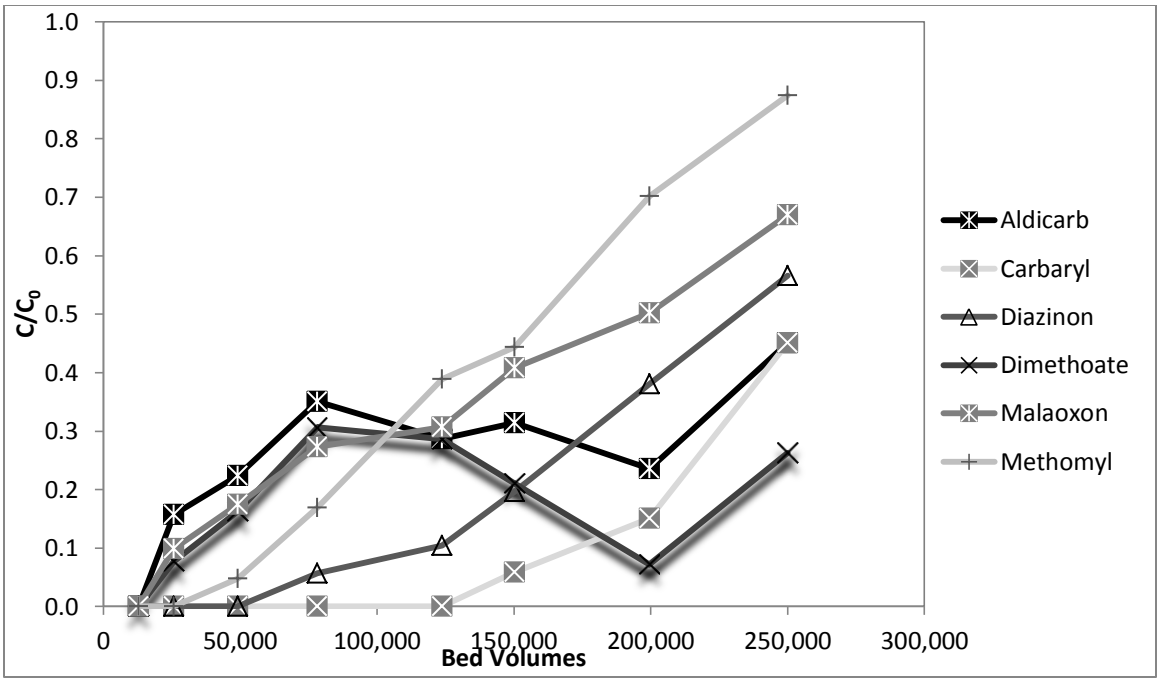

Figure 4.4: Breakthrough Curves for Insecticide Compounds from CD-RSSCT

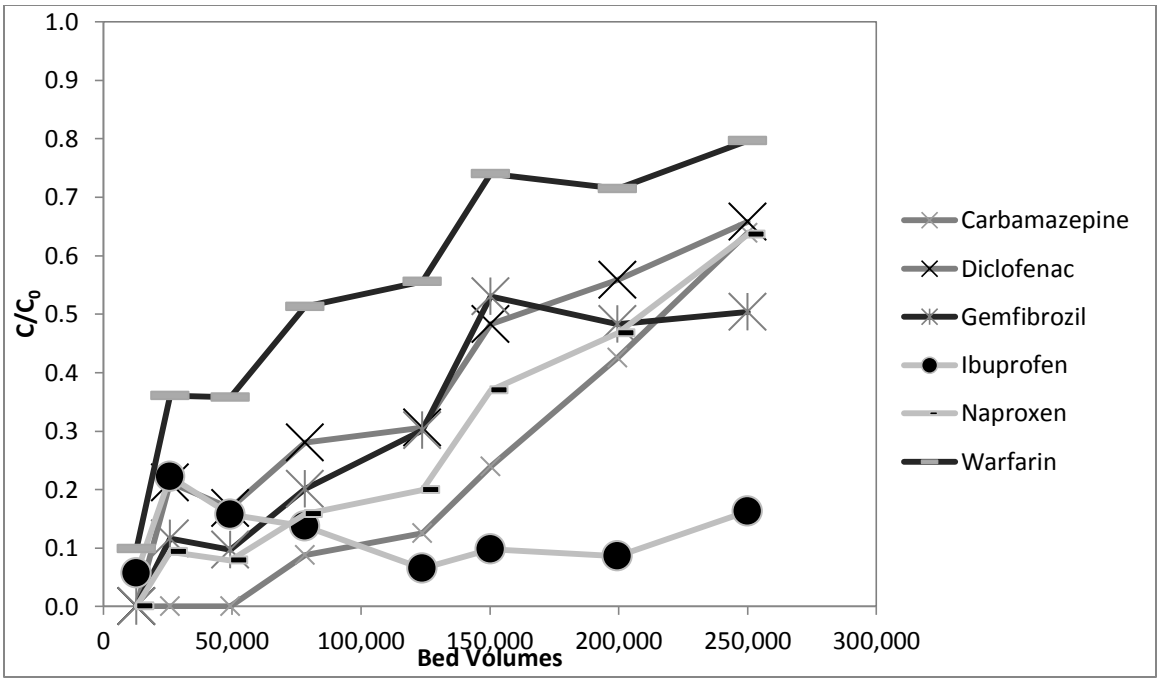

Figure 4.5: Breakthrough Curves for Pharmaceutical Compounds from CD-RSSCT

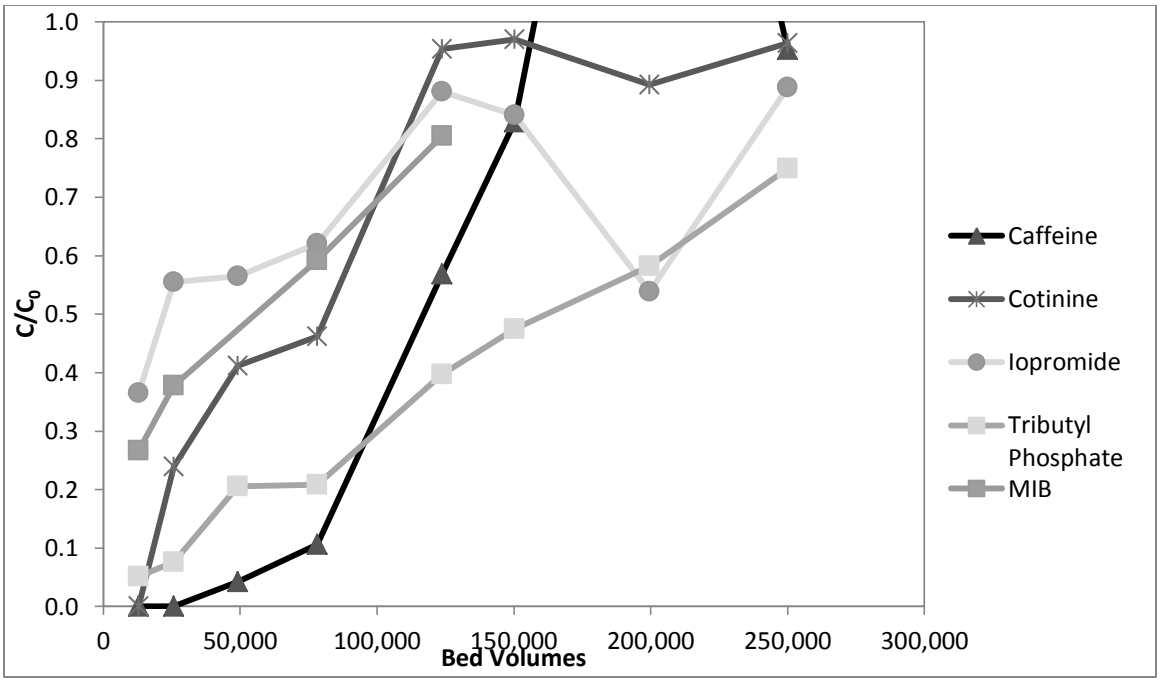

Figure 4.6: Breakthrough Curves for Other Compounds from CD-RSSCT

The MP breakthrough data from the CD-RSSCT shown in Figures 4.2 through 4.6 were used to determine the onset of MP breakthrough as well as the order of MP adsorbability In Table 4.2 the of the onset of MP breakthrough and the adsorption capacity of the GAC, as indicated through the bed volumes to 10% and 50% breakthrough, respectively, are compared for the pilot and the CD-RSSCT data sets for the 11 MPs that broke through to measurable levels in the pilot.

Table 4.2: Onset of MP Breakthrough and Adsorption Capacity for CD-RSSCT and Pilot

Compound	Breakthrough (%)	Pilot Bed Volumes to Indicated % Breakthrough*	CD-RSSCT Bed Volumes to Indicated % Breakthrough*
Acetochlor	10	68,900	50,000
	50	112,000	157,700
Atrazine	10	84,300	115,400
	50	154,000	200,000
Caffeine	10	43,200	84,600
	50	65,900	123,100
Carbamazepine	10	88,500	88,500
	50	205,700	242,300
Cotinine	10	28,800	30,800
	50	51,400	88,500
Iopromide	10	20,600	7,000
	50	40,100	19,200
Methomyl	10	40,100	73,100
	50	62,700	96,200
Metolachlor	10	54,500	65,400
	50	109,000	146,200
Prometon	10	40,100	46,200
	50	78,200	146,200
Simazine	10	63,800	100,000
	50	102,800	211,500
Tributyl Phosphate	10	36,000	38,500
	50	83,300	173,100

* Bed volumes are based on PSDM fits

The comparisons in Table 4.2 illustrate that the CD-RSSCT predicted the onset of breakthrough within 20% of the bed volume estimates from the pilot test for five MPs (carbabazepine, cotinine, metolachlor, prometon, and tributyl phosphate). For the remainder of the MPs, bed volumes to 10% breakthrough were largely overestimated by the CD-RSSCT, exceptions being acetochlor and iopromide. Additionally, the adsorption capacity of

the GAC was overpredicted by the CD-RSSCT for all MPs except iopromide. The late onset to breakthrough and the extended GAC service life in the CD-RSSCT was likely due to the particle size-dependence of NOM fouling. As hypothesized by Corwin and Summers (2010) NOM fouling in the RSSCT caused less carbon surface area to be lost as compared to the pilot due to the difference in carbon particle size.

Additional data analysis was conducted to compare the relative MP adsorbability in the CD-RSSCT and the pilot tests. In order to assess relative adsorbability, the bed volumes to 20% breakthrough for each MP was normalized to the bed volumes to 20% carbmazepine breakthrough. The normalized CD-RSSCT bed volumes were then compared to the normalized pilot bed volumes (Figure 4.7). Carbamazepine was chosen to normalize the bed volumes because there was a good match between the CD-RSSCT and the pilot for the onset of breakthrough and at 20% breakthrough.

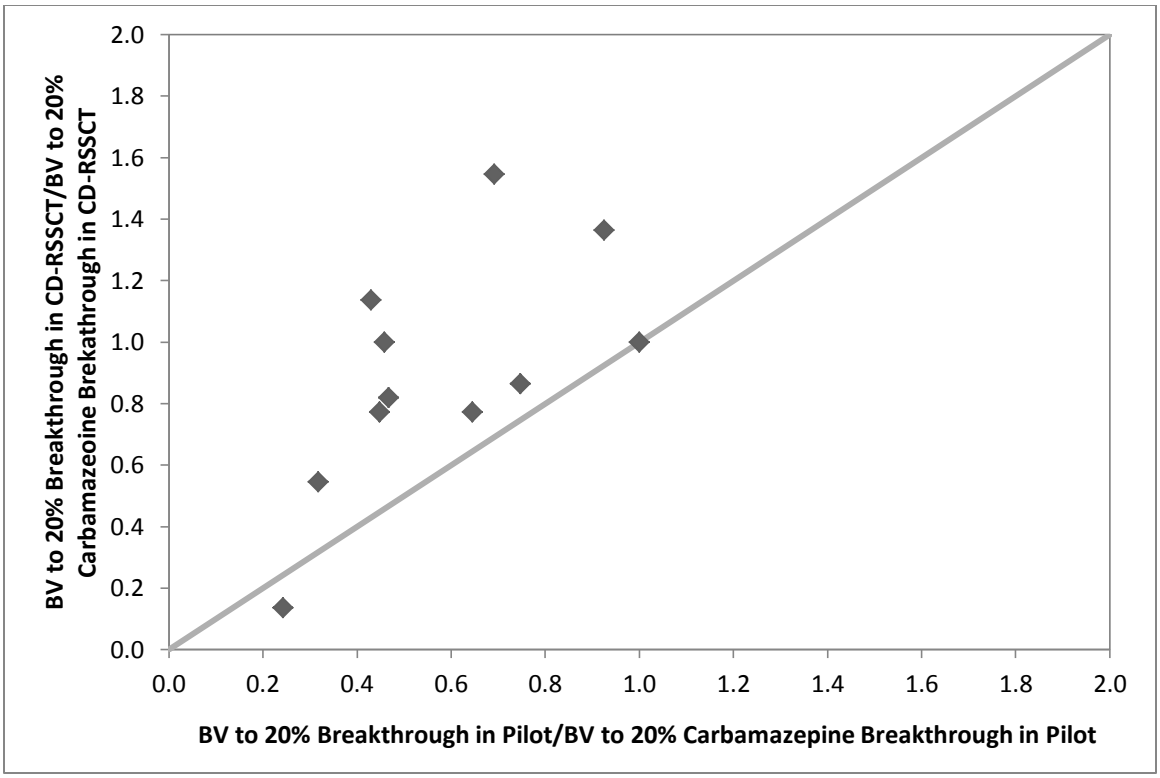

Figure 4.7: Relative MP Adsorbability in CD-RSSCT and Pilot Test

Relative to carbamazepine, the CD-RSSCT had a tendency to overpredict the relative MP adsorbability as compared to the pilot (Figure 4.7). The results in Figure 4.7 and Table 4.2 suggest that it is difficult to directly use the CD-RSSCT data to predict field-scale MP removal.

PD-RSSCT STUDY

RSSCTs based on the proportional diffusivity design were operated for 357,000 bed volumes (8 months). The objectives for the PD-RSSCT study were the following:

1. Determine the effectiveness of GAC for the removal of micropollutants
2. Determine the suitability of the PD-RSSCT design for scale-up

Out of the 34 MPs evaluated in the PD-RSSCT, 27 MPs were detected in the effluent to at least 10% of the influent concentration. Breakthrough was obtained for all MPs but acetaminophen, carbaryl, chlorpyrifos, diuron, BPA, triclosan, and ethinyl estradiol (EE2).

The 27 MPs that were detected at measureable levels in the PD-RSSCT are shown in Figures 4.8 to 4.12. For clarity, compounds were grouped by the following compound classifications: antibiotics/antimicrobials, herbicides, insecticides, pharmaceuticals, and other.

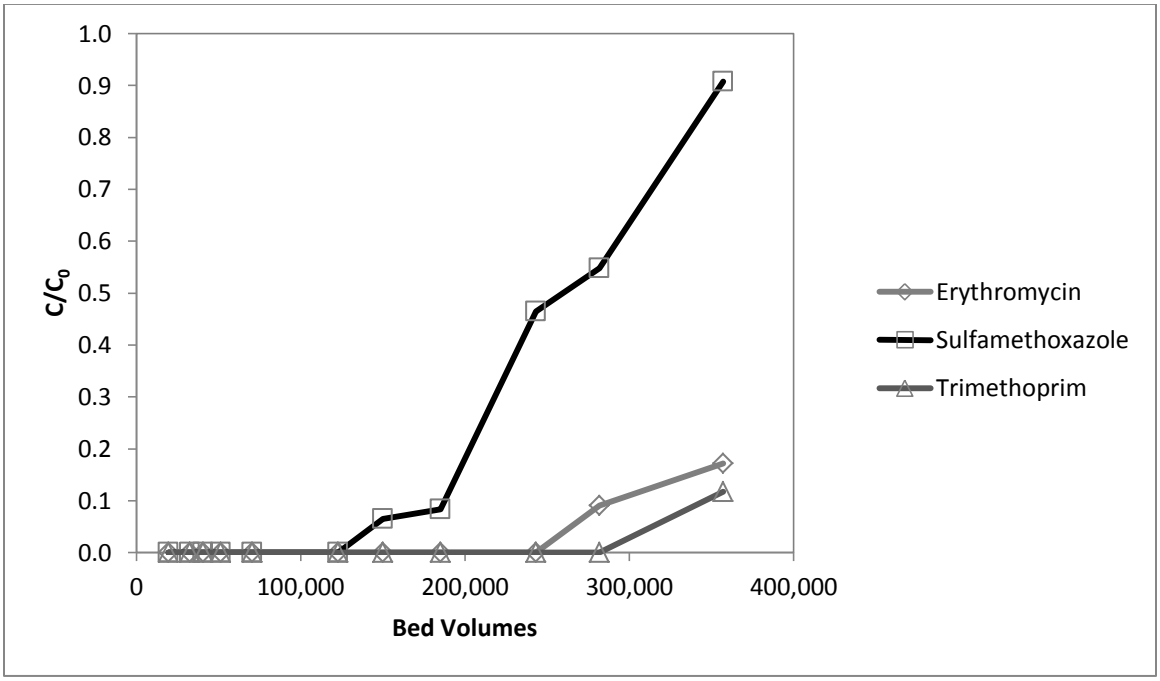

Figure 4.8: Breakthrough Curves for Antibiotic/Antimicrobial Compounds from PD-RSSCT

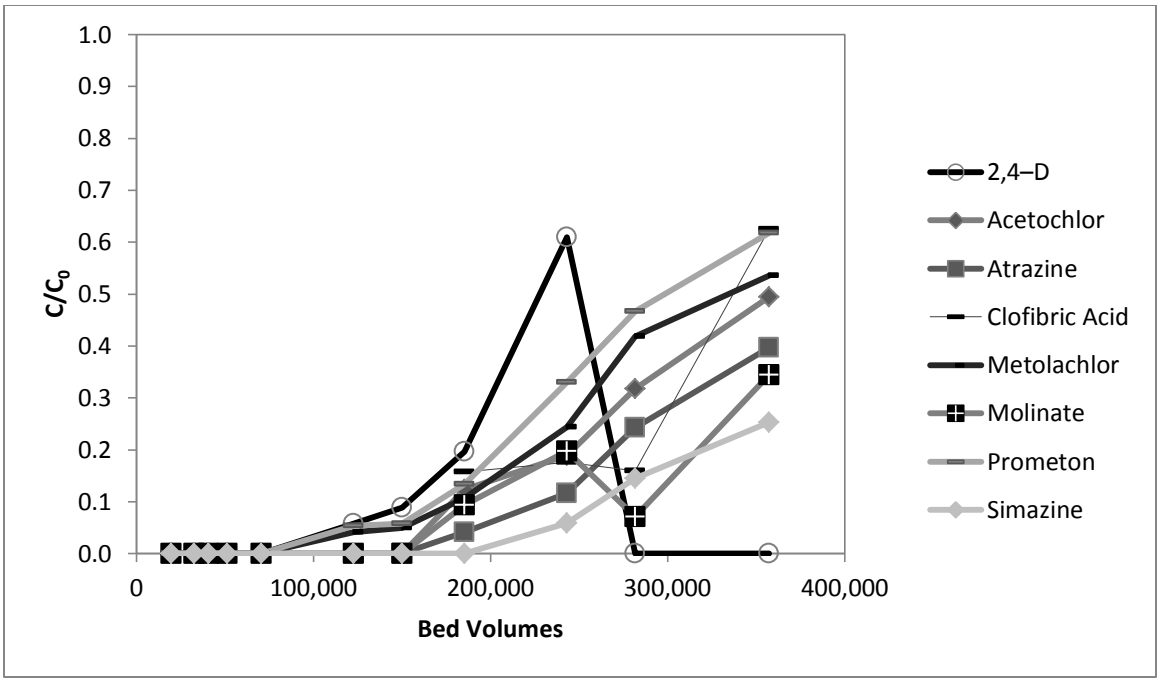

Figure 4.9: Breakthrough Curves for Herbicide Compounds from PD-RSSCT

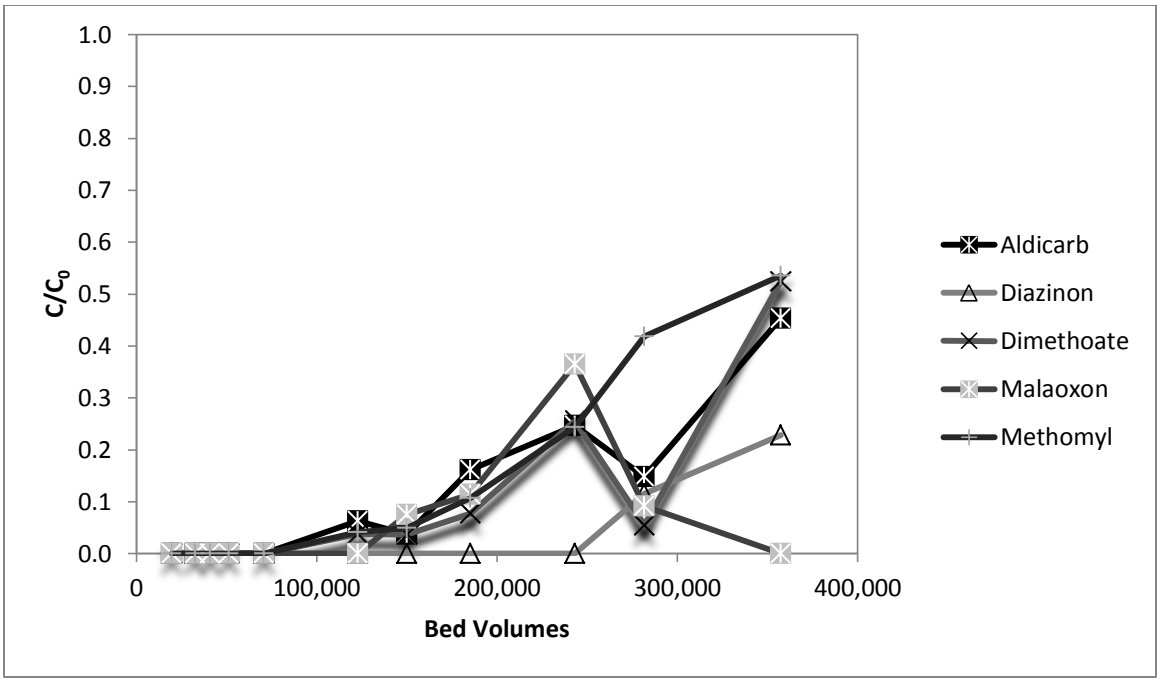

Figure 4.10: Breakthrough Curves for Insecticide Compounds from PD-RSSCT

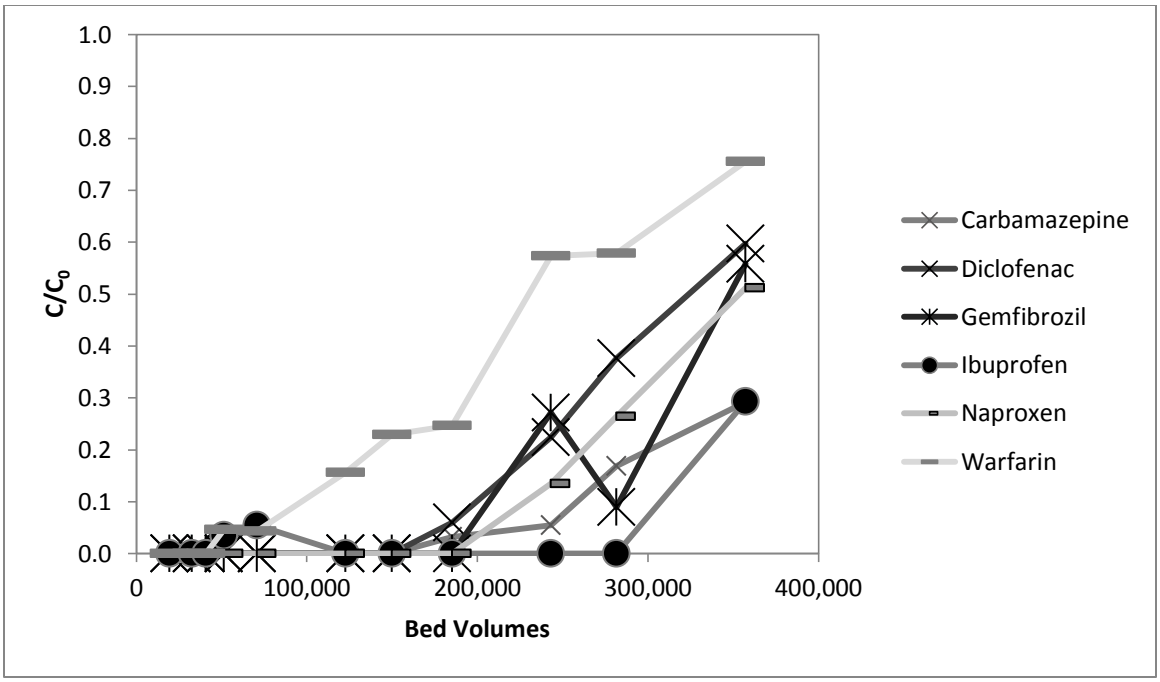

Figure 4.11: Breakthrough Curves for Pharmaceutical Compounds from PD-RSSCT

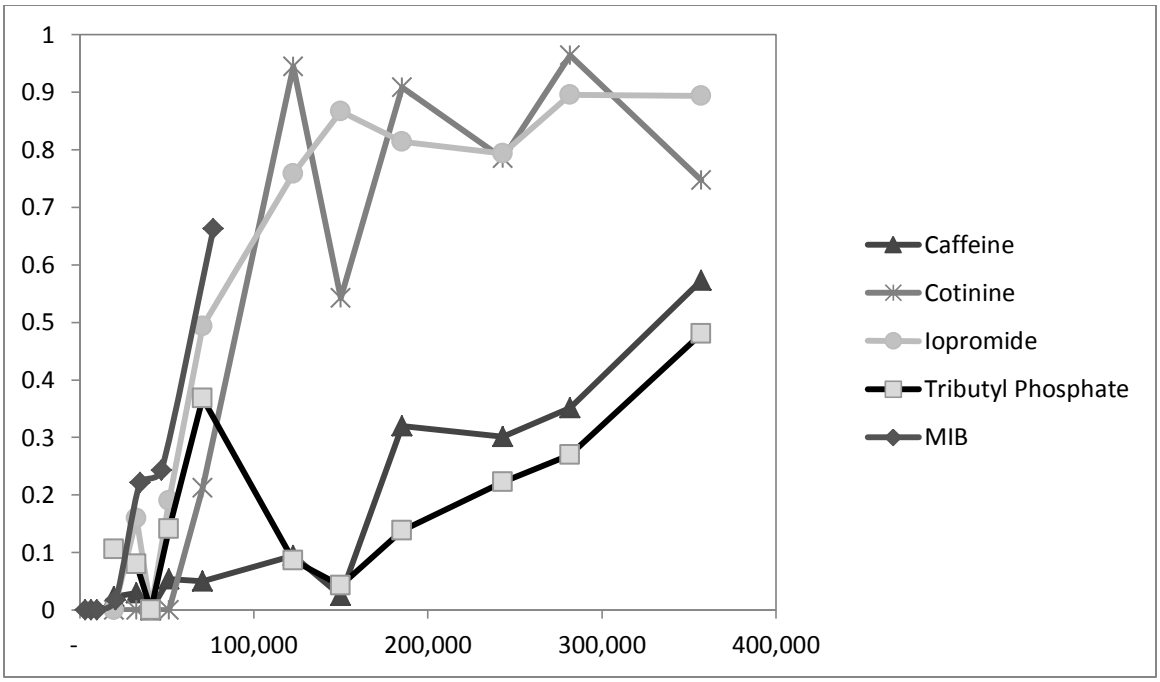

Figure 4.12: Breakthrough Curves for Other Compounds from PD-RSSCT

The MP breakthrough data from the PD-RSSCT shown in Figures 4.8 through 4.12 were used to determine the onset of MP breakthrough as well as the order of MP adsorbability In Table 4.3, the onset of MP breakthrough and the adsorption capacity of the GAC, as indicated through the bed volumes to 10% and 50% breakthrough, respectively, are compared for the pilot and PD-RSSCT data sets for the 11 MPs that broke through to measurable levels in the pilot.

Table 4.3: Onset of MP Breakthrough and Adsorption Capacity for PD-RSSCT and Pilot

Compound	Breakthrough (%)	Pilot Bed Volumes to Indicated % Breakthrough*	PD-RSSCT Bed Volumes to Indicated % Breakthrough*
Acetochlor	10	68,900	218,500
	50	112,000	314,600
Atrazine	10	84,300	236,000
	50	154,000	349,500
Caffeine	10	43,200	218,500
	50	65,900	288,400
Carbamazepine	10	88,500	270,900
	50	205,700	436,000
Cotinine	10	28,800	52,000
	50	51,400	80,000
Iopromide	10	20,600	40,000
	50	40,100	75,000
Methomyl	10	40,100	165,000
	50	62,700	227,200
Metolachlor	10	54,500	183,500
	50	109,000	323,500
Prometon	10	40,100	166,000
	50	78,200	297,100
Simazine	10	63,800	287,000
	50	102,800	410,000
Tributyl Phosphate	10	36,000	183,500
	50	83,300	384,500

* Bed volumes are based on PSDM fits

The comparisons in Table 4.3 indicate that the PD-RSSCT overpredicted both the onset of breakthrough and the MP adsorption capacity (50% breakthrough) for all 27MPs. Similarly to the CD-RSSCT, the late onset of breakthrough and the extended GAC service life was likely due to NOM fouling and a smaller percentage of the internal surface area being lost upon adsorption on smaller GAC particles.

To compare relative MP adsorbability in the pilot and the PD-RSSCT, the bed volumes to 20% breakthrough for each MP were normalized to the bed volumes to 20% carbmazepine breakthrough. The normalized PD-RSSCT bed volumes were then compared to the normalized pilot bed volumes for each MP (Figure 4.13). Carbamazepine was chosen to normalize the bed volumes for the PD-RSSCT to maintain consistency between the two RSSCT design discussions.

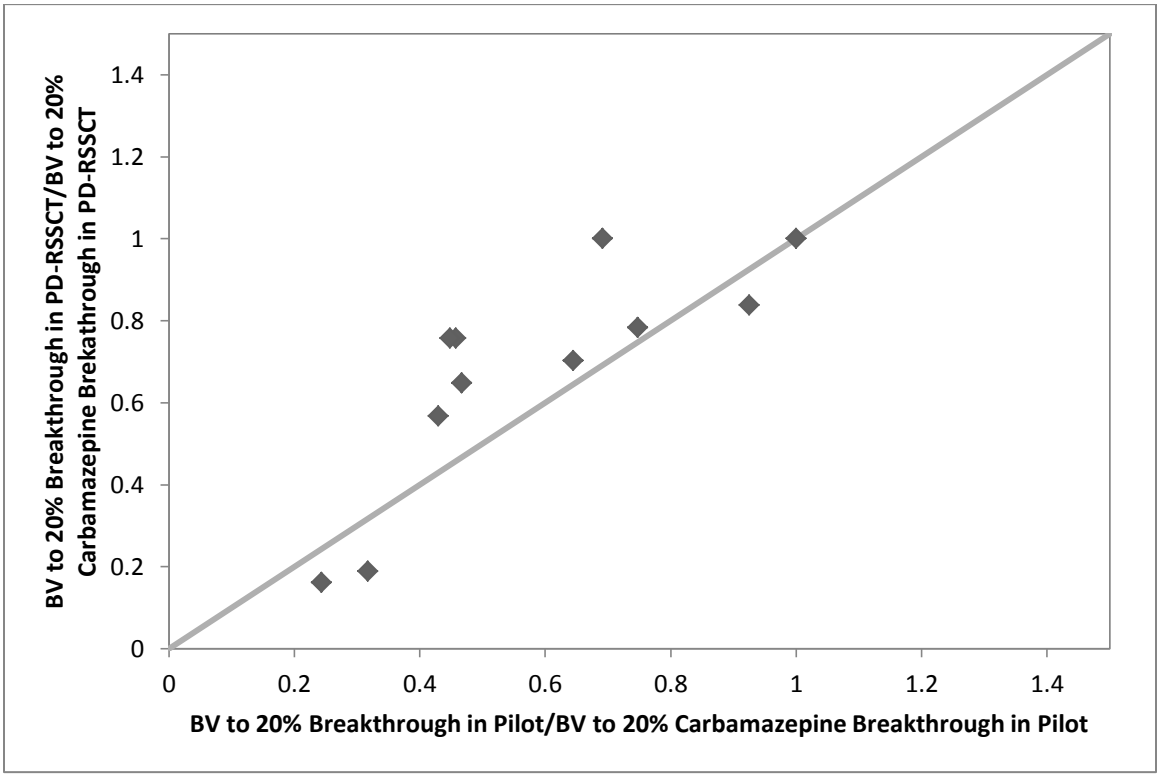

Figure 4.13: PD-RSSCT Relative Adsorbability

Compared to the CD-RSSCT results (Figure 4.7), the PD-RSSSCT data scattered more closely about the 1:1 line in Figure 4.13, indicating that the relative MP adsorbability was more effectively predicted by the PD-RSSCT.

COMPARISON OF CD-RSSCT AND PD-RSSCT

Completion of the CD-RSSCT took less time than the PD-RSSCT and produced a more complete data set. In Table 4.4, the BVs and times to reach 50% MP breakthrough are summarized for the 22 MPs, for which 50% breakthrough was obtained in at least one of the RSSCTs.

Table 4.4: CD-RSSCT and PD-RSSCT Comparison

Compound	CD-RSSCT BV to 50% Breakthrough	CD-RSSCT Time to 50% Breakthrough (days)	PD-RSSCT BV to 50% Breakthrough	PD-RSSCT Time to 50% Breakthrough (days)
2,4-D	140,000	37	--	--
Acetochlor	165,000	43	--	--
Atrazine	192,000	50	--	--
Caffeine	117,000	31	332,000	190
Carbamazepine	217,000	57	--	--
Clofibric Acid	24,000	7	257,000	148
Cotinine	82,000	22	91,000	53
Diazinon	232,000	60	--	--
Diclofenac	161,000	42	324,000	186
Dimethoate	--	--	353,000	202
Erythromycin	236,000	62	--	--
Gemfibrozil	147,000	39	348,000	200
Iopromide	22,000	6	72,000	42
Malaoxon	198,000	52	--	--
Methomyl	161,000	42	196,000	97
Metolachlor	147,000	39	334,000	192
Naproxen	209,000	55	354,000	203
Prometon	150,000	39	298,000	171
Simazine	218,000	57	--	--
Sulfamethoxazole	219,000	57	259,000	149
Tributyl Phosphate	162,000	43	--	--
Warfarin	76,000	20	230,000	132

In the CD-RSSCT, 50% breakthrough occurred first for iopromide on day 6. Twenty additional MPs had broken through to 50% by day 62, the final one being erythromycin. In the PD-RSSCT, 50% breakthrough occurred first for iopromide on day 42. Naproxen was the thirteenth and last compound to break through to 50% on day 203. The results in Table 4.4 illustrate that it took about 2 to 21 times longer to reach 50% breakthrough in the PD-RSSCT than in the CD-RSSCT. Advantages of the PD-RSSCT, on the other hand, are that the PD-

RSSCT (1) effectively predicts NOM removal and (2) more closely predicts relative MP adsorbability.

DETERMINATION OF THE FOULING FACTORS (Y-VALUES)

In order to take into account the particle-size dependent fouling of the GAC as a result of NOM adsorption, fouling factors (Y-Values) were calculates from the differences in MP adsorption capacity between the pilot and either of the RSSCTs. Fouling factors were determined for the 11 micropollutants for which measureable breakthrough was reached in the pilot test. Fouling factors had previously been determined by minimizing the sum of squares between the RSSCT data and pilot data for a particular micropollutant (Corwin, 2010). This method of determining the Y-value is highly dependent upon the breakthrough data available for the compound and does not provide insights into kinetic factors that control MP removal at the field and bench scales. Therefore, Y-values were determined from apparent Freundlich capacity parameters that resulted in the best fit of the pore surface diffusion model (PSDM) to the pilot and RSSCT data. The PSDM, embedded in the software package AdDesignS, was used to determine equilibrium (i.e. Freundlich capacity) and kinetic parameters describing the adsorption of each of the 11 MPs. Fouling factors (Y) were determined from Freundlich capacity parameters (K) as follows:

$$SF^{Y} = \left[\frac{K_{RSSCT}}{K_{Pilot}}\right] \tag{3.9}$$

Where Y is solved for by using:

$$Y = \left[\frac{Log(K_{RSSCT}/K_{Pilot})}{Log(SF)}\right] \tag{3.10}$$

The methods described in Chapter 3 were used to obtain PSDM outputs shown in the subsequent sections.

PSDM Description of Pilot Data

To describe the pilot data with the PSDM, the fixed bed parameters, adsorbent properties, simulation parameters and number of collocation points shown in Table 4.5 were used. These input parameters were the same for all MPs.

Table 4.5: PSDM Input Parameters for Pilot Modeling

Input Type	Parameter	Value
Fixed Bed Properties	Bed Length	58.3 cm
	Bed Diameter	2.54 cm
	Dry GAC Mass	136 g
	Flow Rate	42.2 mL/min
	EBCT	7.00 min
Adsorbent Properties	Apparent Particle Density	0.730 g/mL
	Particle Radius	4.60E-4 m
	Particle Porosity	0.500
	Particle Shape Factor	1.00
Simulation Parameter	Total Run Time	600 days
	First Point Displayed	6.48E-8 days
	Time Step	5 days
	Number of Axial Elements	10
Number of Collocation Points	Axial Direction	8
	Radial Direction	5

Once the input parameters were set in Table 4.5, the adsorption equilibrium and kinetic parameters needed to be determined. Two adjustable parameters were set to describe each MP breakthrough curve. The Freundlich K was initially calculated with

$$K^* = \left[\frac{BV_{50}}{\rho_{bed}}\right] \tag{3.5}$$

and the intraparticle diffusive flux was initially set to the maximum pore diffusion flux (τ=1, SPDFR=1E-30). If the PSDM output resulted in a breakthrough curve that was steeper than the pilot data, the tortuosity was increased until the best fit was achieved. If the PSDM output resulted in a breakthrough curve that was too flat, the tortuosity was kept at a value of one, and surface diffusion was invoked by increasing the value of the SPDFR until a good fit for the experimental breakthrough curve was obtained. Subsequently, the K value was fine-tuned

to obtain the best fit for the experimental data. The Freundlich K, SPDFR, and τ values for each of the 11 MPs, for which measureable breakthrough was obtained in the pilot study, are shown in Table 4.6.

Table 4.6: Equilibrium and Kinetic Parameters for Pilot Test

Compound	**K $(mg/g)(L/mg)^{(1/n)}$**	**SPDFR**	**τ**	**Normalized Total Flux***
Acetochlor	250	10.88	1.00	11.88
Atrazine	315	6.56	1.00	7.56
Caffeine	145	16.28	1.00	17.28
Carbamazepine	360	4.00	1.00	5.00
Cotinine	115	3.32	1.00	4.32
Iopromide	90	7.50	1.00	8.50
Methomyl	140	0.85	1.00	1.85
Metolachlor	250	2.50	1.00	3.50
Prometon	180	2.58	1.00	3.58
Simazine	230	7.64	1.00	8.64
Tributyl Phosphate	200	1.13	1.00	2.13

*Total normalized flux = 1 for maximum pore diffusion (τ = 1, SPDFR=10^{-30})

Using the equilibrium and kinetic parameters shown in Table 4.6 along with the PSDM input parameters in Table 4.5, PSDM outputs were obtained for the 11 MPs for which measureable levels were detected in the pilot column effluent. A comparison between the PSDM outputs and the pilot data are shown in Figure 4.14. For clarity the results of the 11 MPs are shown in two panels (a and b).

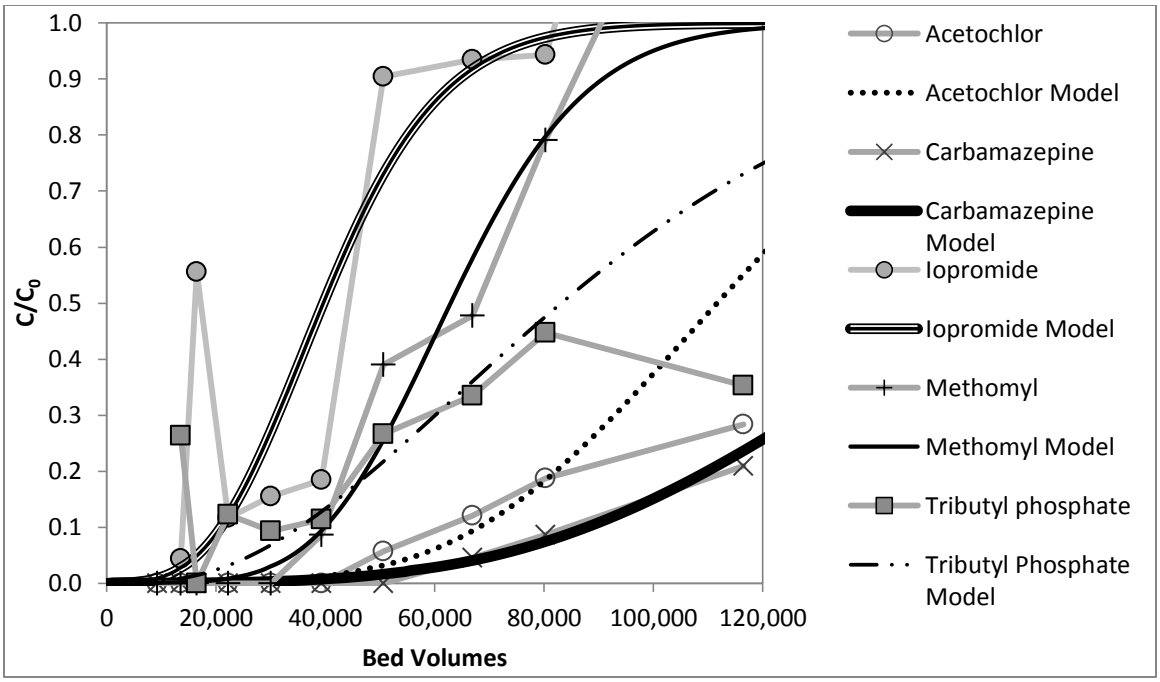

(a)

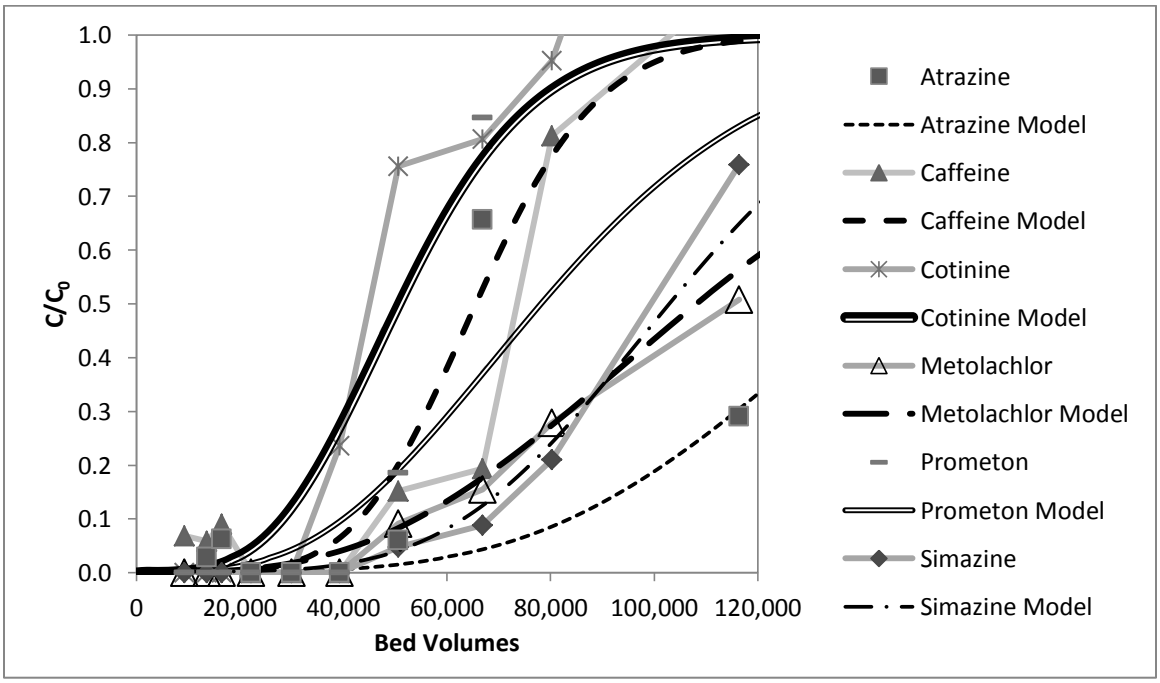

(b)

Figure 4.14: Comparison between PSDM Output and Pilot Column Data

PSDM Description of CD-RSSCT Data

PSDM fits for the CD-RSSCT were obtained in a manner similar to that described for the pilot data. The PSDM input parameters for the CD-RSSCT are shown in Table 4.7.

Table 4.7: Input Parameters for CD-RSSCT PSDM Modeling

Input Type	Parameter	Value
Fixed Bed Properties	Bed Length	13.5 cm
	Bed Diameter	0.754 cm
	Dry GAC Mass	2.78 g
	Flow Rate	16.1 mL/min
	EBCT	0.374 min
Adsorbent Properties	Apparent Particle Density	0.730 g/mL
	Particle Radius	1.07E-4 m
	Particle Porosity	0.500
	Particle Shape Factor	1.00
Simulation Parameter	Total Run Time	100 days
	First Point Displayed	6.48E-8 days
	Time Step	1 day
	Number of Axial Elements	10
Number of Collocation Points	Axial Direction	8
	Radial Direction	5

The equilibrium parameter, K, was calculated as described in the previous section. In contrast, the total CD-RSSCT flux constrained to be a function of the pilot flux and the scaling factor for the CD-RSSCT is as follows:

$$RSSCT\ Flux = \frac{Pilot\ Flux}{Scaling\ Factor} \tag{4.1}$$

Initial attempts were made to describe both pilot and CD-RSSCT breakthrough curves with the same total flux value because the CD-RSSCT design is based on the assumption that intraparticle diffusivity is independent of GAC particle size. However, this approach of constraining the flux resulted in poor fits of the pilot data when the RSSCT flux was used or poor fit of the RSSCT data when the pilot flux was used. PSDM fits for methomyl are shown in Figures 4.15 for the case where the pilot data were described with the intraparticle flux that best described the RSSCT data. In Figure 4.16, the intraparticle flux was scaled linearly with particle size according to equation 4.1. A comparison of Figure 4.15 and 4.16 shows that the latter approach resulted in model outputs that more closely matched the data.

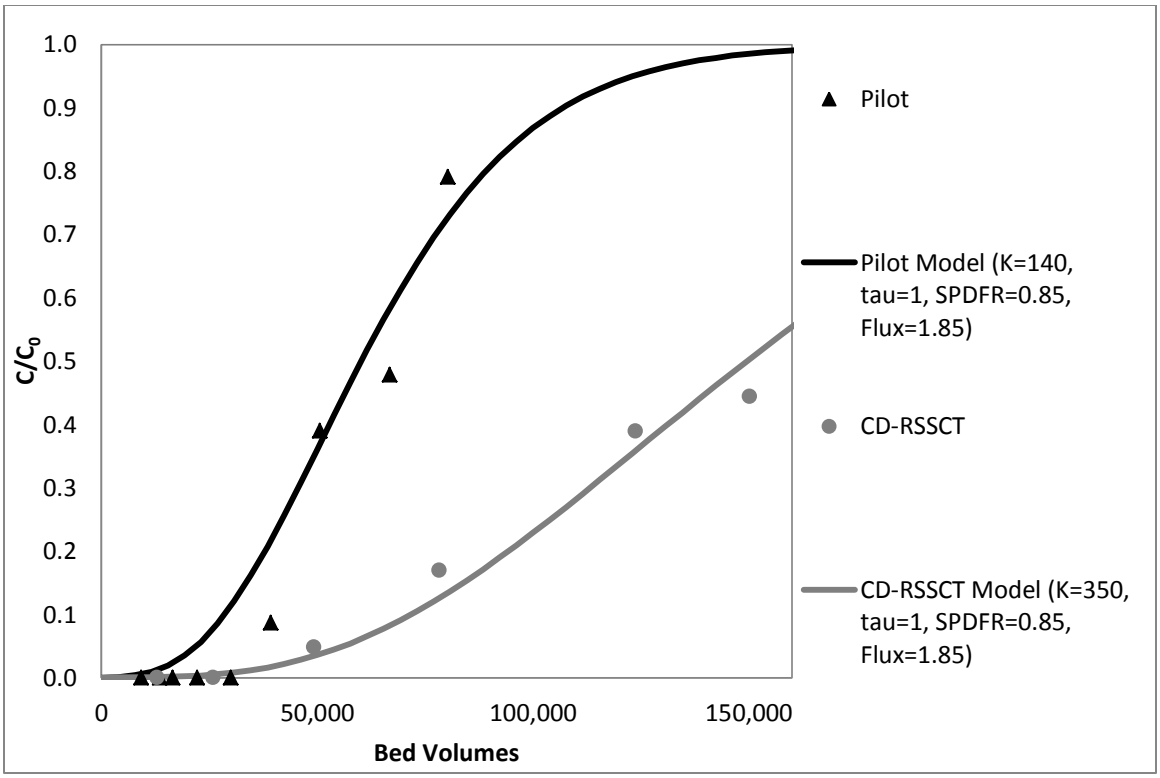

Figure 4.15: PSDM Fits for Methomyl Pilot and CD-RSSCT Breakthrough Data with Intraparticle Flux Kept Constant

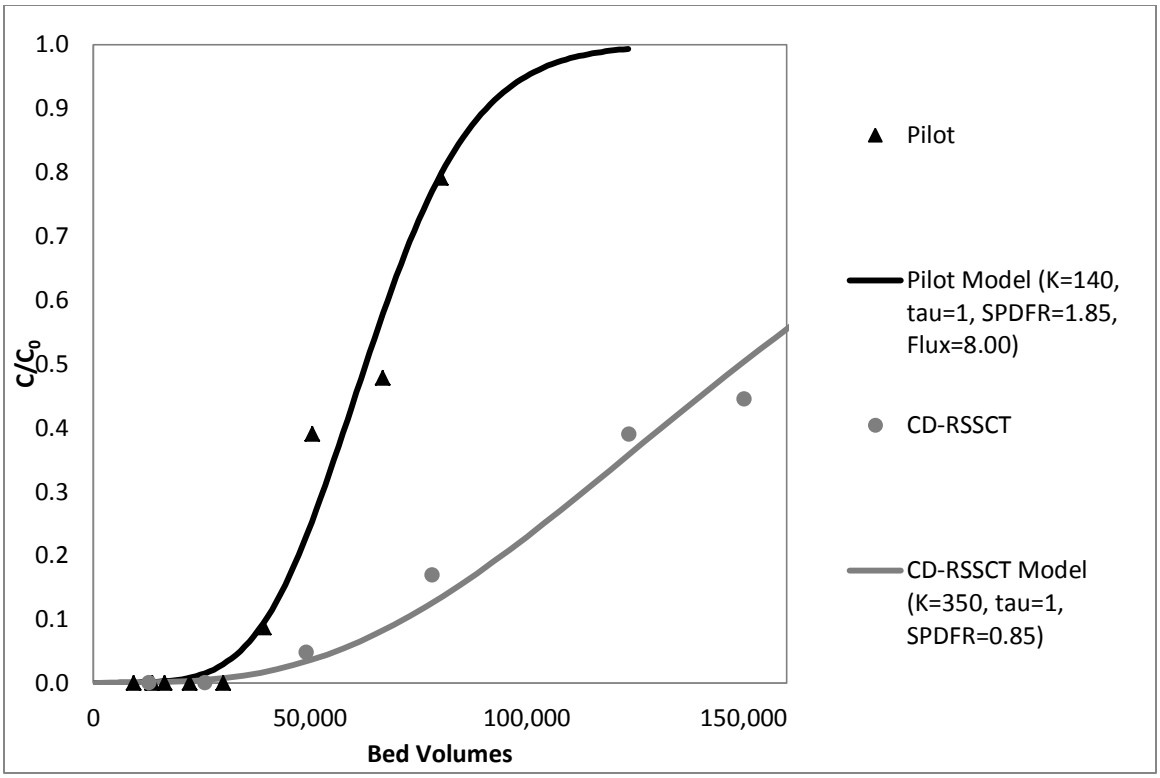

Figure 4.16: PSDM Fits for Methomyl Pilot and CD-RSSCT Breakthrough Data with Particle Size-Adjusted Intraparticle Flux

Thus, the PSDM results suggest that MP diffusivity in the presence of NOM varies linearly with particle size. While the CD-RSSCT design approach does not account for this dependence, the PSDM can be used for scaling purposes to address the particle size dependence of the intraparticle flux.

The Freundlich K, SPDFR, and τ values used to describe the CD-RSSCT data are shown in Table 4.8. The kinetic parameters shown in Table 4.8 illustrate that surface diffusion needed to be involved for 7 of the 11 MPs, and SPDFRs ranged from 0.16 to 3. For the remaining 4 MPs, pore diffusion was sufficient to describe intraparticle mass transfer and τ values ranged from 1 to 2.

Table 4.8: Equilibrium and Kinetic Parameters for CD-RSSCT

Compound	**K** $(mg/g)(L/mg)^{(1/n)}$	**SPDFR**	**τ**	**Flux**
Acetochlor	400	1.75	1.00	2.75
Atrazine	475	0.75	1.00	1.75
Caffeine	275	3.00	1.00	4.00
Carbamazepine	615	0.16	1.00	1.16
Cotinine	225	1E-30	1.00	1.00
Iopromide	45	0.97	1.00	1.97
Methomyl	350	0.85	1.00	1.85
Metolachlor	400	1E-30	1.23	0.81
Prometon	400	1E-30	1.21	0.83
Simazine	500	1.00	1.00	2.00
Tributyl Phosphate	575	1E-30	2.03	0.49

Using the equilibrium and kinetic parameters shown in Table 4.8 along with the PSDM input parameters in Table 4.7, PSDM outputs were obtained for the 11 MPs for which measureable levels were detected in the pilot column effluent. To facilitate comparisons with pilot column data, CD-RSSCT data and corresponding fits are shown by compound class (herbicides in Figure 4.17, insecticide in Figure 4.18, and the remaining MPs in Figure 4.19).

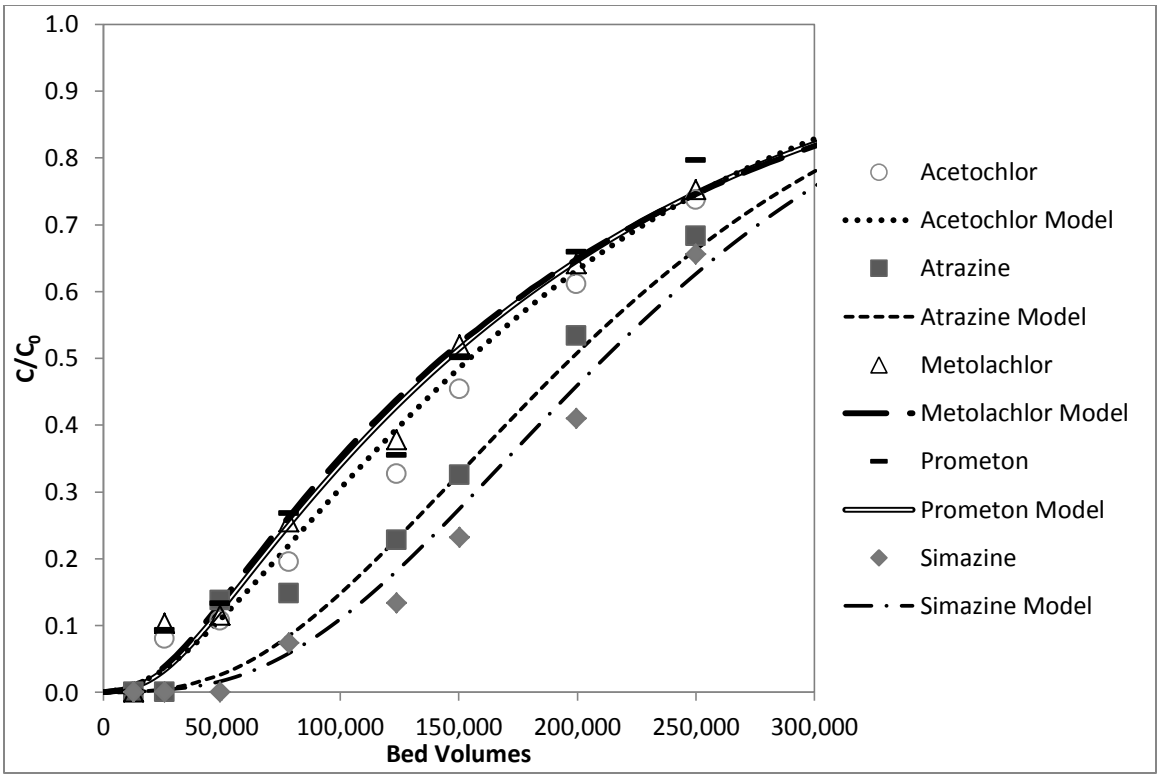

Figure 4.17: Comparison of CD-RSSCT Data and PSDM Fits for 5 Herbicides

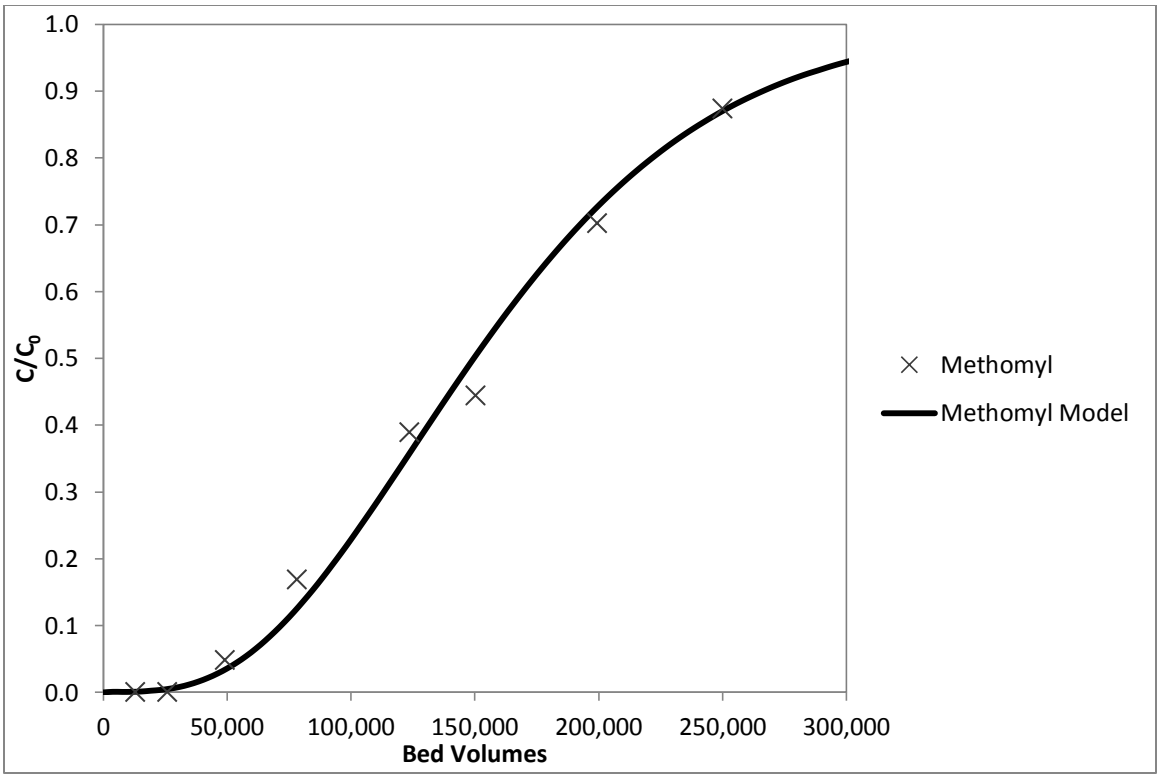

Figure 4.18: Comparison of CD-RSSCT Data and PSDM Fit for the Insecticide Methomyl

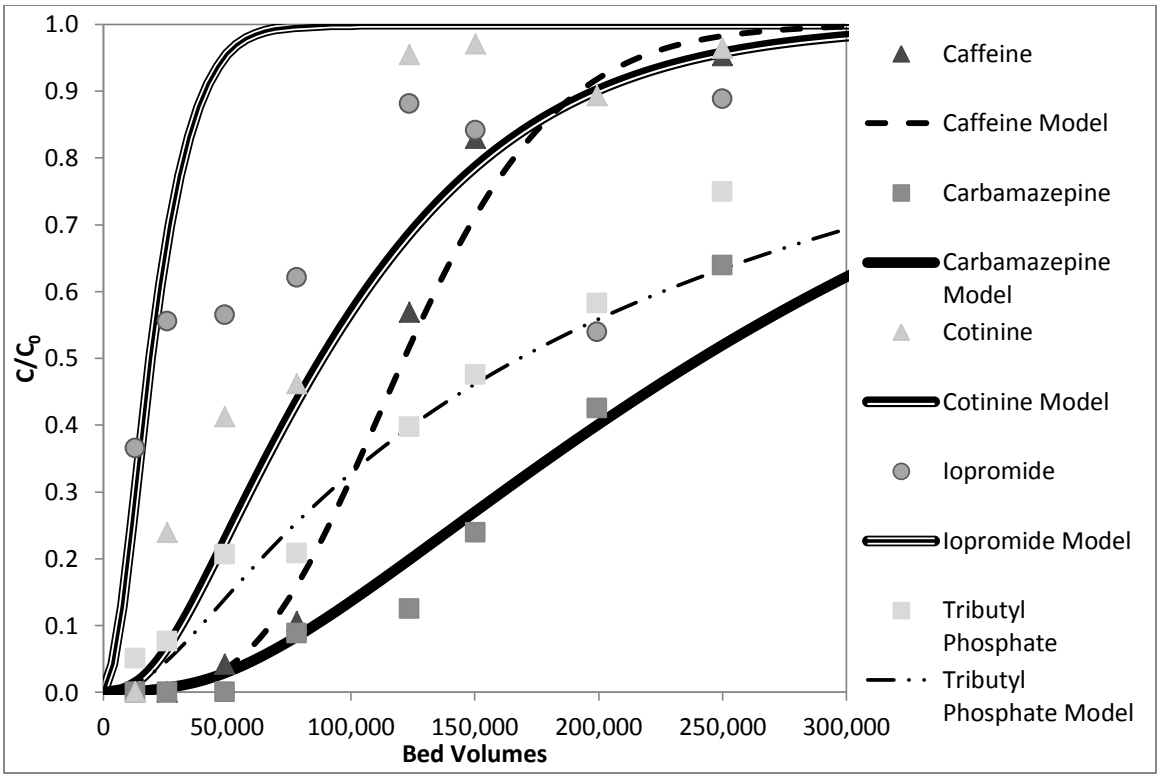

Figure 4.19: Comparison of CD-RSSCT Data and PSDM Fits for Five Additional Compounds

PSDM Description of PD-RSSCT Data

PSDM fits for the PD-RSSCT were obtained in a manner similar to that described for the CD-RSSCT data. The PSDM input parameters for the PD-RSSCT are shown in Table 4.9.

Table 4.9: Input Parameters for PD-RSSCT PSDM Modeling

Input Type	Parameter	Value
Fixed Bed Properties	Bed Length	9.26 cm
	Bed Diameter	4.76E-3 cm
	Dry GAC Mass	0.758 g
	Flow Rate	2.00 mL/min
	EBCT	0.824 min
Adsorbent Properties	Apparent Particle Density	0.730 g/mL
	Particle Radius	5.05E-5 m
	Particle Porosity	0.500
	Particle Shape Factor	1.00
Simulation Parameter	Total Run Time	250 days
	First Point Displayed	13.2 days
	Time Step	5 day
	Number of Axial Elements	10
Number of Collocation Points	Axial Direction	8
	Radial Direction	5

The equilibrium parameter K and the intraparticle flux were calculated by equations 3.5 and 4.1. The PD-RSSCT design is predicated on the assumption that intraparticle diffusivity is linearly dependent on GAC particle size and good fits were achieved with this assumption. For illustrative purposes, PSDM outputs and corresponding RSSCT and pilot breakthrough data for metolachlor are shown in Figure 4.20.

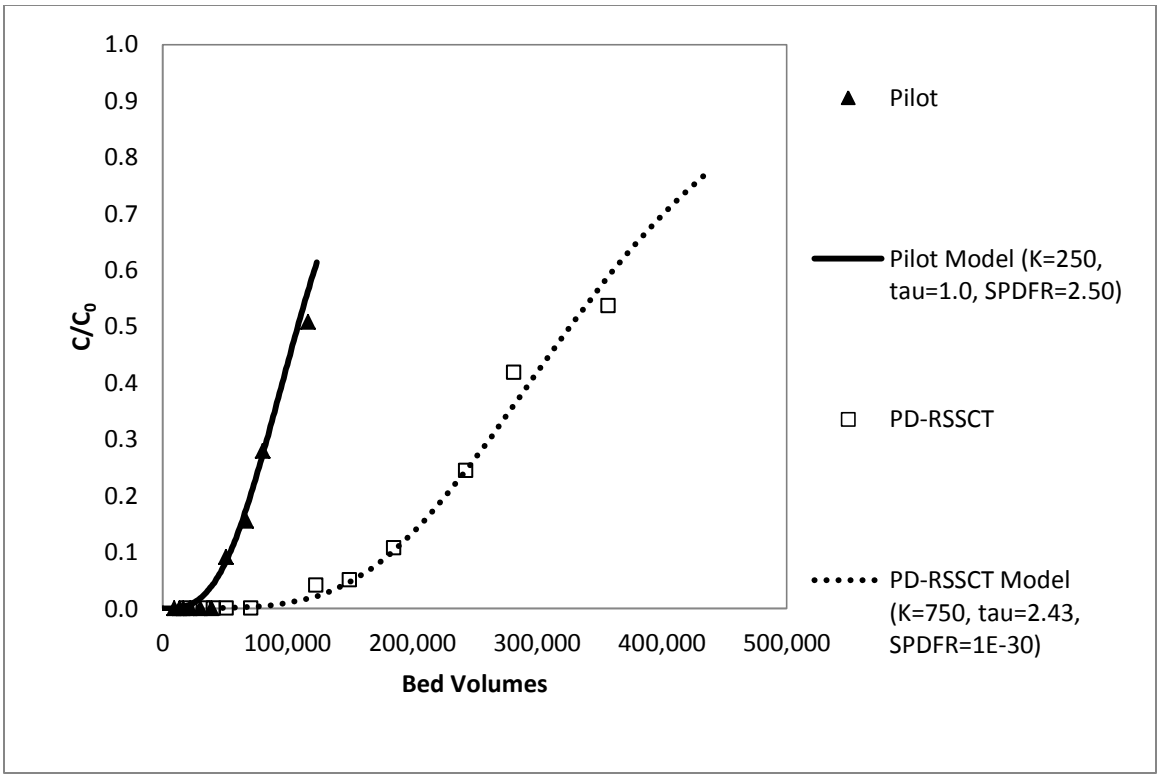

Figure 4.20: Comparison of Metolachlor Breakthrough data Obtained in PD-RSSCT and Pilot Test and Corresponding PSDM Fits

The Freundlich K, SPDFR, and τ values used to describe the PD-RSSCT data are shown in Table 4.10. The kinetic parameters shown in Table 4.10 show that surface diffusion needed to be invoked for acetochlor and caffeine, while, pore diffusion was sufficient to describe adsorption rates of the remaining 9 MPs. Tortuosity values for the latter 9 MPs ranged from 1 to 4.

Table 4.10: Equilibrium and Kinetic Parameters for PD-RSSCT

Compound	K $(mg/g)(L/mg)^{(1/n)}$	SPDFR	τ	Flux
Acetochlor	690	0.40	1.00	1.40
Atrazine	775	1E-30	1.12	0.89
Caffeine	635	1.03	1.00	2.03
Carbamazepine	975	1E-30	1.70	0.59
Cotinine	190	1E-30	1.97	0.51
Iopromide	172	1E-30	1.00	1.00
Methomyl	500	1E-30	1.06	0.94
Metolachlor	750	1E-30	2.43	0.41
Prometon	675	1E-30	2.38	0.42
Simazine	900	0.02	1.00	1.02
Tributyl Phosphate	925	1E-30	4.00	0.25

Using the equilibrium and kinetic parameters shown in Table 4.10 along with the PSDM input parameters in Table 4.9, PSDM outputs were obtained for the 11 MPs for which measureable levels were detected in the pilot column effluent. To facilitate comparisons with pilot column data, PD-RSSCT data and corresponding fits are shown by compound class (herbicides in Figure 4.21, insecticide in Figure 4.22, and the remaining MPs in Figure 4.23).

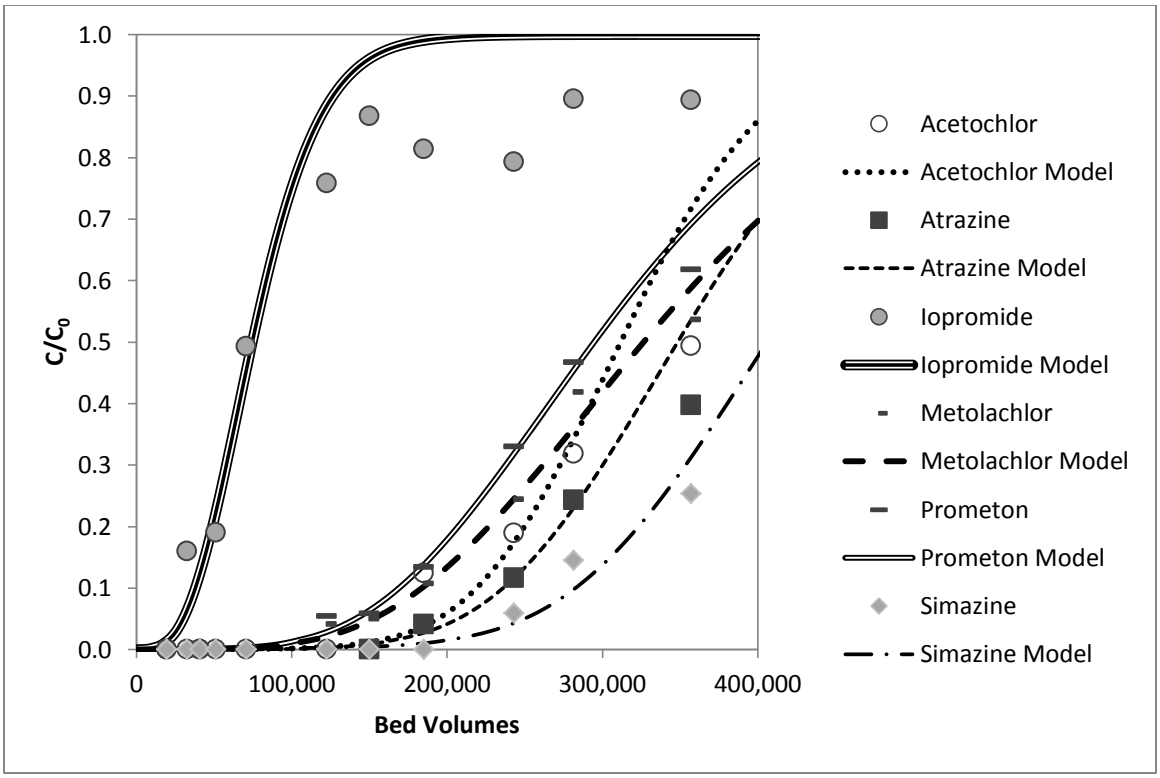

Figure 4.21: Comparison of PD-RSSCT Data and PSDM Fits for 5 Herbicides

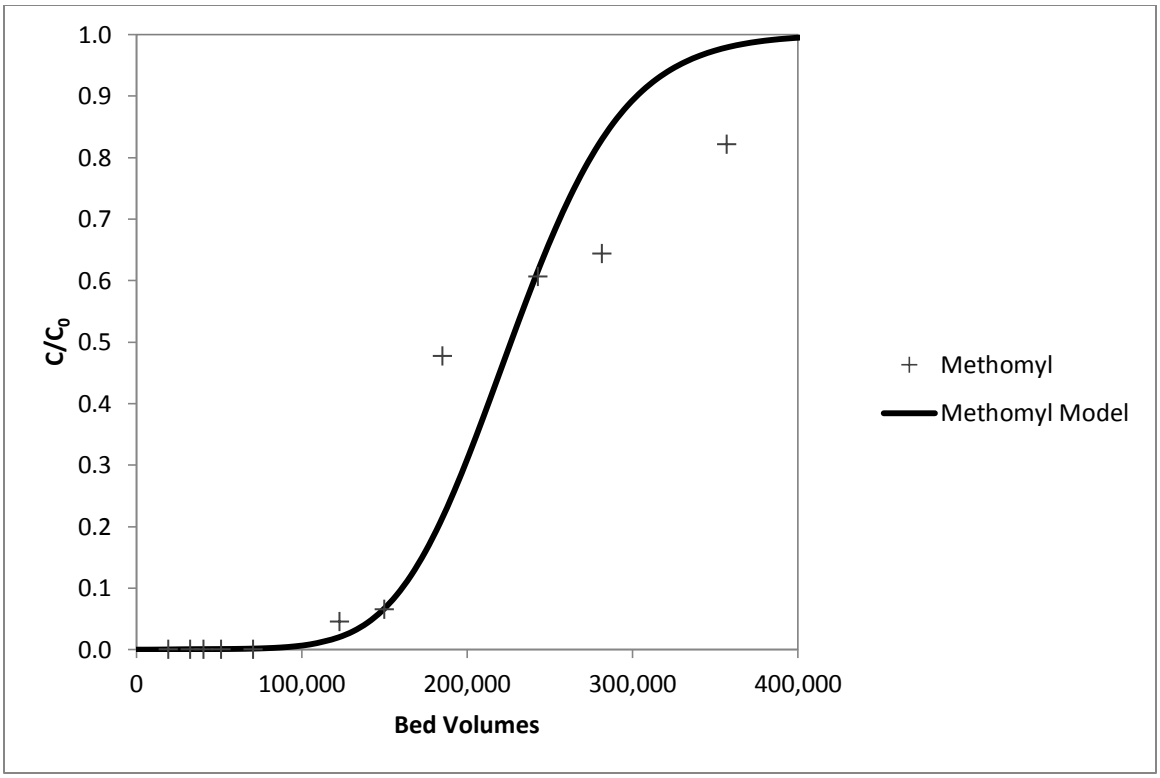

Figure 4.22: Comparison of PD-RSSCT Data and PSDM Fit for the Insecticide Methomyl

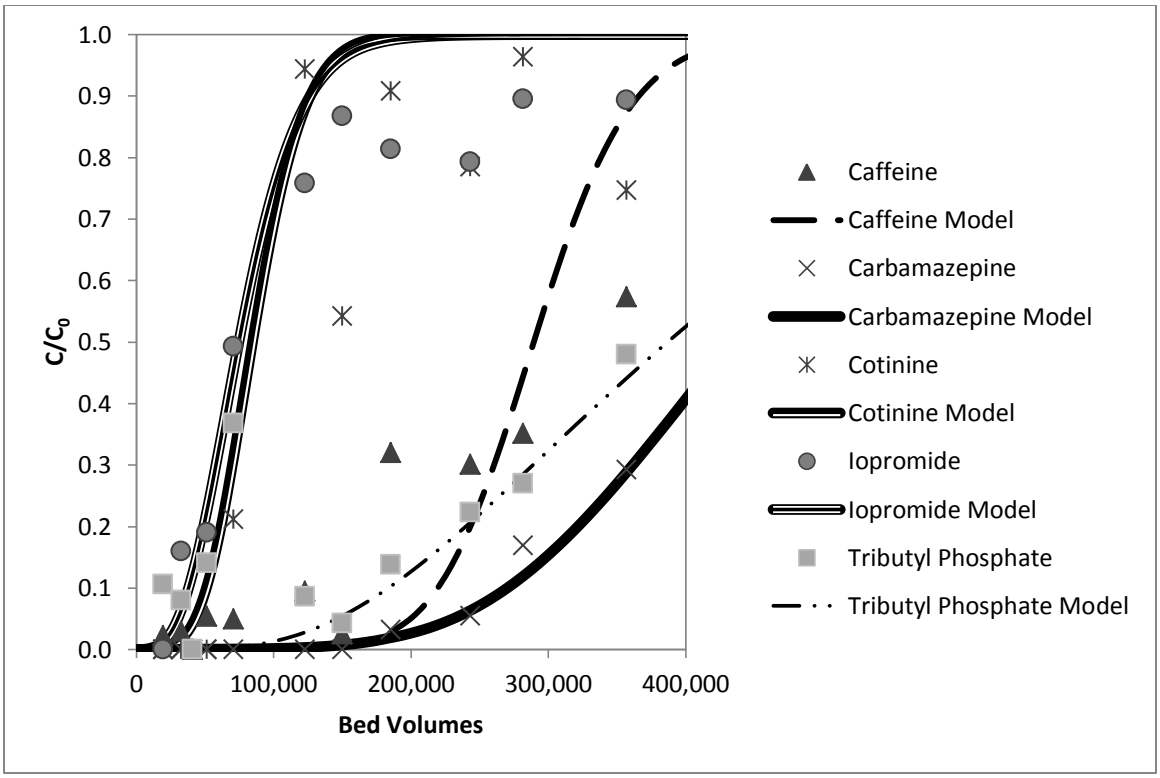

Figure 4.23: Comparison of PD-RSSCT Data and PSDM Fits for Five Additional Compounds

Comparison Between Pilot, CD-RSSCT and PD-RSSCT

This section outlines the differences between the modeled breakthrough curves for the pilot test, CD-RSSCT and the PD-RSSCT for the 11 MPs, for which measureable breakthrough was reached in the pilot test. The test comparisons illustrated in Figures 4.24 through 4.34 in this section are shown for each MP in the order in which they broke through in the pilot test.

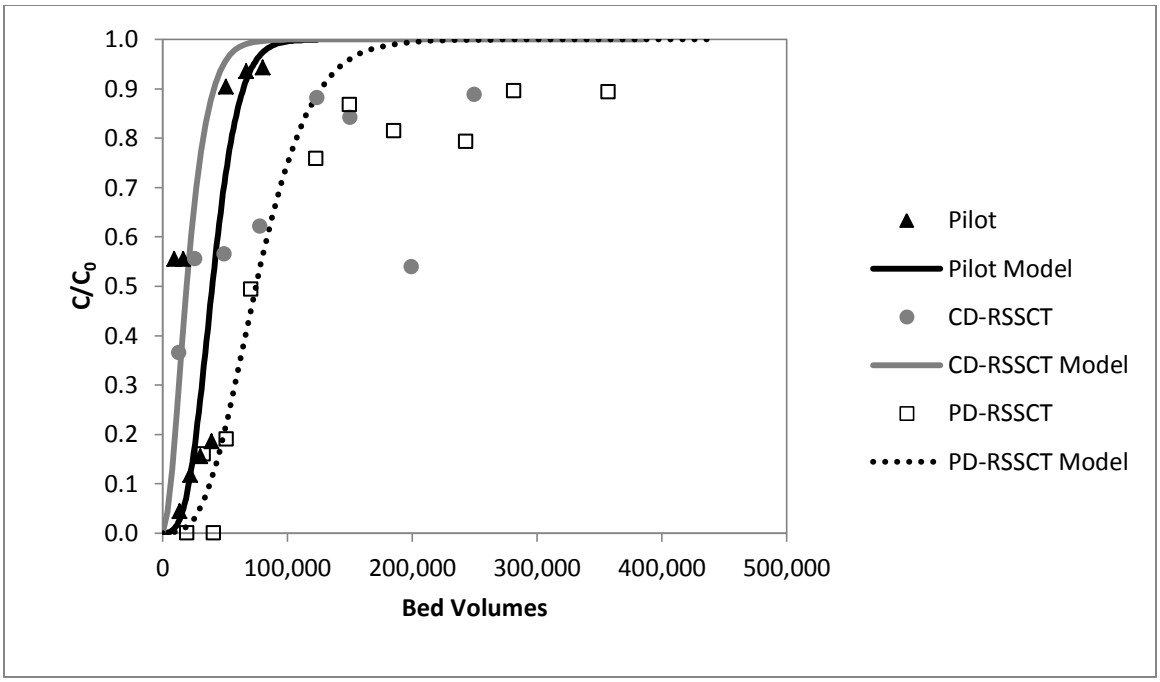

Figure 4.24: Iopromide Breakthrough Data and PSDM Fits

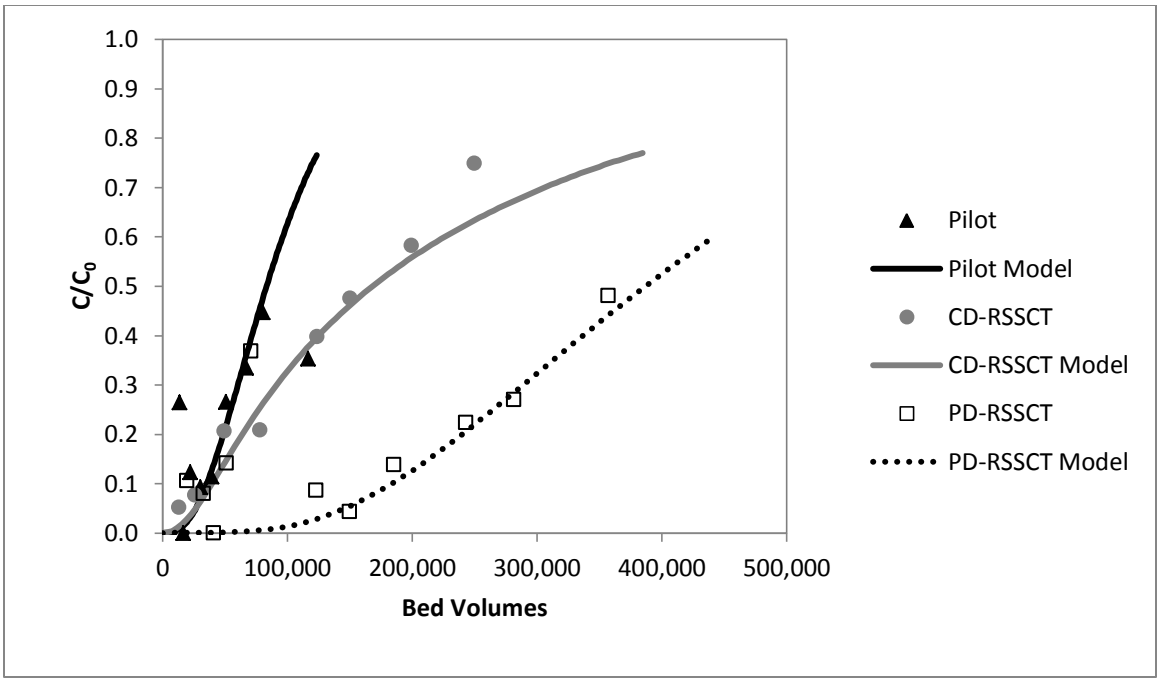

Figure 4.25: Tributyl Phosphate Breakthrough Data and PSDM Fits

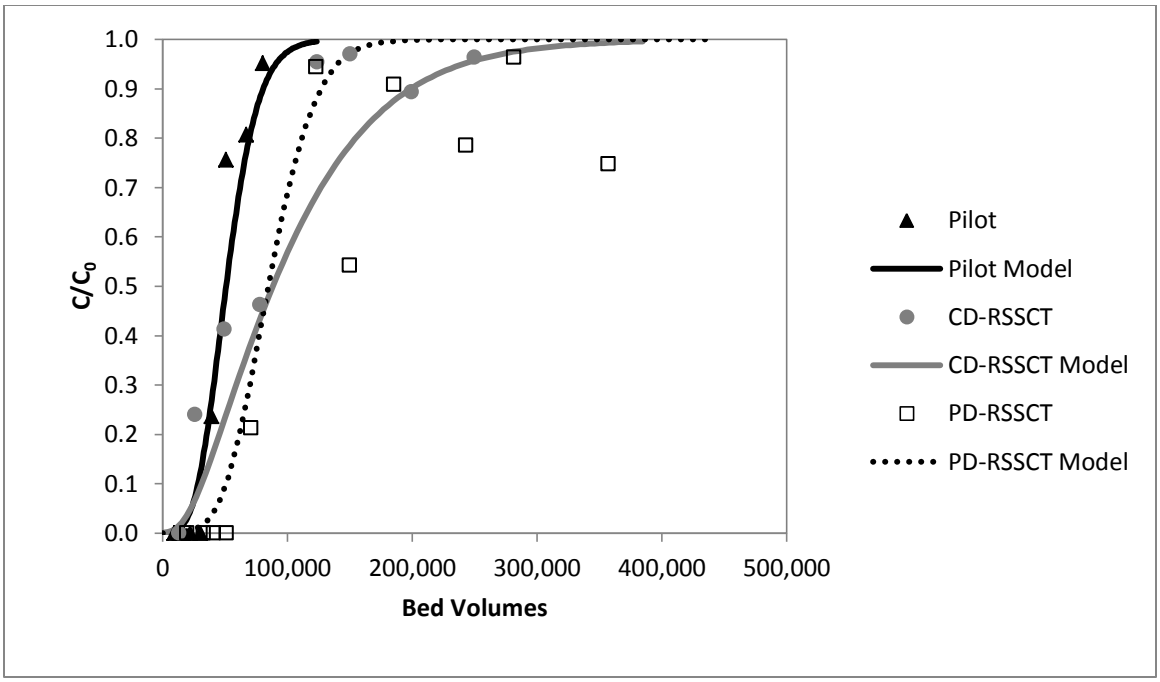

Figure 4.26: Cotinine Breakthrough Data and PSDM Fits

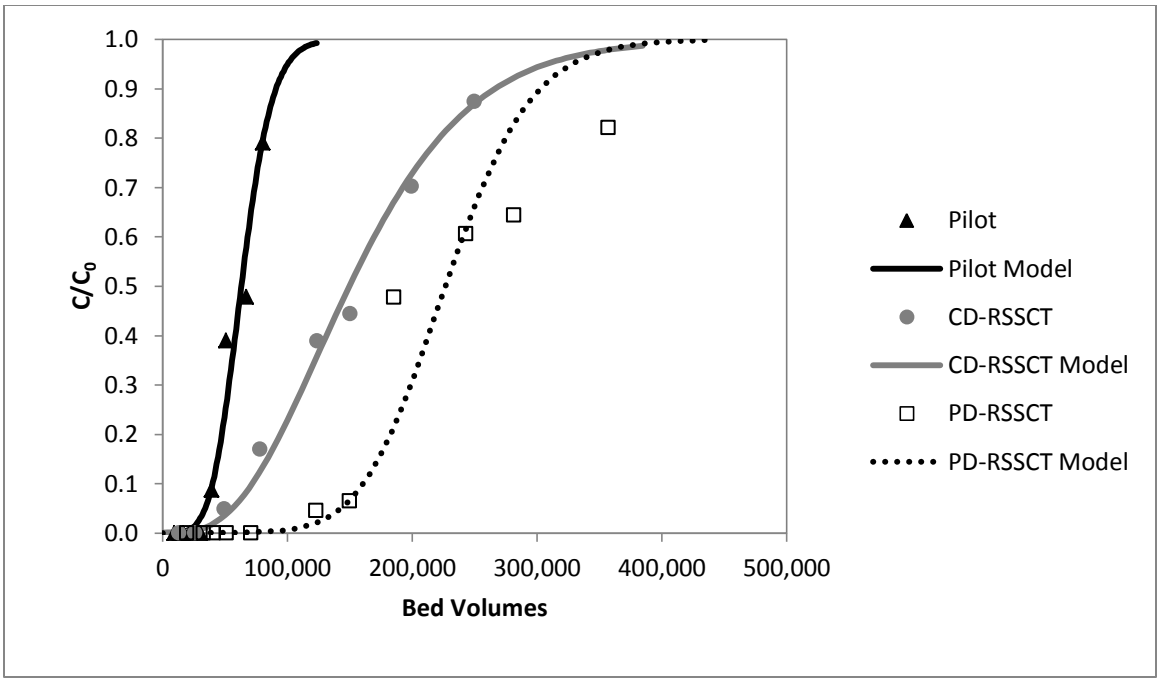

Figure 4.27: Methomyl Breakthrough Data and PSDM Fits

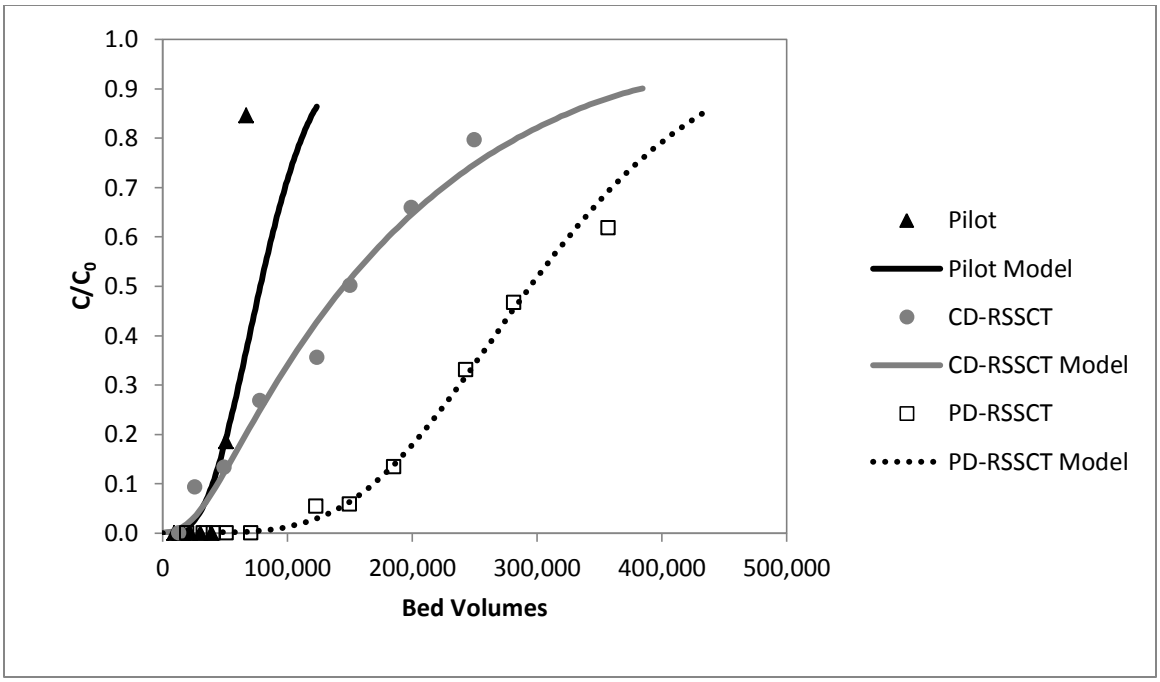

Figure 4.28: Prometon Breakthrough Data and PSDM Fits

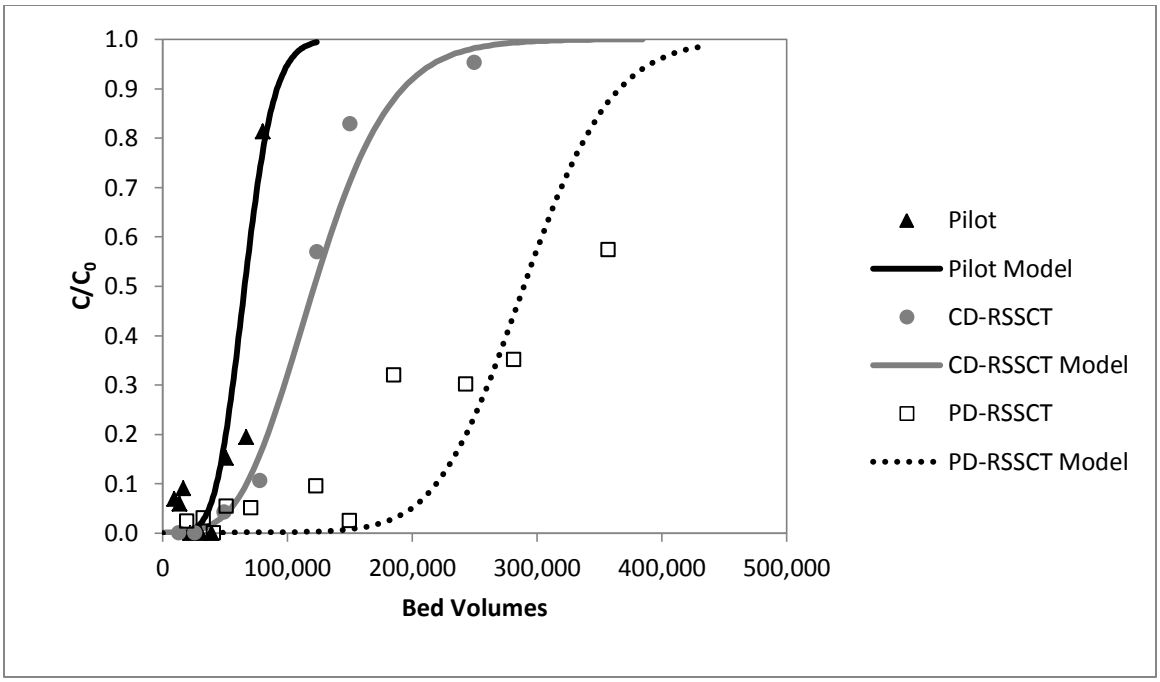

Figure 4.29: Caffeine Breakthrough Data and PSDM Fits

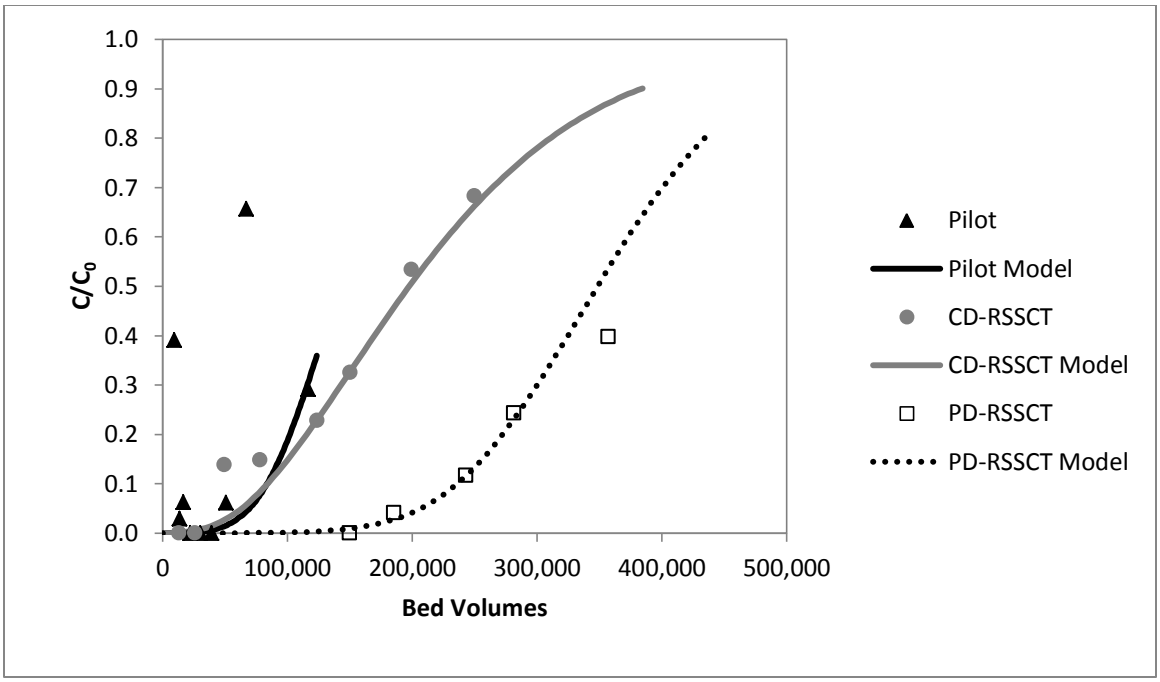

Figure 4.30: Atrazine Breakthrough Data and PSDM Fits

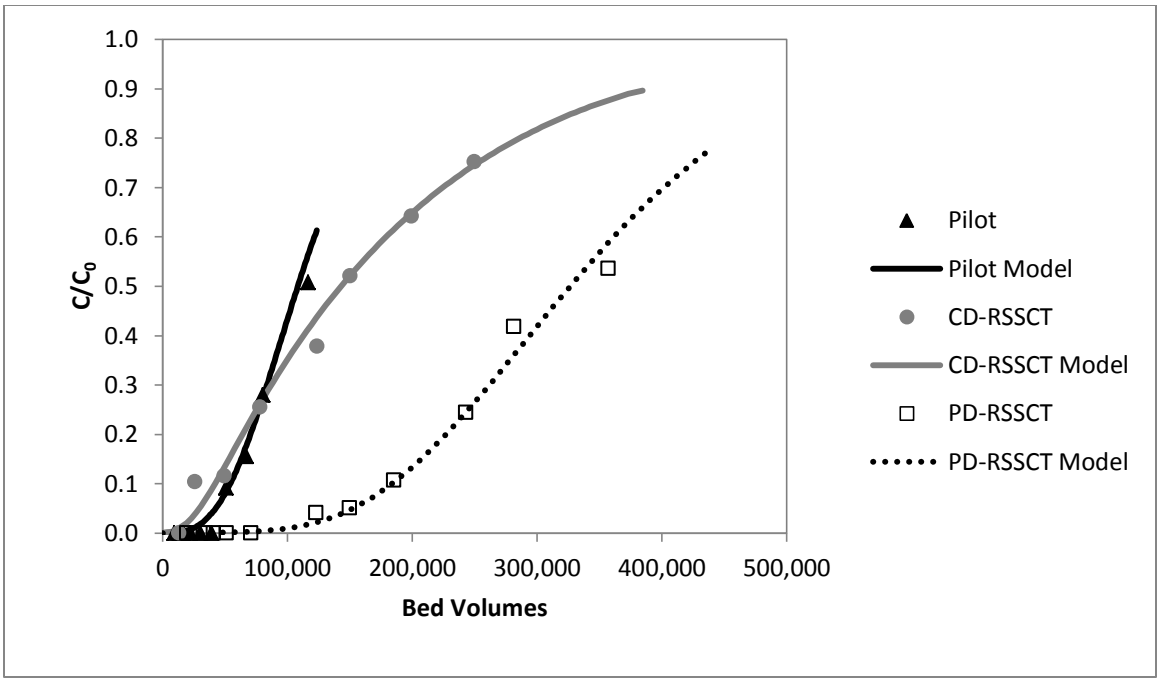

Figure 4.31: Metolachlor Breakthrough Data and PSDM Fits

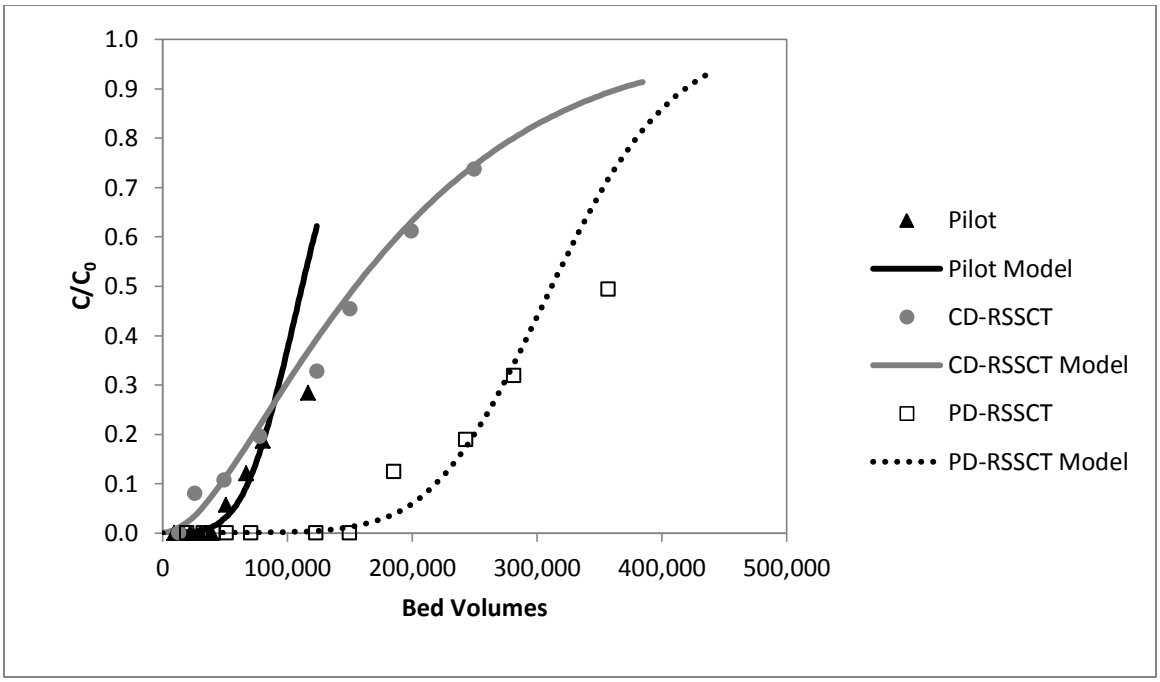

Figure 4.32: Acetochlor Breakthrough and PSDM Fits

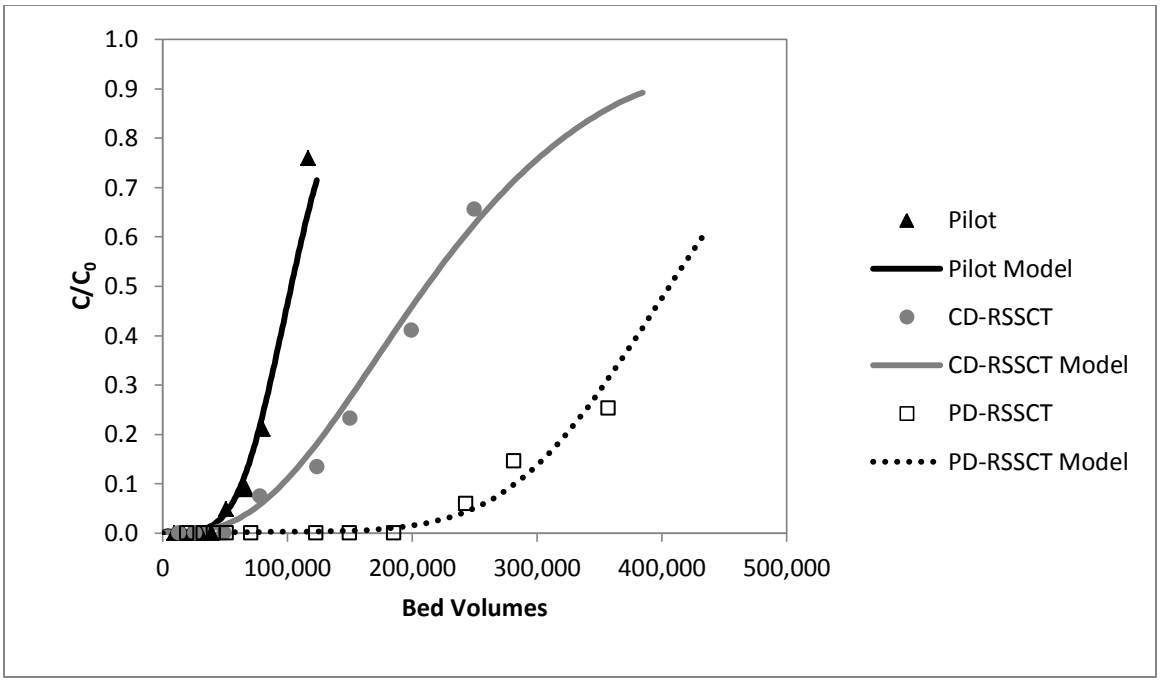

Figure 4.33: Simazine Breakthrough Data and PSDM Fits

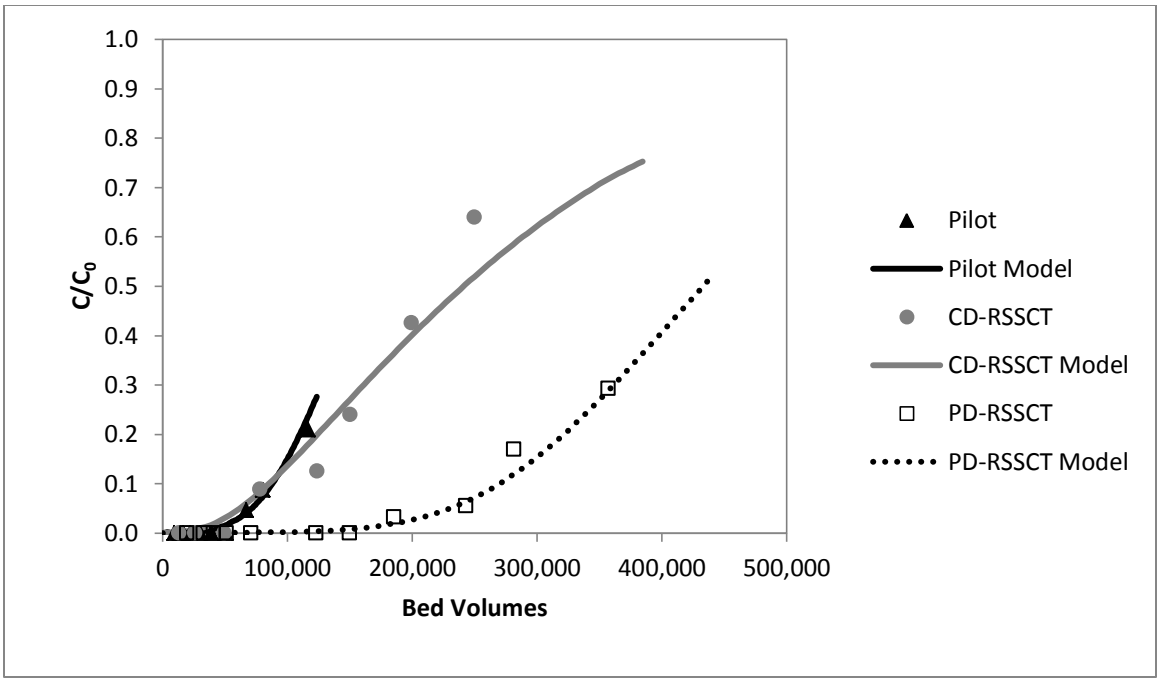

Figure 4.34: Carbamazepine Breakthrough Data and PSDM Fits

For the CD-RSSCT, onset of breakthrough occurred sooner than in the pilot for some MPs (e.g. iopromide) but later than in the pilot for others (e.g. methomyl). With the exception of iopromide, 50% breakthrough in the CD-RSSCT occurred later than in the pilot, indicating that the CD-RSSCT generally overpredicts MP adsorption capacity. For the PD-RSSCT, onset of breakthrough and 50% breakthrough, a measure of adsorption capacity, always occurred later than in the pilot. The PD-RSSCT, therefore, also overpredicts the capacity of the GAC. Relative to the CD-RSSCT, MP breakthrough in the PD-RSSCT may have occurred later because (1) the particle size.

Fouling Indexes for PD- and CD-RSSCT

Once the best PSDM fits for the pilot data and the RSSCT data was achieved were obtained, the fouling index and the fouling factor (Y-Value) were determined using Equation 4.3:

$$Fouling\ Index = \frac{K_{RSSCT}}{K_{pilot}} = SF^{Y} \tag{4.3}$$

K values for the 11 MPs that broke through in the pilot are summarized in Table 4.6, and the corresponding K values for the CD- and PD-RSSCT in Tables 4.8 and 4.10, respectively. Table 4.11 summarizes the fouling indexes for the 11 MPs, for which comparisons between pilot and RSSCT breakthrough data were possible.

Table 4.11: Fouling Index Values

Compound	**PD-RSSCT Fouling Index**	**CD-RSSCT Fouling Index**
Acetochlor	2.76	1.60
Atrazine	2.46	1.51
Caffeine	4.38	1.90
Carbamazepine	2.71	1.71
Cotinine	1.65	1.96
Iopromide	1.91	0.50
Methomyl	3.57	2.37
Metolachlor	3.00	1.60
Prometon	3.75	2.22
Simazine	3.91	2.17
Tributyl Phosphate	4.63	2.88

Using Equation 3.10, the Y-values were determined from the fouling indexes for each compound and are shown in Table 4.12 for the PD-RSSCT and the CD-RSSCT. As an

illustrative example, the fouling index for methomyl was 2.37 for the CD-RSSCT and the associated scaling factor was 4.32. The Y value that resulted from a fouling index of 2.37 and a scaling factor or 4.32 was 0.59.

Table 4.12: Fouling Factor Values

Compound	PD-RSSCT Y-Value	CD-RSSCT Y-Value
Acetochlor	0.47	0.32
Atrazine	0.42	0.28
Caffeine	0.69	0.44
Carbamazepine	0.47	0.37
Cotinine	0.23	0.46
Iopromide	0.30	-0.47
Methomyl	0.63	0.59
Metolachlor	0.51	0.32
Prometon	0.62	0.55
Simazine	0.64	0.53
Tributyl Phosphate	0.72	0.72

Dependence of Y on Compound Characteristics

Octanol-Water Partition Coefficient

Inspection of the Y-values in Table 4.12 shows that the magnitude of Y was different for each adsorbate. Based on the results of Fotta (2012), correlations between Y and the pH-dependent octanol-water partition coefficient (log D) were developed. The Y-values for the PD-RSSCT were found to have some dependence on log D (Figure 4.35), but Y values appear to follow two separate trends.

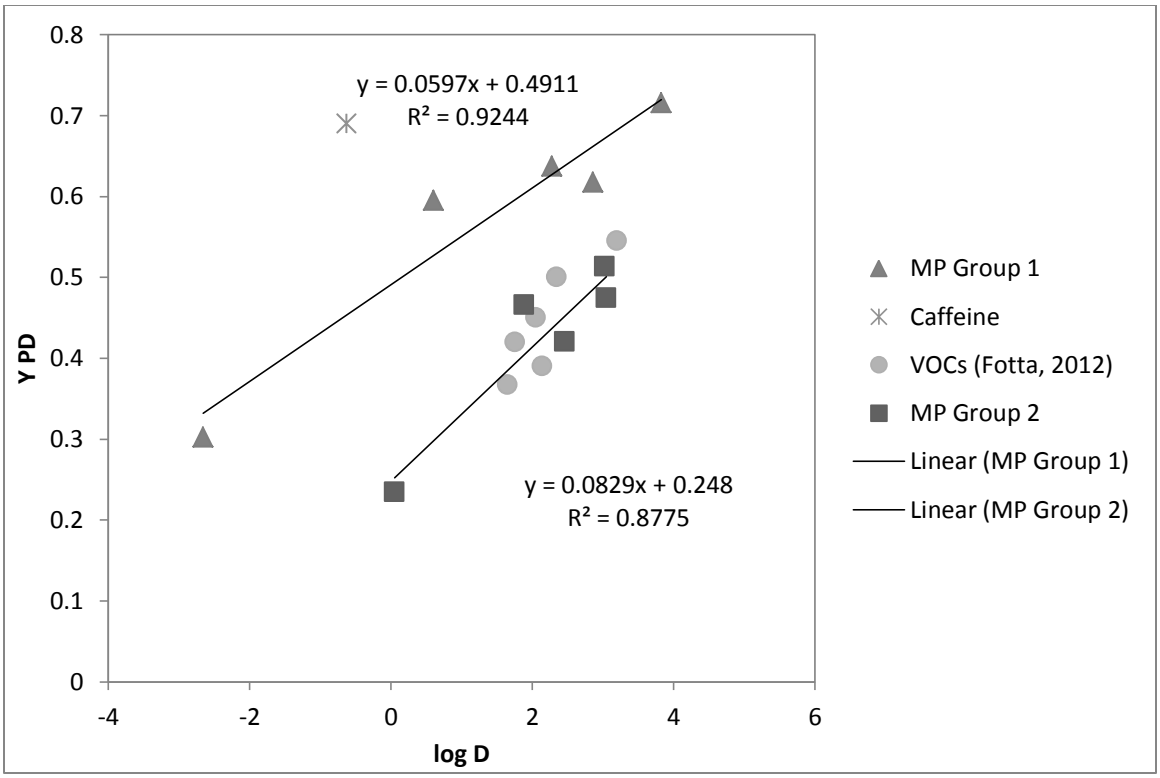

Figure 4.35: Dependence of Y-Values for PD-RSSCT on Log D

The compounds that made up MP Group 1 were iopromide, methomyl, simazine, prometon and tributyl phosphate while those in MP Group 2 were cotinine, carbamazepine, atrazine, acetochlor, and metolachlor. The trend established by MP Group 2 closely matched that determined by Fotta (2012) for the VOCs 1,1,1-trichloroethane, 1,1-dichloroethane, 1,1-dichloroethene, 1,2-dichloroethane, cis-1,2-dichloroethene, and 1,1,2-trichlorotrifluoroethane. No MP characteristics could be identified that can explain why a given MP would fall on one or the other trend line. Caffeine, likely, did not follow either trend because of its biodegradability.

The CD-RSSCT Y-values were also found to have some dependence on log D (Figure 4.36), and similarly to the PD-RSSCT, the Y values appear to follow two separate trends.

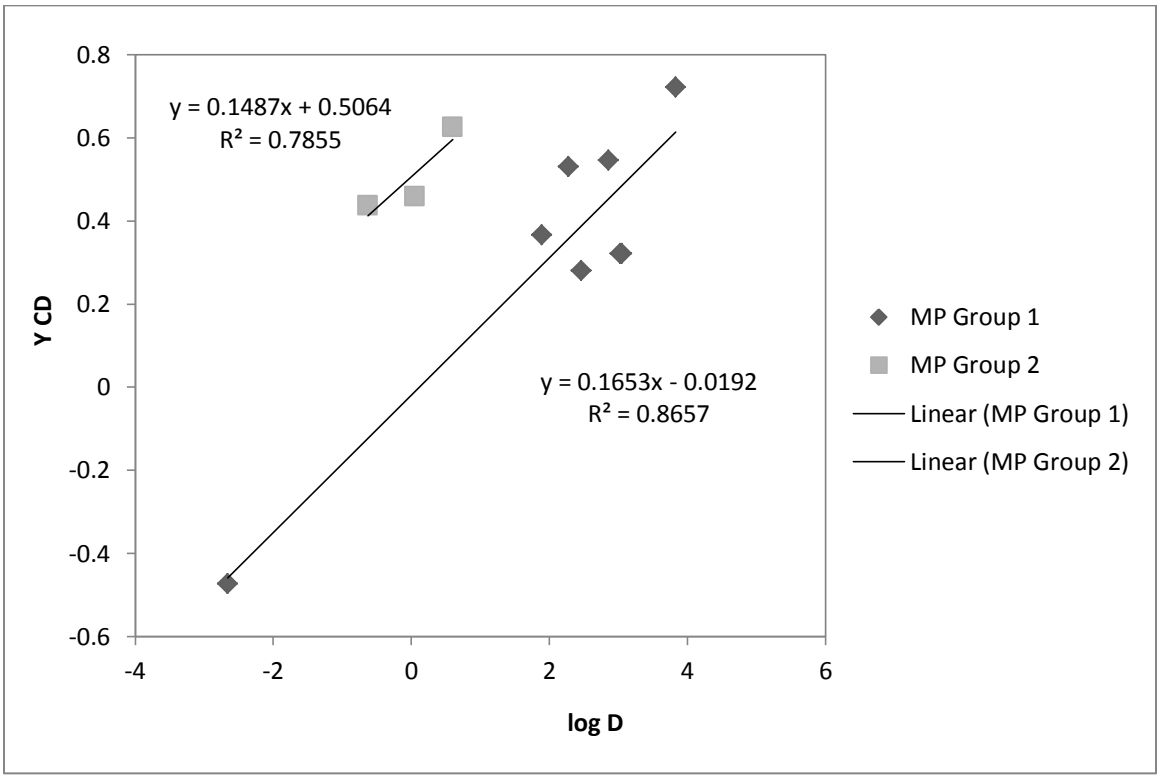

Figure 4.36: Dependence of Y-Values for CD-RSSCT on Log D

The compounds that made up MP Group 1 were caffeine, cotinine, and methomyl, while those in MP Group 2 were acetochlor, atrazine, carbamazepine, iopromide, metolachlor, prometon, simazine, and tributyl phosphate. Again, no MP characteristic could be identified that explains why a certain MP would fall on one or the other trend line. Unlike for the PD-RSSCT, caffeine was not an outlier for the CD-RSSCT.

Linear Free Energy Relationship

As illustrated in the previous section, no single compound characteristics could be identified that could serve as a predictor for Y. It is therefore likely that several compound characteristics and/or other parameters are needed to predict Y. To test the possibility of using multiple compound characteristics that are important in describing sorption processes, Abraham descriptors were used to develop a linear free energy relationship (LFER). A traditional multiple linear regression (MLR) approach was initially pursued to develop LFERs to predict Y for both the PD-RSSCT and CD-RSSCT. However, there were two problems with this approach. First, the training set had at most 11 Y-values, which meant that an MLR approach with six adjustable parameters (one for each Abraham parameter plus the intercept) would overfit the model. Second, through a statistical analysis performed in R-Project, it was determined that the five Abraham parameters for the 11 MPs (and the 6 VOCs studied by Fotta (2012))were highly correlated. Therefore, a principal component analysis and regression was used and is discussed below.

Principal component analysis (PCA) transforms correlated variables into uncorrelated principal components (PCs) and has been widely used for making predictive models (Fekedulegn et al., 2002). PCA is conducted by an eigenvalue decomposition of a data covariance or correlation matrix, resulting in eigenvalues and eigenvectors. The eigenvalues represent the variability explained by the associated eigenvector. Eigenvectors are the vectors showing the dominant variables, and the PCs are the orthogonal linear combinations of the variables. PC1, as shown on Figure 4.37 is the longest axis in the data set and gives the

direction of the maximum spread of the data. This component accounts for as much of the variability in the data as possible. If not enough data variability is explained by PC1 then another axis is created; i.e. PC2 in Figure 4.37. PC2 gives the direction of maximum spread perpendicular to the first direction given by PC1. Essentially, PCA chooses a new coordinate system for the data and the PCs are the unit vectors along the new axes (Bowden et al., 1997).

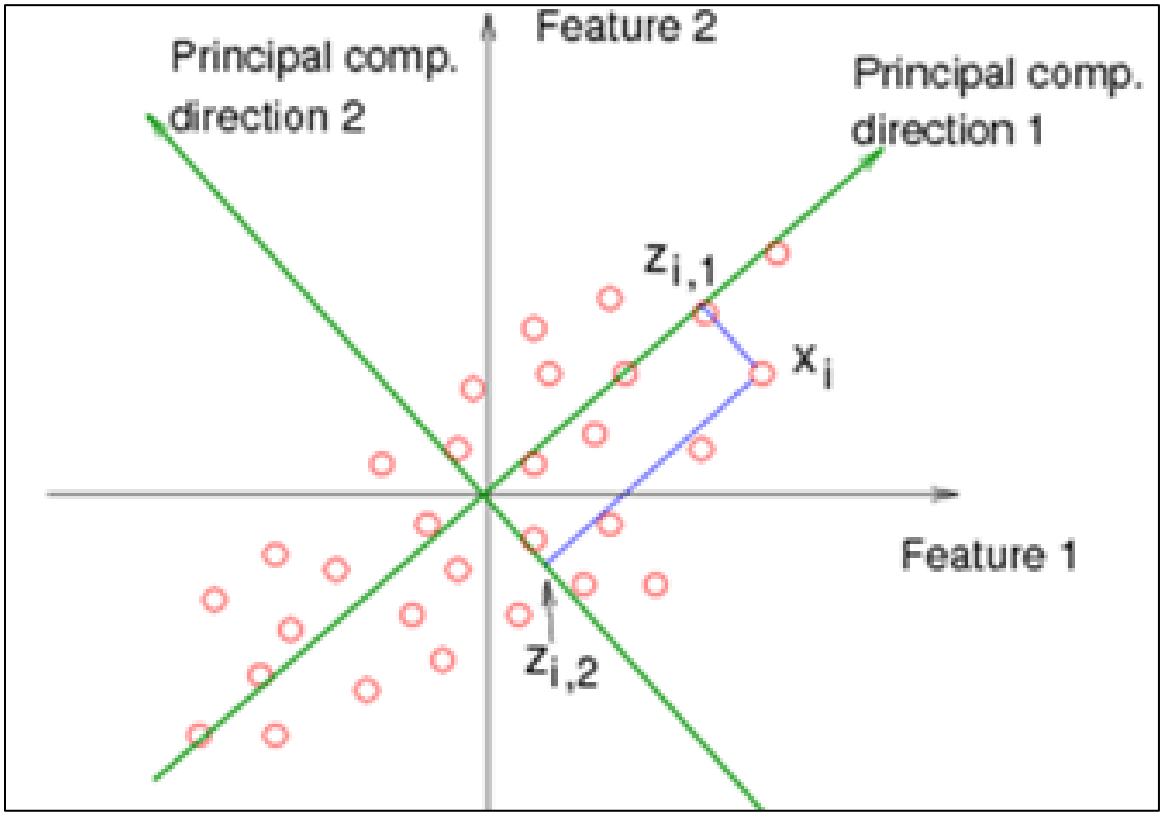

Source: Penn State University Statistics 857 (2011)

Figure 4.37: Principal Component Analysis

The PCA for the CD-RSSCT showed that the variability in Y was well explained by just one PC and an intercept. Equation 4.4 is the result of the PCA for the CD-RSSCT Y-values:

$$Ypca \quad = (0.165 \pm 0.0406)(PC1) + (0.883 \pm 0.143) \tag{4.4}$$

n=11 r^2=0.90 adjusted r^2=0.89

where PC1 is calculated from:

$$PC1 \quad = -0.612S - 0.247A - 0.370B - 0.341V - 0.558E \tag{4.5}$$

Only the first eigenvector was used because it explained 90% of the variance, and inclusion of PC2 did not significantly improve the explanation of the variance. The ability of the PCA relationship shown in Equation 4.4 to describe the variability in Y-values for the 11 MPs in the training set is illustrated in Figure 4.38. The close agreement between predicted and experimental Y-values (Ypca and Yexp) to the 1:1 line in Figure 4.38 illustrates that Equation 4.4 effectively describes the variance in Y values for the 11 MPs.

The value of PC1 used in Equation 4.4 is unique to each MP and is a function of the Abraham descriptors S, A, B, V, and E. The value of the PCs were calculated using the R-Project calculated eigenvectors for each Abraham descriptor. Assuming that the correlation between the Abraham descriptors, S, A, B, V, and E, does not change dramatically for other compounds Equation 4.5 can be used to calculate PC1 for other MPs not used in the training set.

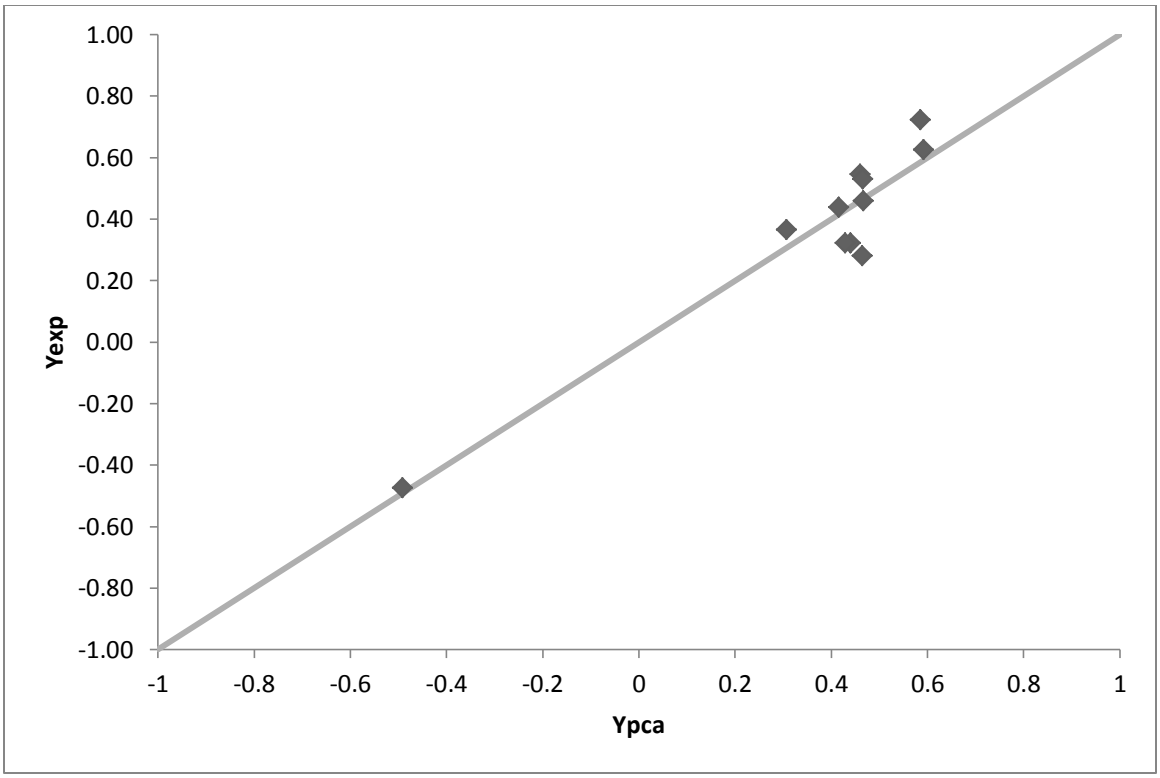

Figure 4.38: Predictive Ability of the PCA Relationship for Y-Values for the CD-RSSCT

To assess the predictive strength of the PC, a leave-one-out (LOO) analysis was conducted. By leaving out one MP and altering the training set to 10 MPs, eleven regression equations were developed that relate Ypca to PC1. Using these equations, the Y-value of the 11 MPs was predicted. The predictive ability with the LOO method is illustrated in Figure 4.39.

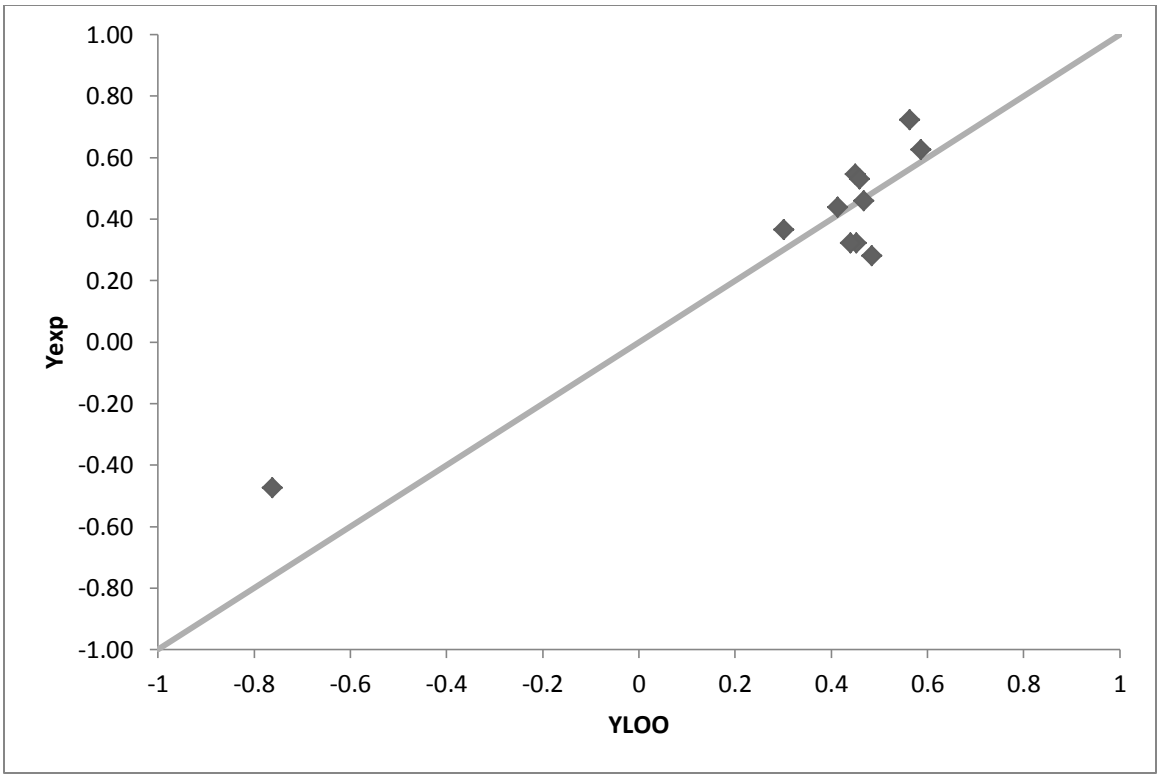

Figure 4.39: Predictive Ability of the PCA Relationship as Assessed by the LOO Method

Through R-Project, the validation with the LOO method returned an r^2 value of 0.78 which confirms the predictive strength of the LFER.

SCALE-UP APPROACHES

In this section, scale-up approaches for both PD-RSSCT and CD-RSSCT data are presented.

PD-RSSCT

When PD-RSSCTs are conducted, the linear dependence of intraparticle flux on particle size is reflected in the RSSCT design. Therefore, only the fouling factor Y is required to address the particle size-dependence of the adsorption capacity. Therefore, PD-RSSCT data can be scaled directly using equation 2.15 once Y for a given MP is known. Estimates of Y can be obtained from the following equations:

$$Y = 0.0597(\log D) + 0.491 \tag{4.6}$$

$$Y = 0.0829(\log D) + 0.248 \tag{4.7}$$

An illustrative example, field-scale GAC breakthrough predictions for naproxen are shown in Figure 4.40.

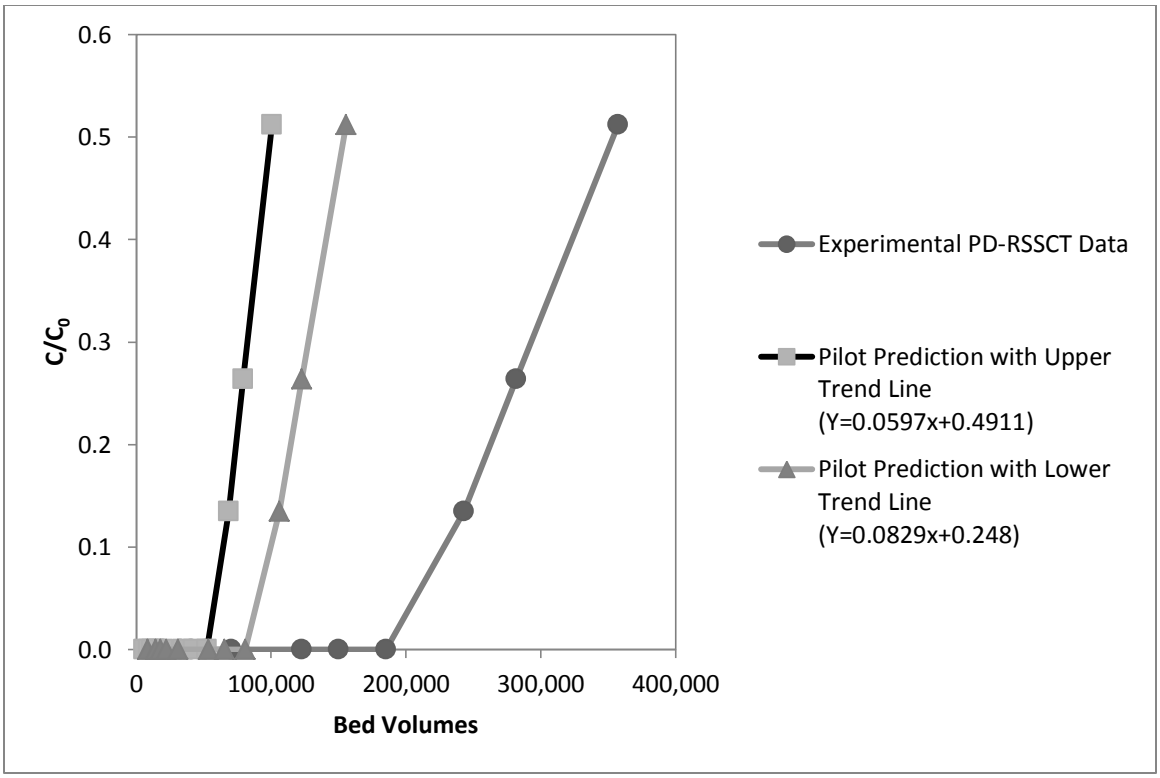

Figure 4.40: PD-RSSCT Scale-Up Predictions for Naproxen

Breakthrough for naproxen was predicted to occur sooner with the upper trend line (Equation 4.6) as compared to the lower trend line (Equation 4.7). With the upper trend line, naproxen was predicted to reach 10% breakthrough at the field-scale at 68,000 bed volumes, whereas, with the lower trend line naproxen was predicted to reach 10% breakthrough at 105,000 bed volumes. Therefore, depending on which trend line, naproxen would fall on, there could be a difference of 37,000 bed volumes to reach 10% breakthrough.

CD-RSSCT

When scaling up CD-RSSCT data, both the dependence of MP adsorption capacity and intraparticle flux on particle size need to be addressed. Therefore, the following approach using the PSDM and developed LFER is proposed:

1. Use PSDM to obtain best fit for CD-RSSCT data. Resulting fitting parameters are $K_{CD\text{-}RSSCT}$ and CD-RSSCT flux (which is a combination of τ and SPDFR as illustrated in Table 3.5)
2. Calculate Y from LFER (Equations 4.4 and 4.5)
3. Calculate fouling index from Y using the desired scaling factor (Equation 4.3)
4. Calculate K_{Pilot} (Equation 4.3)
5. Calculate pilot flux (Equation 3.4)
6. Use PSDM to obtain pilot fit using K_{Pilot} and the pilot flux

For example, for the MP methomyl, the following calculations would be conducted.

1. Best fit of PSDM for CD-RSSCT data resulted in K = 350 (mg/g)(L/mg)$^{1/n}$, τ = 1, SPDFR = 0.85
2. The Y-value from the LFER using the calculated PC1 for methomyl:

$$PC1 \quad = -0.612(0.91) - 0.247(0.21) - 0.370(0.85) - 0.341(1.21) - 0.558(0.77)$$

$$PC1 \quad = -1.77$$

$$Y \quad = (0.165)(-1.77) + (0.883)$$

$$Y \quad = 0.59$$

3. The fouling index was calculated from

$$FoulingIndex = 4.32^{0.59}$$

$$FoulingIndex = 2.37$$

4. K_{Pilot} was calculated as

$$K_{pilot} = \frac{350\left(\frac{mg}{g}\right)\left(\frac{L}{mg}\right)^{1/n}}{2.37\left(\frac{mg}{g}\right)\left(\frac{L}{mg}\right)^{1/n}}$$

$$K_{pilot} = 148\left(\frac{mg}{g}\right)\left(\frac{L}{mg}\right)^{1/n}$$

5. The pilot flux resulted in a value of 8.00 when using a scaling factor of 4.32 in combination with the CD-RSSCT flux of 1.85; i.e. 1.85x4.32 = 8.00
6. The PSDM prediction of the pilot is then obtained with a K of 148 $(mg/g)(L/mg)^{1/n}$, τ = 1, and SPDFR= 7.00

Figure 4.41 illustrates how the scale-up approach was conducted for methomyl by first fitting the CD-RSSCT, then adjusting K, and finally the intraparticle flux.

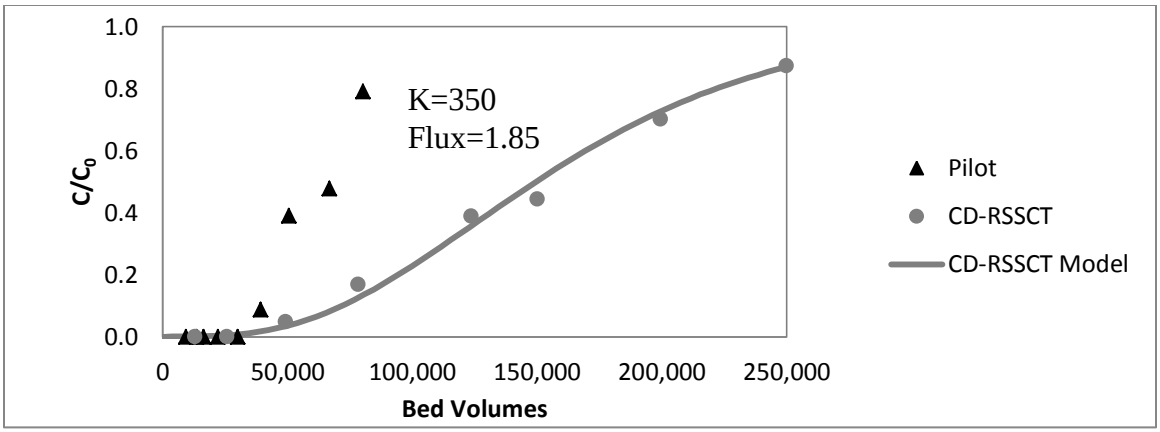

(a)

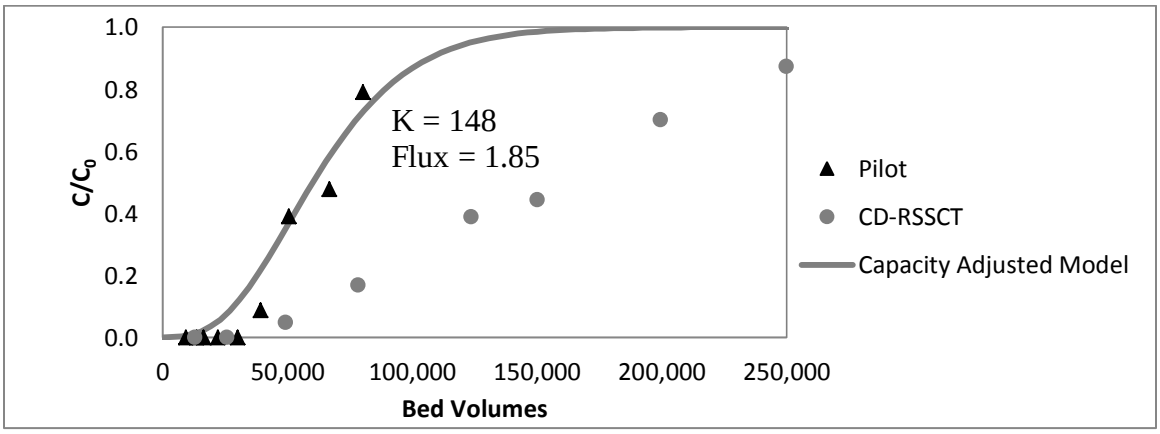

(b)

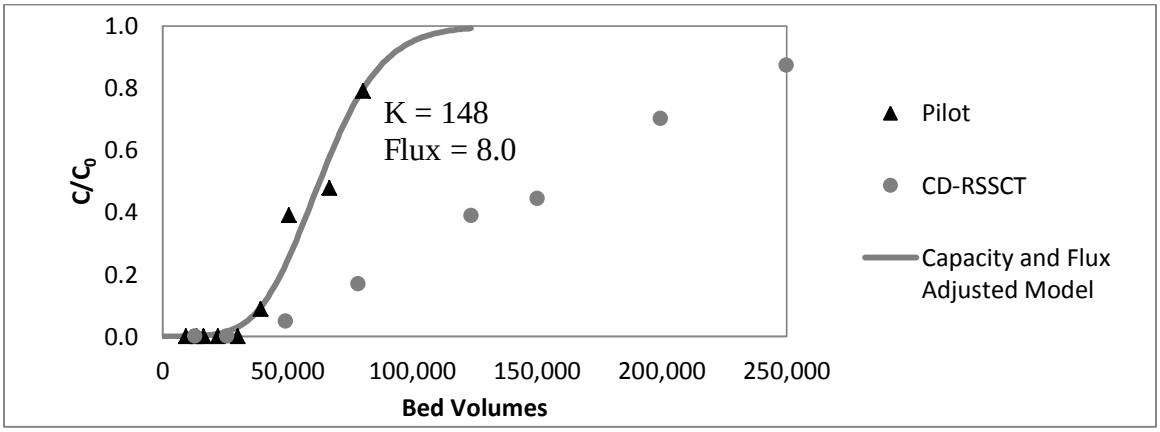

(c)

Figure 4.41: Scale-Up Procedure for CD-RSSCT

Additionally, three additional MPs were chosen to illustrate the CD-RSSCT scale-up approach. Diclofenac, naproxen, and diuron were chosen to represent MPs that broke through in the CD-RSSCT relatively early, in the middle of the run, and near the end of the run, respectively. These three compounds were not detected in the pilot effluent and therefore were used to illustrate the predicitve application of the CD-RSSCT scale-up approach. The predictions for field-scale removal of diclofenac, naproxen, and diuron by GAC are illustrated in Figures 4.42, 4.43, and 4.44, respectively.

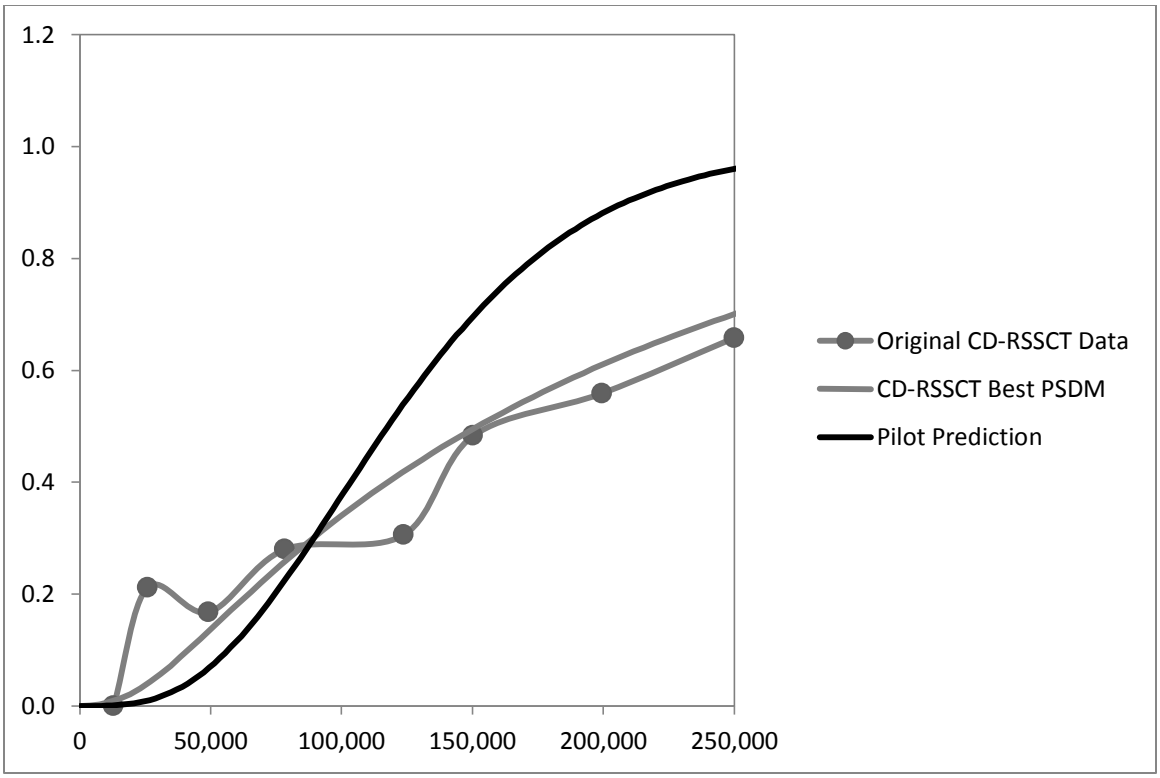

Figure 4.42: Application of CD-RSSCT Scale-Up Approach for Diclofenac

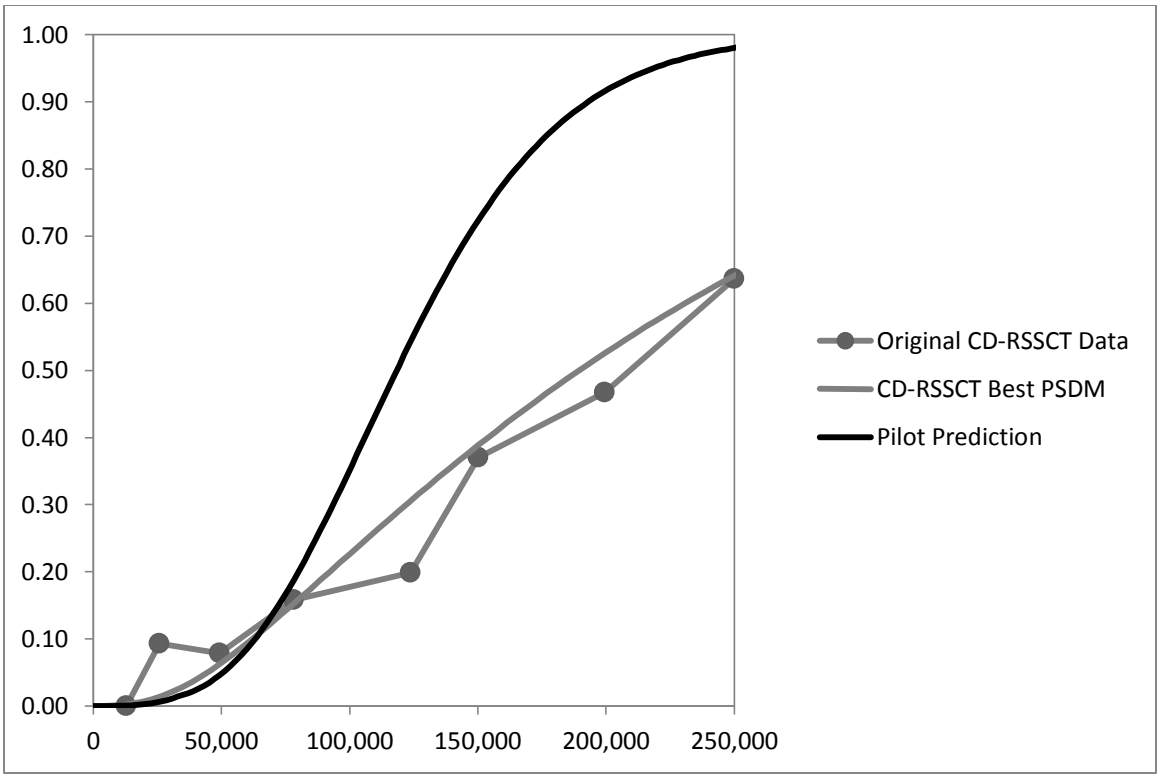

Figure 4.43: Application of CD-RSSCT Scale-Up Approach for Naproxen

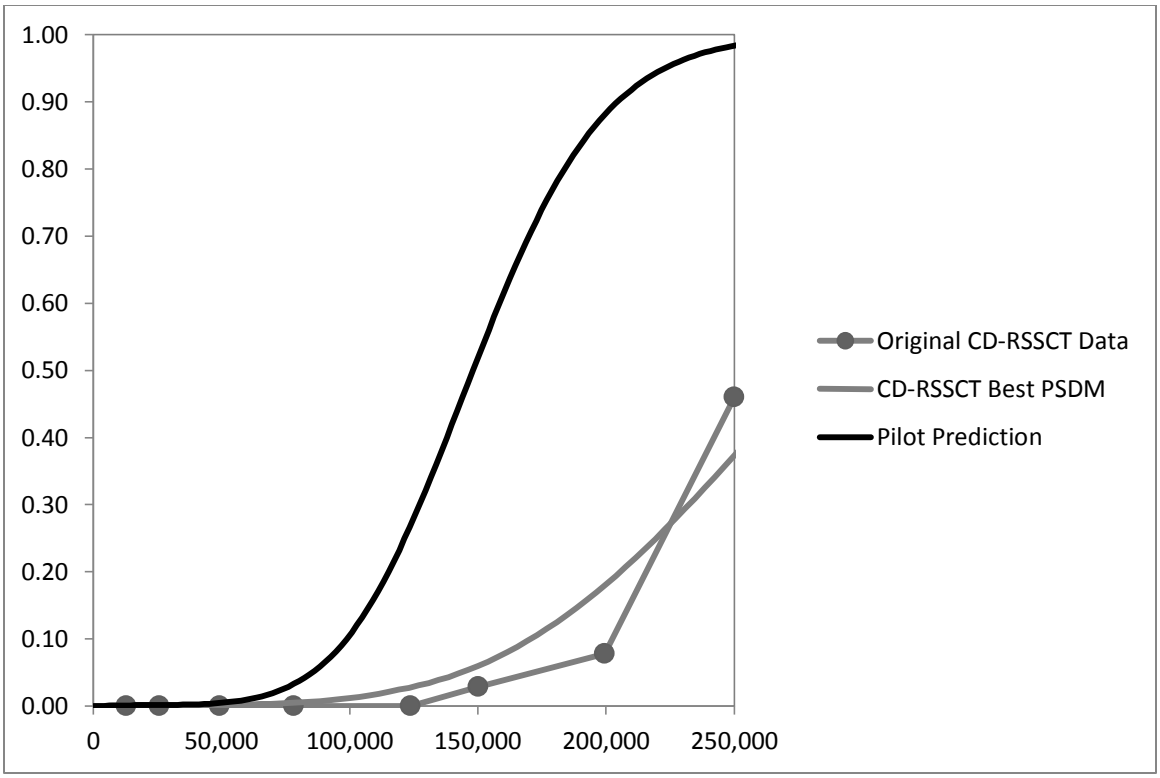

Figure 4.44: Application of CD-RSSCT Scale-Up Approach for Diuron

The first step to apply the CD-RSSCT scale-up procedure was to determine K, τ, and SPDFR that resulted in the best fit PSDM for the CD-RSSCT breakthrough data of each compound. The resulting equilibrium and kinetic parameters are shown in Table 4.13.

Table 4.13: CD-RSSCT Best Fit PSDM Parameters

Input	**Diclofenac**	**Naproxen**	**Diuron**
K_{RSSCT}	450	500	625
τ	1.5	1	1
SPDFR	1E-30	1E-30	8
RSSCT Flux	0.67	1	9

Based on Table 4.13 the predicted pilot equilibrium and kinetic parameters were calculated in steps 4 and 5. The calculated parameters for the field-scale adsorber performance are shown in Table 4.14.

Table 4.14: Pilot Prediction PSDM Parameters

Input	**Diclofenac**	**Naproxen**	**Diuron**
K_{Pilot}	275	270	327
τ	1	1	1
SPDFR	1.88	3.32	38
Pilot Flux	2.88	4.32	39

The prediction for field-scale capacity for diclofenac, naproxen, and diuron to 20% breakthrough are shown in Table 4.15.

Table 4.15: Application Results of CD-RSSCT Scale-Up Approach

Compound	**Model BV for CD-RSSCT 20% Breakthrough**	**Model BV to Pilot 20% Breakthrough**
Diclofenac	65,400	74,050
Naproxen	92,300	80,225
Diuron	207,690	115,200

Based on the results from Table 4.15, both naproxen and diclofenac should have reached 20% breakthrough during the pilot run. Due to possible slow and fast biodegradability for diclofenac and naproxen, respectively, neither of these compounds were detected. Diuron was also not detected in the pilot, but the anticipated bed volumes value to 20% breakthrough in the pilot was very end of the pilot run and therefore not enough bed volumes had been processed to see diuron breakthrough.

In order to assess if the scale-up approach for the PD-RSSCT and the CD-RSSCT had reasonable agreement, the pilot predictions for dicofenac and naproxen were each compared in Figures 4.45 and 4.46, respectively. Diuron was not included in this analysis since this MP did not reach measurable detection in the PD-RSSCT.

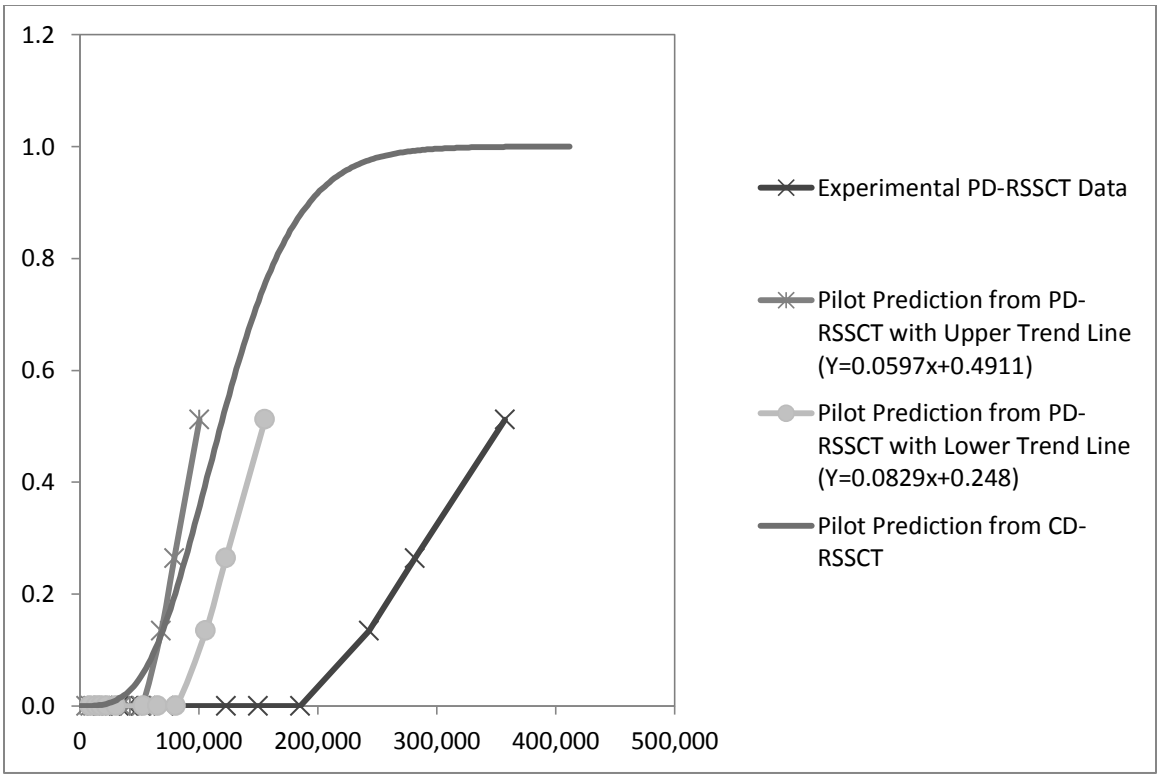

Figure 4.45: Comparison between PD-RSSCT and CD-RSSCT Scale-Up Approaches for Naproxen

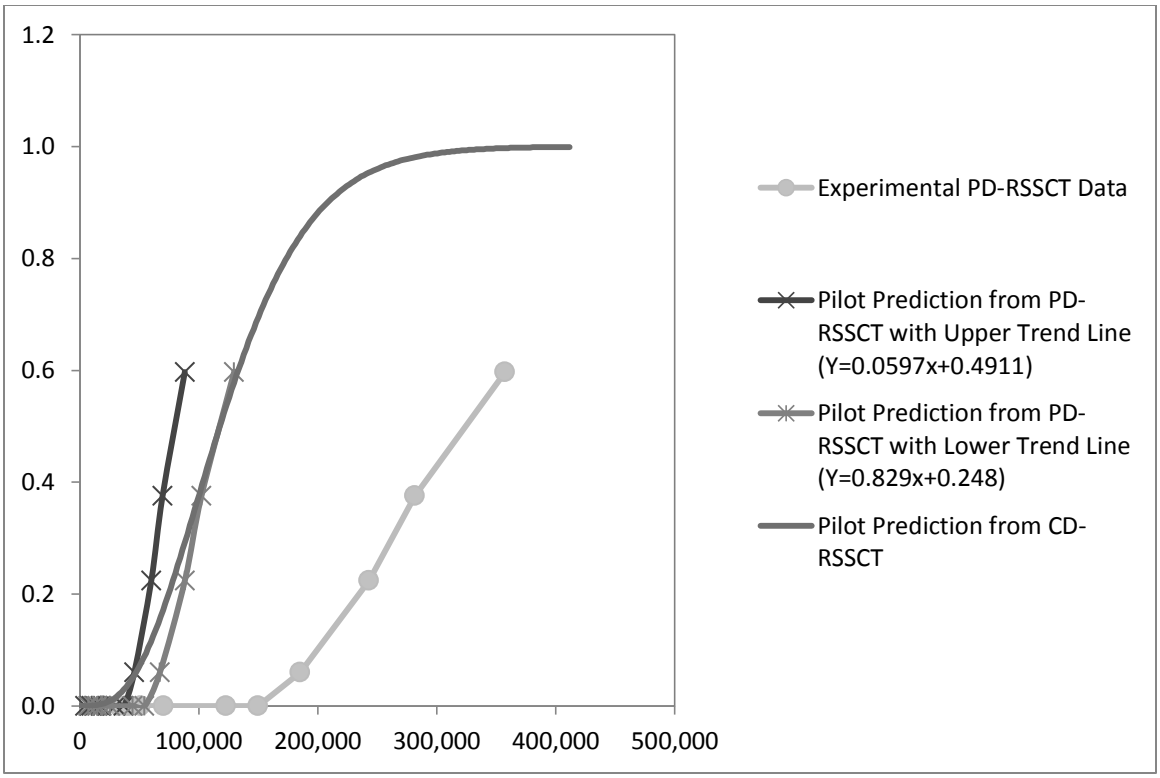

Figure 4.46: Comparison of PD-RSSCT and CD-RSSCT Scale-Up Approaches for Diclofenac

There is reasonable agreement between the pilot prediction from the CD-RSSCT scale-up approach and the range of the pilot predictions from the two trend lines from the PD-RSSCT. As such, the scale-up approaches can be used with a good degree of confidence.

CHAPTER 5: SUMMARY AND CONCLUSIONS

The principal objectives of this research were to (1) conduct a pilot test to evaluate the effectiveness of granular activated carbon (GAC) adsorption for the removal of 34 micropollutants (MPs) from coagulated surface water, (2) evaluate two common rapid small scale column test (RSSCT) designs, the CD-RSSCT and the PD-RSSCT, for predicting field-scale MP removal, and (3) develop a comprehensive scale up procedure that will ultimately save utilities time and money when determining GAC adsorber life and performance. To meet the research objectives, the following tasks were completed:

1. Designed, built, and operated a GAC pilot column at the Orange Water and Sewer Authority (OWASA) to evaluate the removal of 34 MPs.
2. Designed, built, and operated a PD-RSSCT to evaluate the removal of 34 MPs.
3. Designed, built, and operated a CD-RSSCT to evaluate the removal of 34 MPs.
4. Analyzed the pilot and RSSCT data sets to develop a scale-up approach that permits the prediction of field-scale GAC performance from RSSCT data.

PILOT STUDY

Results from the pilot column (bituminous coal-based GAC, EBCT=7 min) showed that GAC adsorption is an effective treatment option for the removal of MPs. Only 11 out of the 34 tested MPs broke through to measureable levels (10% breakthrough) in the filter

effluent over the run time of 120,000 bed volumes. The least adsorbable MP was iopromide, followed by cotinine and tributyl phosphate. Iopromide broke through to 10% of the influent concentration after about 20,000 bed volumes of water had been treated, which corresponds to operating the GAC adsorber continuously for about 3 months. For reference, about 13,000 bed volumes of water could be treated before DOC breakthrough reached 50%. In terms of carbon usage rate (CUR), results from the pilot study translated into 34.6 mg/L (0.289 lb/1000 gal) to reach 50% DOC removal. For 90% MP removal, CURs for the 11 MPs, for which at least 10% breakthrough was obtained in the pilot study, ranged from 21.9 mg/L (0.183 lb/1000 gal) for iopromide to 5.0 mg/L (0.042 lb/1000 gal) for carbamazepine. For the remaining 23 MPs, CURs would be less than 5 mg/L, suggesting that GAC adsorption is a cost effective technology for the removal of many MPs.

RSSCT STUDY

Both the CD-RSSCT and the PD-RSSCT were evaluated in this study. The CD-RSSCT was operated for 2 months with a total of 250,000 bed volumes processed. In the CD-RSSCT, at least 10% breakthrough was obtained for all MPs but chlorpyrifos, BPA, triclosan, and ethinyl estradiol (EE2). The PD-RSSCT was run for 357,000 bed volumes (8 months) and at least 10% breakthrough was obtained for all MPs but acetaminophen, carbaryl, chlorpyrifos, diuron, BPA, triclosan, and ethinyl estradiol (EE2). Both RSSCT approaches offered significant time and water volume savings as compared to the pilot test.

However, both particle size-dependent differences in MP adsorption capacity and kinetics needed to be addressed to predict field-scale MP removal from the RSSCT data.

FOULING FACTOR

With the exception of iopromide in the CD-RSSCT, the RSSCTs overpredicted the field-scale MP adsorption capacity of the GAC. The particle size-dependence of fouling caused by the adsorption of background NOM was the likely cause for the differences in MP adsorption capacities. To scale differences in MP adsorption capacity, a fouling factor (Y) was determined for the 11 MPs, for which at least 10% breakthrough was obtained in both the pilot study and the RSSCTs. An analysis of the resulting Y-values showed that the magnitude of Y was compound specific. For the CD-RSSCT, a linear free energy relationship (LFER) was developed that relates Y to the 5 Abraham descriptors (S, A, B, V, and E) for each MP using principal component analysis (PCA). The LFER explained the variability of the Y-values with one principal component as follows:

$$Y = (0.165 \pm 0.0406)(PC1) + (0.883 \pm 0.143) \tag{4.4}$$

where PC1 is the first principal component and is calculated from:

$$PC1 = -0.612S - 0.247A - 0.370B - 0.341V - 0.558E \tag{4.5}$$

The variability in the Y-values obtained from the PD-RSSCT, on the other hand, were not well described by the LFER. Instead, two distinct correlations between Y and log D were found as follows:

$$Y = 0.0597(\log D) + 0.491 \tag{4.6}$$

$$Y = 0.0829(\log D) + 0.248 \tag{4.7}$$

However no compound characteristic could be identified to place MPs on one or the other regression line.

SCALE-UP APROACH

While the fouling factor (Y) addresses differences in MP adsorption capacity between bench-scale and full-scale adsorbers, differences in adsorption kinetics also needed to be addressed. Results from the pore surface diffusion model (PSDM) indicated that the intraparticle diffusive flux of MPs varied linearly with GAC particle size and, as such, the RSSCT flux needs to be scaled with GAC particle size. The PD-RSSCT design explicitly addresses the linear particle size-dependence of MP adsorption kinetics. In contrast, the linear dependence of the intraparticle diffusive flux on particle size must be addressed with the PSDM in order to predict full-scale adsorber performance from CD-RSSCT data. The scale up process to predict field-scale adsorber performance from the CD-RSSCT is shown in Figure 5.1.

Figure 5.1: CD-RSSCT Scale Up Procedure

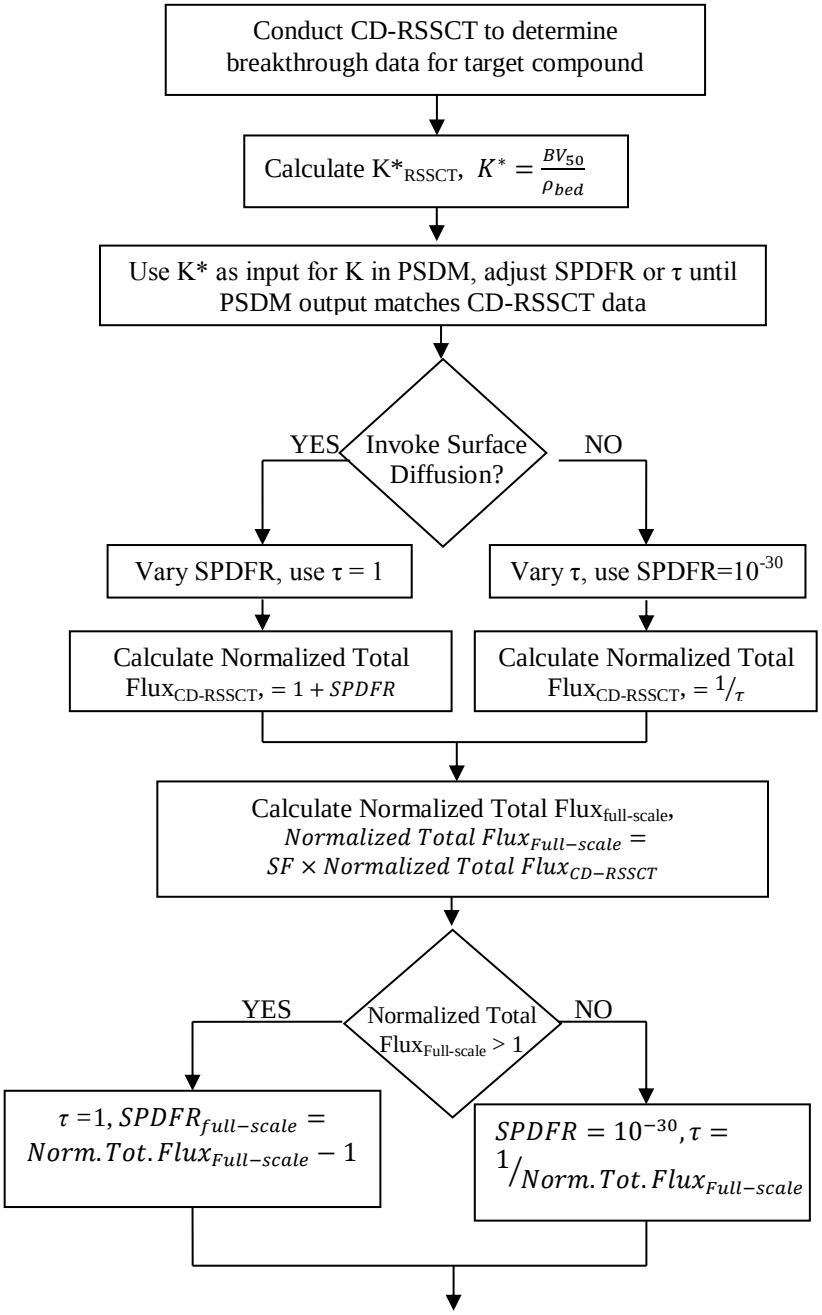
Conduct CD-RSSCT to determine breakthrough data for target compound
Calculate K*RSSCT, $K^* = \frac{BV_{50}}{\rho_{bed}}$
Use K* as input for K in PSDM, adjust SPDFR or τ until PSDM output matches CD-RSSCT data
Invoke Surface Diffusion?
YES
NO
Vary SPDFR, use τ = 1
Vary τ, use SPDFR=10-30
Calculate Normalized Total FluxCD-RSSCT, = $1 + SPDFR$
Calculate Normalized Total FluxCD-RSSCT, = $1/\tau$
Calculate Normalized Total Fluxfull-scale, $Normalized\ Total\ Flux_{Full-scale} = SF \times Normalized\ Total\ Flux_{CD-RSSCT}$
Normalized Total FluxFull-scale > 1
YES
NO
$\tau = 1, SPDFR_{full-scale} = Norm.Tot.Flux_{Full-scale} - 1$
$SPDFR = 10^{-30}, \tau = 1/Norm.Tot.Flux_{Full-scale}$

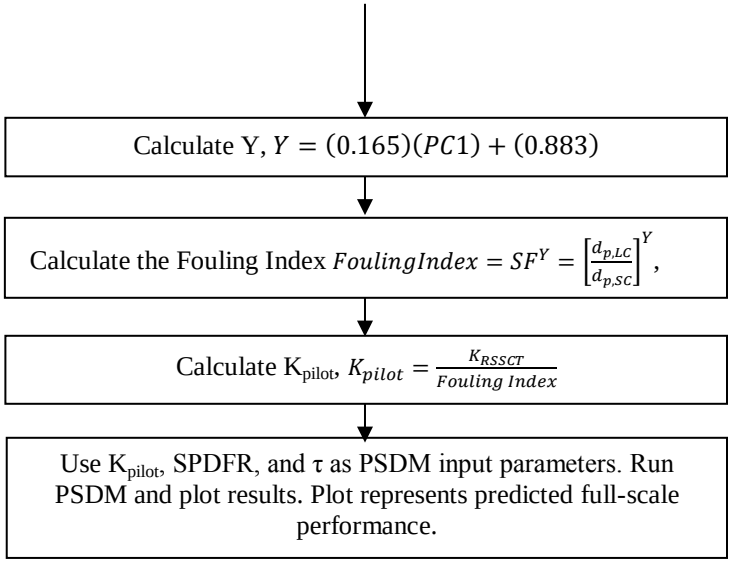
Calculate Y, $Y = (0.165)(PC1) + (0.883)$
Calculate the Fouling Index $FoulingIndex = SF^Y = \left[\frac{d_{p,LC}}{d_{p,SC}}\right]^Y$,
Calculate K_{pilot}, $K_{pilot} = \frac{K_{RSSCT}}{Fouling\ Index}$
Use K_{pilot}, SPDFR, and τ as PSDM input parameters. Run PSDM and plot results. Plot represents predicted full-scale performance.

The PSDM is also able to model the PD-RSSCT for scale-up, but determining a unique Y-value from the regressions shown in Equations 5.1 and 5.2 is not possible. As such, it is suggested that the CD-RSSCT design should be used to predict field-scale MP removal.

RECOMMENDATIONS AND FUTURE WORK

For utilities and consultants looking to run a bench-scale study instead of a pilot study to ascertain GAC life for MP removal, the CD-RSSCT is the more convenient choice. The CD-RSSCT takes less time as compared to the PD-RSSCT. Additionally, a distinct LFER to predict Y-values for the CD-RSSCT was developed using Abraham descriptors. However, to simulate TOC removal, the PD-RSSCT is better suited.

Future work is needed to assess whether or not the scaling approach developed for the CD-RSSCT in this research can be applied to predict TOC removal from CD-RSSCT data. If this future work is successful, CD-RSSCTs could be used to accurately predict both MP and TOC removal at the field-scale.

REFERENCES

Abraham, Michael H., Ibrahim, Adam, and Zissimos, Andreas M. (2004). Determination of Sets of Solute Descriptors from Chromatographic Measurements. *Journal of Chromatography A,* 1037, 29-47.

Abraham, Michael, H. (1993). Review on Hydrogen Bonding Scales. *Chemical Society Review*, 22, 73.

Apul, Onur G., Qiland Wang, Ting Shao, James R. Rieck, Tanju Karanfil. (2012). *Environemtnal Science and Technology.*

Baynes, Alice, Green, Christopher, Nicol, Elizabeth. Additional Treatment of Wastewater Reduces Endocrine Disruption in Wild Fish-A Comparative Study of Tertiary and Advanced Treatments. (2012). *Environmental Science and Technology*. 46, 5565-5573.

Binetti, Roberto, Costamagna, Francesca Marina, and Marcello, Ida. (2008) Exponential Growth of New Chemicals and Evolution of Information Relevant to Risk Control.

Bowden, R, Mitchell, T.A., Sarhadi, M. (1997). Cluster Based Nonlinear Principle Component Analysis. *Electronics Letters*, 33, 1858-1859.

Brasquet, C., P. Le Cloirec. (1999). QSAR For Organic Adsorption onto Activated Carbon in Water: What About the Use of Neural Networks? *Water Resources,* 33, 3603-3608.

Clarke, Eric D. (2009). Beyond Physical properties-Appicaltion of Abraham Descriptors and LFER Analysis in Agrochemical Research. *Bioorganic and Medicinal Chemistry.* 17, 4153-4159.

Corwin, C.J. and Summers, R.S. (2010). Scaling Trace Organic Contaminant Adsorption Capacity by Granular Activated Carbon. *Environmental Science & Technology,* 44**,** 5403-5408.

Corwin, C.J. (2010). Trace Organic Contaminant Removal from Drinking Waters by Granular Activated Carbon: Adsorption, Desorption, and the Effect of Background Organic Matter. (PhD Dissertation), University of Colorado-Boulder.

Corwin, C.J. and Summers, R.S. (2011). Adsorption and desorption of trace organic contaminants from granular activated carbon adsorbers after intermittent loading and throughout backwash cycles. *Water Research,* 45**,** 417-426.

Creek, Daniel, Davidson, James. 2000. National Water Resource Institute. *Chapter 4.0 Granular Activated Carbon*. NWRI-USA.

Crittenden, J.C., Berrigan, J.K. and Hand, D.W. (1986). Design of rapid small-scale adsorption tests for a constant diffusivity. *Journal Water Pollution Control Federation,* 58**,** 312-319.

Crittenden, J.C., Berrigan, J.K., Hand, D.W. and Lykins, B. (1987). Design of rapid fixed-bed adsorption tests for nonconstant diffusivities. *Journal of Environmental Engineering-ASCE,* 113**,** 243-259.

Crittenden, J.C., Reddy, P.S., Hand, D.W., and Aoroa, H. (1989). Prediction of GAC performance using rapid small-scale column tests. American Water Works Association Research Foundation report; American Water Works Association: Denver, CO.

Crittenden, J. C., Reddy P. S., Arora, H., Trynoski, J., Hand, D.W., Perram, D. L. and Summers, R. S. (1991). Predicting GAC performance with rapid small-scale column tests. *Journal American Water Works Association,* 83**,** 77-87.

Crittenden, John, R.R. Trussell, D.W. Hand, K.J. Howe, and G. Tchobanoglous. (2005). *Water Treatment: Principles and Design*.(2nd edition). Hoboken: John Wiley and Sons.

Dickenson, E.R.V.,J.E. Drewes. (2010). Quantitative structure property relationships for the adsorption of pharmaceutucals onto activated carbon. *Water Science & Technology,* 62, 2270-2276.

Dunn, Susan. (2011). Effect of Powdered Activated Carbon Base Material and Size on Disinfection By-Product Precursor and Trace Organic Pollutant Removal (MS Thesis). North Carolina State University.

Elhadi, S. L. N., Huck, P.M., Slawson, R.M. (2006) Factors Affecting the Removal of Geosmin and MIB in Drinking Water Biofilters. *American Water Works Association Journal,* 98, 108-119.

Eriksson, Lennart, Jaworska, Joanna, Worth, Andrew P., Cronin, Mark T.D., McDowell, Robert M., and Gramatica, Paola. (2003). Methods for Reliability and Uncertainty Assessment and for Applicability Evaluations of Classification- and Regression-Based QSARs. *Environmental Health Perspectives*. 111, 1361-1375.

Fekedulegn, B. Desta, Colbert, J.J., Hicks, R.R., Schuckers, Michael E. (2002). Coping with Multicollinearity: An Example on Application of Principal Component Regression in Dendroecology. US Department of Agriculture. Research Paper NE-721.

Fotta, Meredith. (2012). Effect of Granular Activated Carbon Type on Adsorber Performance and Scale-Up Approaches for Volatile Organic Compound Removal (MS Thesis). North Carolina State University.

Gonzalez, Susana, Lopez-Roldan, Ramon, and Cortina, Jose-Luis. (2012). Presence and Biological Effects of Emerging Contamainants in Llobregat River Basin: A Review. *Environmental Pollution*. 161, 83-92.

Hand, D. W., Crittenden, J. C., Arora, H., Miller, J. M., and Lykins, B. W. (1989). Designing fixed-bed adsorbers to remove mixtures of organics. *Journal American Water Works Association* 81(1), 67-77.

Intertox, Inc. (2009). Comparison of Analytical Results for Trace Organics in the Santa Ana River at the Imperial Highway to Health Risk-Based Screening Levels. Prepared for the Orange County Water District.

Japertas, Pranas, Sazonovas, Andrius, Clarke, Eric D., and Delaney, John S. Prediction of Abraham Descriptors for Agrochemicals. *Pharma Algorithms.*

Karanfil, Tanju, James E. Kilduff. (1999). Role of Granular Activated Carbon Surface Chemistry on the Adsorption of Organic compounds. 1. Priority Pollutants. *Environmental Science and Technology,* 33, 3217-3224.

Kilduff, James E., Srivastava, Reena, Karanfil, Tanju. (2002). Preloading of GAC by natural organic matter: effect of surface on TCE uptake. *Studies in Surface Science and Catalysis*, 144, 553-560.

Knappe, D. R. U. (1996). Predicting the Removal of Atrazine by Powdered and Granular Activated Carbon. PhD Dissertation. University of Illinois.

Knappe, D.R.U. and Summers, S.R. (2010). Evaluation of Available Scale-Up Approaches for the Design of Granular Activated Carbon Adsorbers. Water Research Foundation project #4235.

Mastropole, Angela. (2011). Evaluation of Available Scale-Up Approaches for the Design of GAC Contactors. (MS Thesis). North Carolina State University

Matamoros, Victor, Arias, Carlos A., Nguyen, Loc Xuan, Salvado, Victoria, and Brix, Hans. (2012). Occurrence and Behavior of Emerging Contaminants in Surface Water and Restored Wetland. *Chemosphere.* 88, 1083-1089.

McDowall, B., Ho, L., Saint, C. P., Newcombe, G. (2007). Removal of Geosmin and 2-Methylisoborneol Through Biologically Active Sand Filters. *International Journal of Waste Management,* 1, 311-320.

McGowan, J. C. (2010). Molecular Volumes and Structural Chemistry. *Recueil des Travaux Chimiques des Pays-Bas.* 75, 193-208.

Mertz, K.A., Gobin, F., Hand, D.W., Hokanson, D.R., Crittenden, J.C.(1994) *Manual Adsorption Design Software for Windows (AdDesignS).* Michigan Technological University: Houghton, MI.

Mezzari, Isabella Anna. (2006). Predicting the Adsorption Capacity of Activated Carbon for Organic Contaminants from Fundamental Adsorbent and Adsorbate Properties. (MS Thesis). North Carolina State University.

Murray, Kyle E., Thomas, Sheeba M., and Bodour, Adria A. (2010). Prioritizing Research for Trace Pollutants and Emerging Contaminants in the Freshwater Environment. *Environmental Pollution.* 158, 3462-3471.

Oliveiral, Robson C., Palmieril, Mauricio C., Garcia, Oswaldo. (2011) Biosorption of Metals: State of the Art, General Feature, and Potential Applications for Environmental and Technological Processes.

Owen, Douglas M. (1998). *Removal of DBP Precursors by GAC Adsorption.* AWWA Research Foundation. p.82.

Penn State University Statistics Department. *Lecture 9.* Retrieved from https://onlinecourses.science.psu.edu/stat857/book/export/html/11 (Accessed on 20 December 2012)

Reynolds, T. D. and Richards, P. A. (1996). *Unit Operations and Processes in Environmental Engineering.*(2nd edition). Boston: PWS Publishing Company.

Roberts P.V., and Summers R.S. (1982). Granular Activated Carbon Performance for Organic Carbon Removal, *Journal of American Water Works Association*. 74,113-118.

Rossner Campos, Alfred Armin. (2008). Removal of Polar and Emerging Organic Contaminants by Alternative Adsrobents. (MS Thesis). North Carolina State University.

Shih, Yang-Hsin, Philip M. Gscgwend. (2009). Evaluating Activated Carbon-Water Sorption Coefficients of Organic Compounds Using a Linear Solvation Energy Relationship Approach and Sorbate Chemical Activities. *Environmental Science and Technology,* 43, 851-857.

Snyder, S. A., Vanderford, B. J., Drewes, J. Dickenson, E., Snyder, E. M., Bruce, G. M., Pleus, R. C. (2008) State of Knowledge of Endocrine Disruptors and Pharmaceuticals in Drinking Water. AWWA Research Foundation. Denver Co. 123-137.

Sprunger, Laura, Blake-Taylor, Brooke H., Wairegi, Angeline, Acree, William E., Abraham, Michael H. (2007). Characterization of the Retention Behavior of Organic and Pharmaceutical Drug Molecules on an Immobilized Artificial membrane Column with the Abraham Model. *Journal of Chromatography A.* 1160, 235-245.

Summers, R.S., Hooper, S.M., Solarik, G., Owen, D.M., and Hong, S. (1995). Bench-scale evaluation of GAC for NOM control. *Journal American Water Works Association*. 87, 69-80.

Summers, R.S., Knappe, D.R.U., and Snoeyink, V.L. (2010). Adsorption of Organic Compounds. In *Water Quality and Treatment: A Handbook on Drinking Water*. Edited by American Water Works Association and J.K. Edzwald. McGraw Hill

Schwarzenbach, Rene P., Gschwend, Philip M., Imboden, Dieter M. (2003). Environmental Organic Chemistry: Second Edition. Wiley-Interscience. 58-93.

U.S. Environmental Protection Agency, (2009). *Contaminant Candidate List 3-CCL*. USEPA 815-F-09-001. Retrieved from http://water.epa.gov/scitech/drinkingwater/dws/ccl/ccl3.cfm#ccl3.cfm#List (Accessed 20 December, 2012)

U.S. Environmental Protection Agency, (2012). *National Primary Drinking Water Regulations*. USEPA 816-F-09-004. Retrieved from http://www.epa.gov/drink/contaminants/index.cfm#List (Accessed 18 August, 2012) (a)

U.S. Environmental Protection Agency, (2012). *Unregulated Contaminant Monitoring Rule3-UCMR3*. Retrieved from http://water.epa.gov/lawsregs/rulesregs/sdwa/ucmr/ucmr3/index.cfm.cfm#List (Accessed 20 Decmeber, 2012)
(b)

U.S. Environmental Protection Agency (2012). *2012 edition of the Drinking Water Standards and Health Advisories*. Retrieved from http://water.epa.gov/action/advisories/drinking/upload/dwstandards2012.pdf (Accessed on 9 January 2013) (c)

Walker, John D., Jaworska, Joanna, Comber, Mike H.I., Schultz, Wayne, and Dearden, John C. (2003). Guidelines for Developing and Using Quantitative Structure-Activity Relationships. *Environmental Toxicology and Chemistry*. 22, 1653-1665.

Westerholff, P., Summers, R. S., Chowdhury, Z. K., Kommineni, S. N. (2005). Ozone-Enhanced Biofiltration for Geosmin and MIB Removal. *AWWA Research Foundation.*

Wiesner, M.R., Rook, J.J., and Fiessinger, F. (1987). Optimizing the placement of GAC filtration units. *Journal of American Water Works Association* 79(12), 39-49.

Yuncu, Bilgen. (2010). Removal of 2-Methylisoborneol and Geosmin by High-Silica Zeolites and Powdered Activated Carbon in the Absence and Presence of Ozone. (PhD Dissertation). North Carolina State University.

Zearly, Thomas L., R. Scott Summers. (2012). Removal of Trace Organic Micropollutants by Drinking Water Biological Filters. *Environmental Science and Technology*, 46, 9412-9419.